The Grapefruit Flavonoid Naringenin as a Hepatitis C Virus Therapy: Efficacy, Mechanism And Delivery

By

Jonathan Goldwasser

B.A. Chemistry
Princeton University, 2004

SUBMITTED TO THE DIVISION OF HEALTH SCIENCES AND TECHNOLOGY IN PARTIAL
FULFILLMENT OF THE REQUIREMENTS FOR THE DEGREE OF

DOCTOR OF PHILOSOPHY IN BIOMEDICAL ENGINEERING
AT THE
MASSACHUSETTS INSTITUTE OF TECHNOLOGY
JANUARY 2010

Signature of Author: _____
Harvard-MIT Division of Health Sciences and Technology
January 14, 2010

Certified by: _____
Dr. Martin L. Yarmush
Professor of Surgery and Bioengineering HST, HMS, MGH
Thesis Supervisor

_____
Dr. Yaakov Nahmias
Instructor in Surgery and Bioengineering
Thesis Co-Supervisor

Accepted by: _____
Ram Sasisekharan, PhD/Director, Harvard-MIT Division of Health Sciences and Technology/Edward Hood Taplin Professor of Health Sciences & Technology and Biological Engineering.

Table of Contents

Abstract

Hepatitis C virus (HCV) infection accounts for approximately 40% of chronic liver disease in the United States and results in an estimated 8,000-10,000 deaths annually. Simulations suggest that in the next decade morbidity and mortality associated with HCV infections will result in approximately 200,000 deaths and direct medical expenditures of over $10 billion. Furthermore, recent WHO estimates of worldwide prevalence suggest that up to 2% of the world population is infected with HCV, representing between 120 and 200 million people.

For reasons that are still poorly understood, the current standard of care is effective only in a subset of patients, and depends on both patient-related and disease-related characteristics. Sustained virological response (SVR) – HCV RNA in patient plasma drops below detectable levels at week 24 following completion of treatment, which is thought to be indicative of curing the disease – is attainable in only ~50% of patients.

In recent years, HCV production has been shown to be inextricably linked to lipid metabolism and to the secretion of very low density lipoproteins (VLDL) from hepatocytes. This suggests that by modulating lipid metabolism in the cell, viral production may be reduced in a clinically relevant manner. This work begins by characterizing the link between VLDL secretion and HCV production in the Huh7.5.1/JFH-1 system.

We proceed to examine the effects of naringenin, a grapefruit flavonoid, on the production of HCV. Naringenin has been shown previously to reduce VLDL secretion from hepatocytes, and we demonstrate its ability to block HCV production, as well. We explore the mechanism of naringenin's effect on HCV, and show that the flavonoid prevents the assembly of infectious viruses in the cell.

Despite previous success by several groups in describing the mechanisms involved in naringenin's effect on VLDL secretion, these mechanisms are thought to account only for ~50% of the observed inhibition, suggesting a deeper understanding of the underlying principals is still lacking. We suggest that naringenin exerts its metabolic, and consequently, antiviral effects through modulation of nuclear recepetor (NR) activity. NRs are a superfamily of ligand-regulated transcription factors known to have an important role in maintaining the homeostasis of metabolites. We show that naringenin activates peroxisome proliferator activated receptors (PPARs), NRs known to drive β-oxidation; and inhibits the liver X receptor (LXR), known to drive lipogenesis and cholesterol synthesis.

Despite naringenin's promise as a possible treatment for HCV, its low bioavailability, limits its clinical potential. We conclude this work by showing that naringenin's solubility and bioavailability – and thus, clinical relevance – can be greatly enhanced by complexation with β-cyclodextrins.

Acknowledgements

First, I would like to thank my research advisor, Dr. Martin L. Yarmush. Maish took me under his wing very early in my academic career and allowed me a great amount of freedom in my work. I was privileged to be able to wake up in the morning and work on a project the was entirely my brainchild and about which I was enthusiastic – not many graduate students enjoy that liberty, and I am thankful to Maish for that.

Next, to my co-adviser, Dr. Yaakov Nahmias, thank you for introducing the notion of battling HCV with naringenin to me. It was a brilliant idea and it allowed me to explore a topic closer to the "bedside" than the "bench" for a change. Also, thank you for giving me a better understanding of how science works in the big, cold world. To quote the great physicist, Robert Oppenheimer: "When you see something that is technically sweet, you go ahead and do it and you argue about what to do about it only after you have had your technical success."

My deep thanks to my dear friend and first mentor, Dr. Monica Casali. Not only did you inspire me to think creatively and help me solve problems in my research, you also taught me how to correctly use a cuvette and that it is never OK to use the same plate for both salad and pasta.

I also would like to express my most sincere gratitude to my thesis committee members: Dr. Lee Gehrke, who agreed to become the chair of the committee, Dr. Raymod Chung, and Dr. Mehmet Toner. They all accepted the challenges of getting involved in this research, kept me focused on the big picture, yet encouraged me to pursue all of my ideas. Many people helped me learn techniques and conduct the research described in this work. Special thanks to Drs. Zak Megeed, Alejandro Soto-Gutierrez and Hiroshi Yagi and to Dr. Wenyu Lin from Dr. Raymond Chung's lab.

As with all my successes in life, I would like to thank my parents, who have encouraged and guided me through some tough times. Thank you for inspiring me to pursue this course. Although I eventually decided not to go into a life in academia, I consider myself lucky to have had the chance to go down this path for the past five years, and to do so without having to endure the slings and arrows of graduate student fortunes (or lack there of). You guys are great.

To my two friends-cum-mentors, Eric Yang and Piyush Koria, a special thanks. No doubt that without your support, right now I would be humming to myself in a padded room somewhere. You have been true friends to me through the most difficult of times, and I am truly thankful to have had a chance to be your friend and lab mate.

I would like to thank all my friends and supporters at the CEM, especially Ilana Reis and Lynne Stubblefield. Your willingness to help and professional skill was matched by your kindness and patience. Thank you to Cathy Modica who was a constant cheerleader along the way, especially in the dark early days. I hope to find more people like you in my future.

Thank you to all of my friends here in Boston, especially to Saurabh, Marco and Monica, Michael, Uri, Yibo, Maria Louisa, Seth, Mridula and Raj, Amy, Jack and Jenny, Alex, Danilo, Stephanie, Erkin, Oaz, Eli, Joe, Kyle, Rumi, Todd, Luke, Erika, Eugene, Helen, Ben, Tom, Nick, Christine, and Ping.

Finally, I would like to thank my beloved Amanda. Words fail me as I try to explain the difference you have made in my life here. Others have helped me academically; some have kept me sane and made me laugh. But no one has made me as happy as you have. My experience at MIT would have been entirely different without you, and many times since we have met I have had the chance to reflect on how your presence in my life has shed a bright beam of light on everything I have experienced here. Thank you for being my love, my anchor, and my muse.

1 Introduction

1.1 Hepatitis C Virus

Hepatitis C virus (HCV) infection accounts for approximately 40% of chronic liver disease in the United States and results in an estimated 8,000-10,000 deaths annually. Simulations suggest that in the next decade morbidity and mortality associated with HCV infections will result in approximately 200,000 deaths and direct medical expenditures of over $10 billion (1). Furthermore, recent WHO estimates of worldwide prevalence suggest that up to 2% of the world population is infected with HCV, representing between 120 and 200 million people (2). In the developed world, most new cases are acquired through blood-to-blood transmission (i.e., needle sharing) (3).

The natural history of hepatitis C infections is highly variable between patients (**Figure 1**) (3). 75-85% of all infected individuals develop a long-term infection, while approximately 15% clear the infection following the acute phase. The chronic phase of the disease is asymptomatic for an extended period, and may remain so. However, 10-15% of chronic patients develop fibrosis and cirrhosis of the liver, usually over several decades. Approximately 6% of patients with cirrhosis will then develop decompensated liver disease and will require transplant. Consequently, HCV infection is the leading indication of liver transplant in the US and most parts of the world (4). Lastly, patients with established cirrhosis have a 3-4% annual risk of developing hepatocellular carcinoma (HCC). The exact reasons for the variability in natural history among individuals have not been entirely clarified, but associations with multiple demographic factors, co-morbidities, and behavioral factors have been described (3).

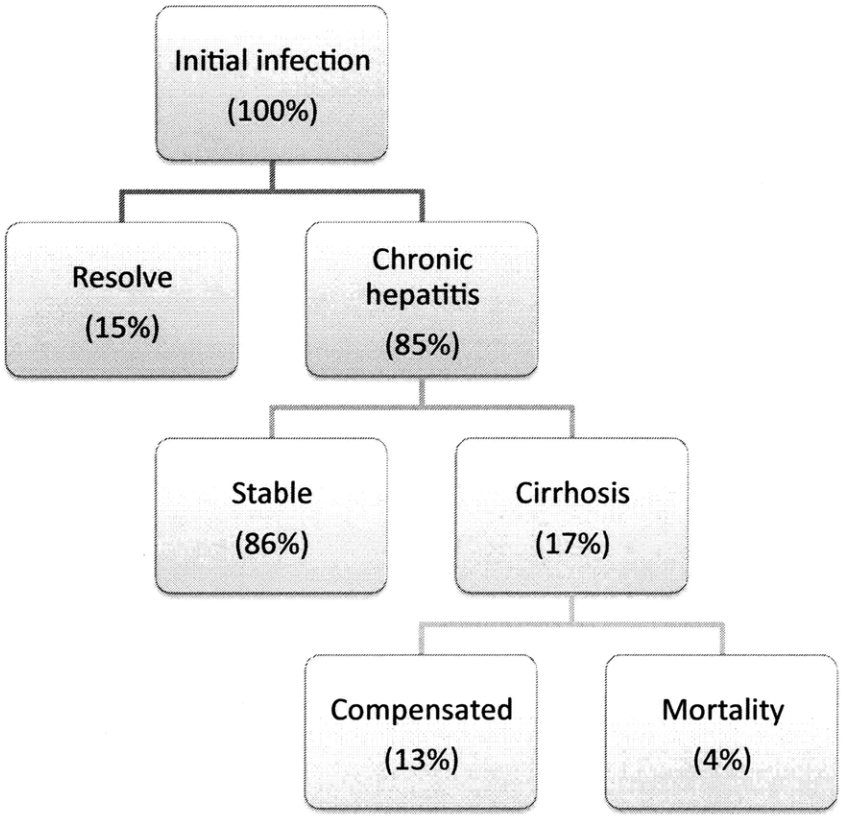

Figure 1 - HCV has a highly variable natural history. For every 100 people infected, 85 will develop chronic hepatitis. In the majority of these, the disease will be stable, but over several decades, 17 people will develop liver fibrosis and cirrhosis. These people will be at an increased risk for decompensated liver disease and hepatocellular carcinoma. The factors that lead patients to have such variable courses of disease are not known, although several associations have been made to demographic factors, co-morbidities, and behavioral factors. More recently, genetic links have been invistagted. *Adapted from McHutchison (2004).*

Since the discovery of the HCV virus in 1989 (5), the standard of care for treating HCV-infected individuals has developed from interferon α (IFNα) monotherapy through a combination of ribavirin and interferon, to the current standard of pegylated IFNα and ribvirin (6). For reasons that are still poorly understood, this regimen is effective only in a subset of patients, and depends on both patient-related and disease-related characteristics (7). Sustained virological response (SVR) – HCV RNA in patient plasma drops below detectable levels at week 24 following completion of treatment, which is thought to be indicative of curing the disease – is attainable in only 42-46% of genotype 1 infections, the most common genotype in the US and Europe (6, 8). Beyond its low efficacy, combination treatment exacts a high toll in terms of drug-induced side effects, including flu-like illness, fever, fatigue, hematological disease, anemia, leucopenia, thrombocytopenia, alopecia, and depression (9). These adverse effects, along with other barriers, prevent the completion of treatment in patients, leading to discontinuation of treatment in 10-20% of cases.

Several drugs are currently in development for HCV to improve efficacy and reduce adverse effects. Most efforts focus on inhibiting viral enzymes, specifically the viral protease and polymerase (*see below*), although attempts have been made to develop nucleic acid-based treatments (6). The propensity of the virus to mutate, however, makes it difficult to consistently produce an SVR in patients. Previous drug candidates have led to the evolution of escape mutants within patients (*quasi-species*) and could lead to the evolution of resistant strains in the patient population (10, 11). Strategies borrowed from the treatment of HIV, including timing of treatments and drug cocktails hold some promise in averting the development of resistance (12). Nonetheless, therapies that target *host* factors hold more promise, as these are immutable. Specifically, agents are being developed to either elicit an immune response against the virus (13), or to exploit the virus' dependence on certain host factors for the completion of its lifecycle (14, 15).

1.1.1 The Viral Life Cycle

HCV is an enveloped, ~9500 bp, positive-strand RNA virus, a member of the *Flaviviridae* family. The viral genome encodes a single open reading frame (ORF) of approximately 3000 amino acids. The viral life cycle begins upon entry into the host cell (**Figure 2**). The process of cellular entry has yet to be clarified completely, but seems to involve several receptors. Both CD81 (16) and claudin-1 (17) seem to be required for successful entry of the virus into the cell. It seems however, that these receptors are involved in later steps of viral entry, and that early steps may involve either the low-density lipoprotein receptor (LDLR) or the scavenger receptor, SR-BI (16, 18, 19).

Upon introduction of the viral genetic material into the host cytoplasm, translation is initiated via the viral 5' nontranslated region (NTR), which functions as a ribosomal entry site (20). The viral polyprotein is threaded in and out of the endoplasmic reticulum (ER), and is then cleaved both by host enzymes and autocatalytically by proteases that are part of the nascent polyprotein. This leads to the production of mature structural proteins, including core, E1, and E2; and nonstructural (NS) proteins (21, 22). The accumulation of viral proteins, and specifically core protein, in the cellular ER induces morphological changes in the cell with the formation of a *membranous web*, where viral replication has been reported to occur (23). HCV budding occurs either at the ER membrane or in ER-associated lipid droplets (*see below*) (24) and is driven by the viral core protein (24, 25), after which the virus is exported from the cell via the Golgi apparatus by exocytosis (26).

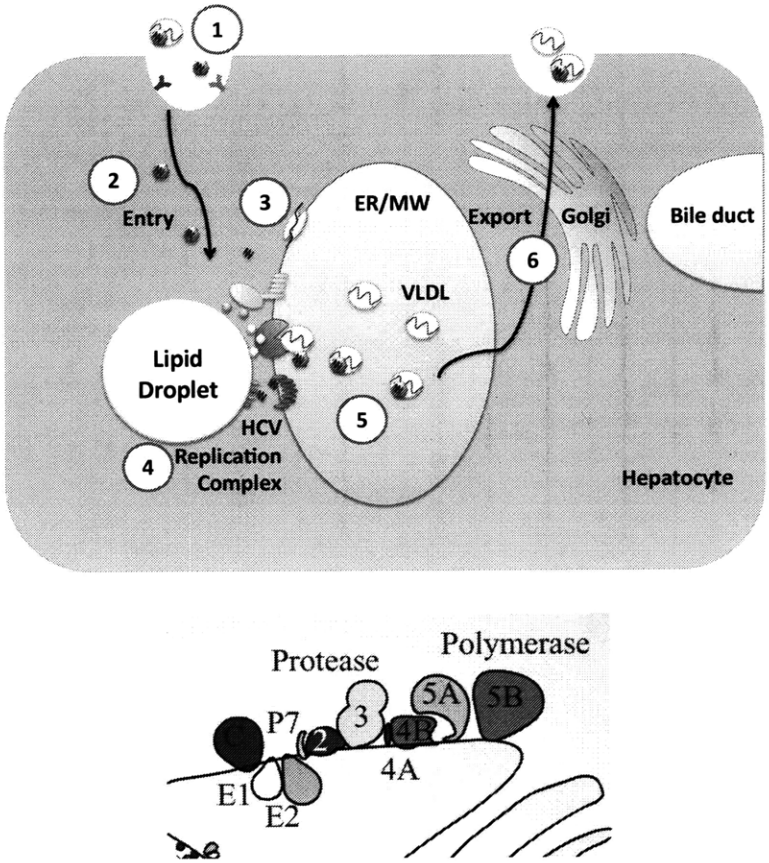

Figure 2 - Illustration of the viral lifecycle. (*Top*) Cell entry (1) has been shown to be dependent on several receptors, including SR-BI, LDLR, CD81, and claudin-1. It is not clear whether receptors recognize a lipoviral particle (a virion physically associated with a lipoprotein), or whether the interaction occurs with virions directly. Viruses enter the cytoplasm and uncoat (2), and their RNA is used to synthesize the viral polyprotein (3). This induces the formation of the membranous web, which is closely associated with lipid droplets. The viral replication complex (4) has been reported to be associated with both of these ER-related structures. Finally, the sense strand genome and structural proteins are assembled into an infectious virion (5), probably as a lipoviral particle, which exits the cell via the Golgi apparatus by exocytosis (6). ER/MW – endoplasmic reticulum/membranous web. (*Bottom*) The viral polyprotein depicted inserted into the ER membrane.

1.1.2 Viral particle production is dependent on host metabolic processes

The link between HCV and lipid metabolism was suggested early on, both by the association of steatosis with chronic HCV infection (27), and the finding that HCV particles are physically associated with lipoporoteins in patient plasma (28). Early experiments were limited by the lack of a cell culture system capable of sustaining the full viral life cycle. Nonetheless, the HCV core protein expressed in HepG2 hepatoma cells was shown to associate with cytoplasmic lipid droplets (29) – lipid storage organelles that are closely associated with the ER (30). Furthermore, viral replication in replicon-based systems was shown to be inhibited by statins, inhibitors of HMG CoA, the rate-limiting enzyme in the mevalonate pathway (31, 32). Further investigation revealed that this was due to the dependence of viral replication on the availability of geranylgeranyl (33). This lipid was shown to be required in order to anchor the FBL2 protein to the ER membrane, and that interaction of the viral NS5A protein with the anchored FBL2 was essential for viral replication (34). Lastly, it was observed that livers of chimpanzees infected with HCV showed steatotic changes and changes in gene expression consistent with pro-lipogenic metabolic changes (35), provided further evidence of the link between HCV and altered lipid metabolism.

The development of the Huh7.5.1 cell line capable of supporting the full life cycle of JFH-1-derived HCV strains (36, 37) has allowed the further elucidation of both the dependence of the HCV lifecycle on lipid metabolism, and of the alterations in cellular metabolism as a consequence of HCV infection. Huang *et al.* demonstrated that HCV assembled in vesicles enriched in ApoB, the main protein component found in very low-density lipoprotein (VLDL); and in microsomal triglyceride transfer protein (MTP), the rate-limiting enzyme in VLDL assembly (**Figure 3**) (38). Using a similar system, Gastaminza *et al*. demonstrated the existence of high density intracellular HCV precursors suggesting the virus binds to low density lipoproteins in the ER to form lipoviral particles (39). Lastly, HCV has been found to be actively secreted while bound to (VLDL), and blocking the production of ApoB using RNAi or by inhibiting MTP has been shown to lead to a decrease in the amount of secreted virus (38).

Conversely, there is evidence to suggest that chronic viral infection is correlated with the development of steatosis, especially in HCV genotype 3 (40). Yang *et al.* showed that the HCV core protein leads to the upregulation of the fatty acid synthase gene (41), and others have shown an upregulation of the lipogenic SREBP-1c signaling pathway (42, 43). Significantly, HCV has been shown to regulate nuclear receptors (NRs; *see below*), a family of ligand-activated transcription factors, which function as master regulators of cellular metabolic processes (44). HCV core associates with RXRα, a transcriptional co-regulator of multiple metabolic processes (45), and downregulates the PPARα NR, a known driver of fatty acid β-oxidation (46), leading to downregulation of the rate-limiting enzymes CPT-1 and AOX. Studies of liver biopsies of chronic HCV patients suggest these effects occur *in situ*, as well (40). Furthermore, HCV core protein has been recently shown to enhance the activity of the pro-lipogenic LXRα NR (43). Interestingly, the hepatitis B viral X protein has recently been shown to activate LXRα, suggesting the possibility of a more general mechanism for virus-cell interaction in the liver (47, 48).

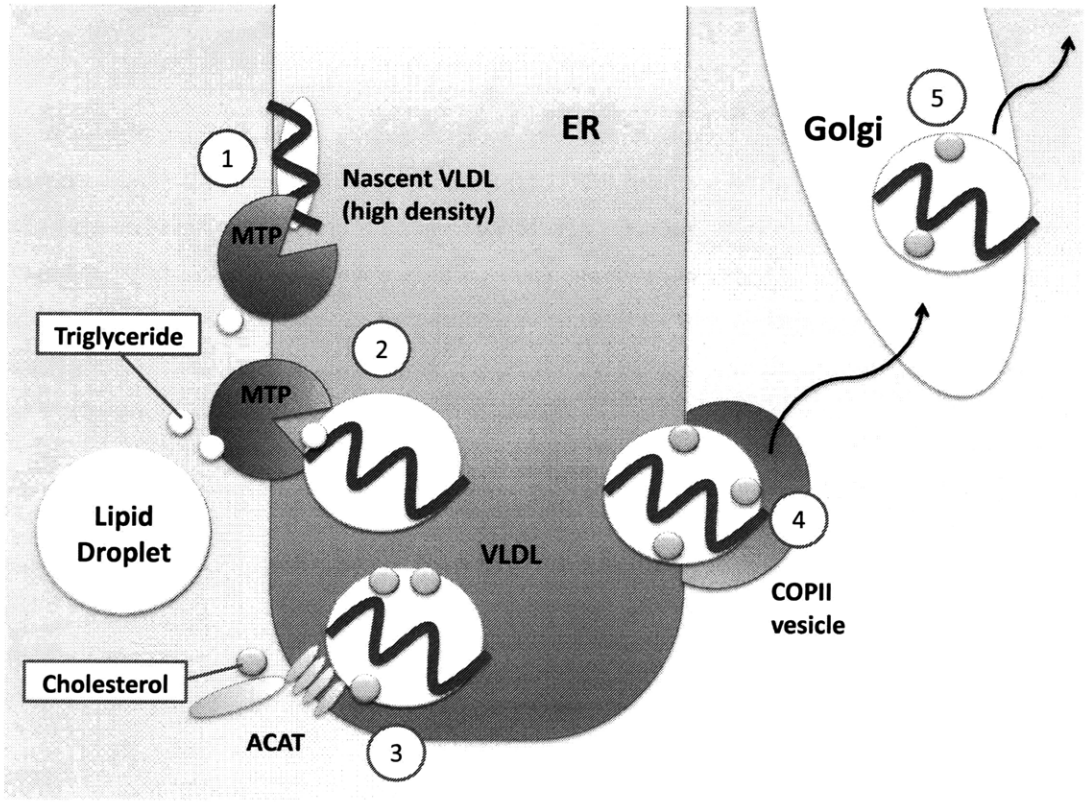

Figure 3 - VLDL assembly in the ER-Golgi. Nascent ApoB is threaded into the ER lumen, where it becomes associated with triglycerides (TG) and cholesteryl esters (CE). Microsomal triglyceride transfer protein (MTP), the rate-limiting enzyme in VLDL assembly, actively transports TGs into the ER. In the absence of TG and CE, ApoB is co-translationally degraded, preventing an accumulation of ApoB in the ER and the export of VLDL. A pre-VLDL particle is exported from the ER to the Golgi apparatus, where it fuses with bulk TGs in the form of lipid droplets, forming the mature VLDL particle which is then exported from the cell by exocytosis (49, 50). *Adapted from Ikonen (2008).*

This evidence suggests that *infectious particle production is inextricably linked to lipid metabolism and to the secretion of VLDL from hepatocytes.* This hypothesis is both consistent with the above-mentioned observations, and may explain the tropism of the virus. Furthermore, *by modulating lipid metabolism in the cell, viral production may be reduced in a clinically relevant manner.*

1.2 Host lipid metabolism is controlled by a family of nuclear receptors

Over the past decade, a superfamily of proteins called *nuclear receptors* (NRs) has been identified and characterized. This family of receptors is involved in embryonic development, cell death, and maintenance of cellular differentiation (51). Among their many functions, *NRs have an important role in maintaining the homeostasis of metabolites* (52).

All NRs share a similar, modular structure, with three major domains (53). The N-terminal domain is known as the *transactivation domain*, which allows the NR to interact with coactivators and other transcription factors. The central, *DNA binding domain* (DBD) allows the NR to recognize *response elements* in specific genes. Lastly, the C-terminal, *ligand binding domains* (LBDs) of all NRs share a common structure. The LBD is generally constructed of a core of 11 helices and a twelfth helix (H12) that forms a lid structure over a binding pocket in the core. The orientation of H12 is determined by the ligand that is bound to the core of the LBD. In the absence of a ligand, the conformation of H12 allows the NR to bind co-repressors; while ligand binding leads to an allosteric shift that allows co-activators to interact with the LBD and the transactivation domain.

Several barriers complicate the study of NR activities in cells. First, nuclear receptors regulate gene function through interactions with multiple co-repressors and co-activators, whose function is often cell-specific and condition-specific (54). Second, NRs are known to be phosphoproteins, and are regulated by multiple kinases (55). Third, nuclear receptors are known to regulate each other's function through transcriptional (56) and non-transcriptional (e.g., competitive inhibition) mechanisms (57, 58). Lastly, the LBDs of several NRs have been shown to be flexible in accommodating multiple ligands, leading to conformational changes that exert differential regulatory effects (59-63). Nonetheless, the benefits of understanding and controlling NR function is evident when considering their involvement in a plethora of disease states, such as cancer, infertility, diabetes, and obesity (64); and the success of therapeutic agents that target these receptors: tamoxifen for the estrogen receptor (65, 66), fibrates for PPARα,

thiazolidinediones (TZDs) for PPARγ (67, 68), and dexamethasone for the glucocoticoid receptor (44).

1.2.1 Three families of NRs control metabolism

Within the complex web of interacting NRs, three major families are involved in the regulation of lipid and carbohydrate metabolism (Table 1): peroxisome proliferator-activated receptors (PPARs), which bind fatty acids; liver X receptors (LXRs), which are known to bind both glucose and products of the mevalonate pathway, most notably cholesterol derivatives; and farnesoid X receptor (FXR), which binds bile salts (44).

Name	Abbreviation	Nomenclature	Ligand
Peroxisome proliferator-activated receptor	PPARα	NR1C1	Fatty acids, leukotriene B4, fibrates
	PPARβ/δ	NR1C2	Fatty acids
	PPAR γ	NR1C3	Fatty acids prostaglandin J2
Liver X receptor	LXRα	NR1H3	Oxysterols, T0901317, GW3965, glucose
	LXRβ	NR1H2	Oxysterols, T0901317, GW3965
Farnesoid X receptor	FXRα	NR1H4	Bile acids, fexaramine

Members of these three families are differentially expressed in various tissues, and their activation has been reported to lead to different responses – contrary responses, when viewed at the level of the single cell – in different tissues and cell types (54, 69). Importantly, when viewed from the point of view of the organism, the different effects exerted by similar stimuli (i.e., metabolite abundance) *should* lead to differing responses in different tissues. For example, low glucose levels should signal adipocytes

to mobilize fat back to the liver (i.e., fat secretion), while signaling the liver to take up and break down lipid (70).

Two NR families – the PPARs and LXRs – sense opposing metabolic states, driving different transcriptional programs in the organism (69, 70). The PPAR family of NRs includes PPARα, PPARγ, and PPARδ (71). The prevalence of these receptor subtypes varies in different tissues, with PPARα being the most prevalent subtype in the liver, and PPARγ the most abundant in adipose tissue (72). PPARα is activated by fatty acids released in a physiological *fasting* state, leading to increased β-oxidation and gluconeogenesis (73). PPARα agonists in particular are known to upregulate genes involved in the β-oxidation of fatty acids and gluconeogenesis (74). PPARγ is similarly activated by long-chain fatty acids and certain prostaglandins, and leads to increased storage of fat in adipocytes (75). In clinical practice, PPARα agonists (fibrates) are used to treat hyperlipidemia, whereas PPARγ agonists (TZDs) are used to increase insulin sensitivity (68, 76).

The LXR family of NRs includes both LXRα and LXRβ (77-79). The latter is ubiquitously expressed, while the former is found primarily in the liver, adipose tissue, and macrophages and is activated by the abundance of glucose and sterols (80), typical of a physiological *fed* state. Following activation by its ligands, LXRα activates lipogenic and glycolytic genes, including genes involved in the production of VLDL and its secretion by hepatocytes (81), partly through activation of SREBP-1c (82, 83).

Following the binding of an agonist, both PPARs and LXRs become activated and heterodimerize with another NR, the retinoid X receptor (RXR) (44). The activated heterodimer then binds conserved response elements in specific genes, while recruiting other co-regulatory molecules, such as the co-activators PGC1α (84) and Trap220 (85) for PPARα and LXRα, respecitvely. The requirement of both LXR and PPAR for the RXR binding partner leads to competitive inhibition at the level of receptor activation, offering a transcriptional layer of control over fasted-to-fed transition (57, 58, 86). The existence of both a PPAR response element (PPRE) and an LXR response element (LXRE)

in the regulatory region of the LXRα gene (56, 87) suggests further levels of cross-regulation. Lastly, other coactivators, corepressors and kinases, such as PI3K and ERK, can regulate NR activity by non-transcriptional mechanisms (**Figure 4**) (54, 55, 88).

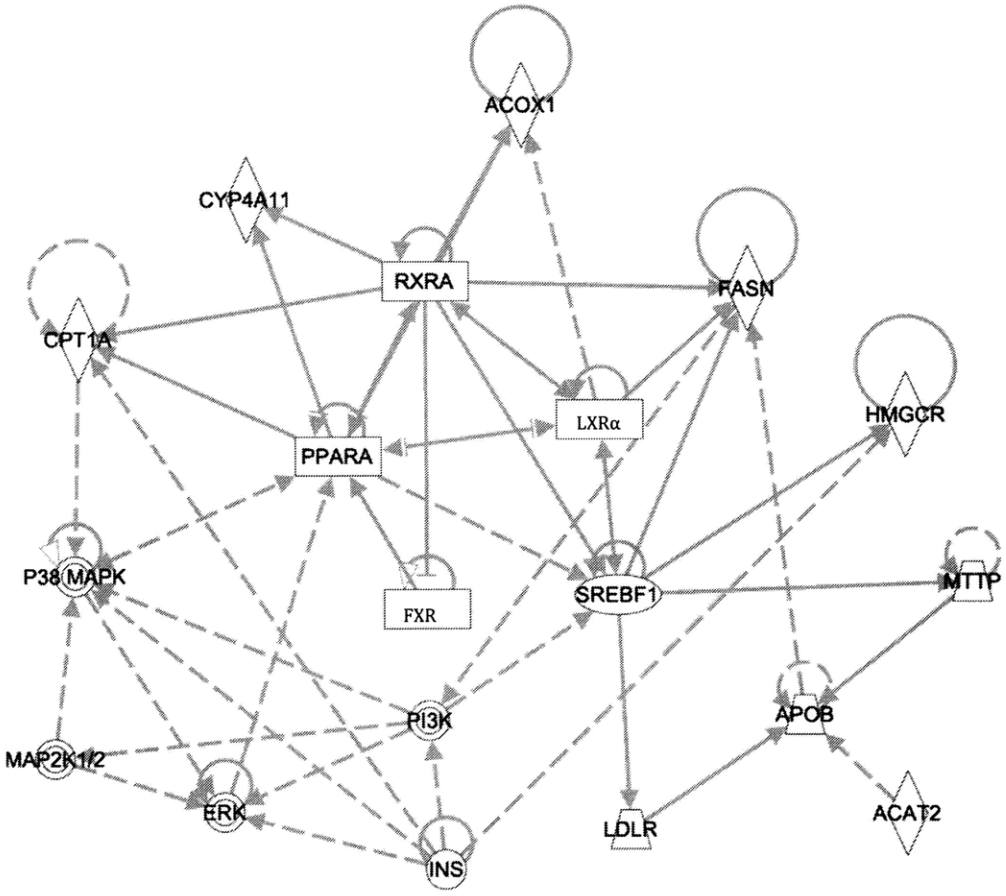

Figure 4 - Lipid and carbohydrate metabolism signaling network. Some of the important regulators of lipid vs. glucose neogenesis mentioned in the text are presented. LXRα, PPARα, and FXRα are master regulators of lipid and cholesterol metabolism. The induction of LXRα leads to the activation of SREBP-1c and other pathways leading to the production of fat and cholesterol; whereas activation of PPARα leads to gluconeogenesis. FXR stimulation induces the conversion of cholesterol into bile salts. The three NRs bind with RXR resulting in transrepression between PPARα and LXRα due to their need for RXR binding in order to become fully active. This diagram captures only a few of the multiple interacting regulators of metabolism in the cell, and is meant to illustrate the high level of complexity related to NR metabolic regulation. *Created using Ingenuity Pathways Analysis software package (Ingenuity systems, Redwood City, CA).*

Given the control these NRs exert over lipid metabolism, and given the association between the HCV life cycle and lipid metabolism, we hypothesize that *modulating the activities of these NRs will allow the modulation and suppression of HCV production*.

1.3 Naringenin

Naringenin is part of a 4000-member polyphenolic family of structurally related molecules called *flavonoids* (**Figure 5**) (89). More specifically, naringenin belongs to a class called *flavonones*, members of which are commonly found in citrus fruits. Naringenin is highly insoluble in water, and is found as a glycoside conjugate, naringin (*naringenin-7-rhamnoglucoside*), in grapefruit. Naringenin has been reported to be an antioxidant with demonstrated hypolipidemic, anti-carcinogenic and anti-inflammatory properties (89). Naringenin is known to interact with multiple drugs as a result of its competitive inhibition of cytochrome P450 enzymes (90).

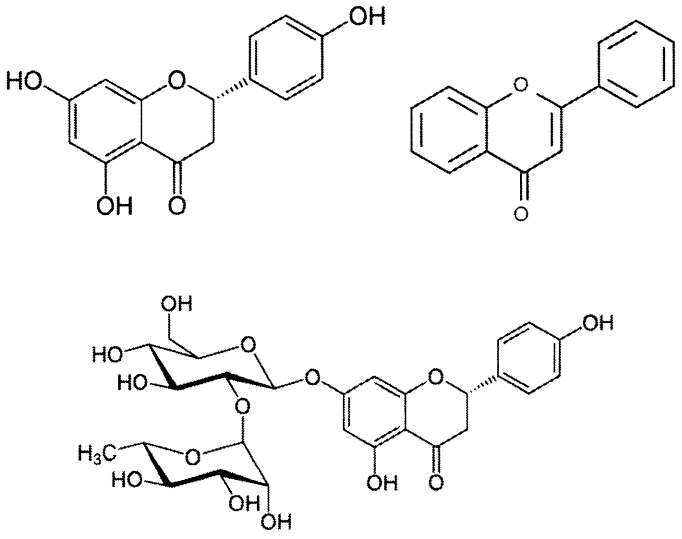

Figure 5 - Naringenin is a flavonoid. Naringenin (*top left*) is a molecule of the flavonone class. Related molecules share the flavonoid backbone structure (*top right*). Many flavonoids are secondary plant metabolites and are attached to glycones (sugar moieties). Indeed, naringenin is naturally found in plants – most abundantly in grapefruits – as naringin (*bottom*) and is hydrolyzed to its aglycone form in the intestine.

1.3.1 Naringenin reduces VLDL secretion

Naringenin has previously been shown to reduce the secretion of VLDL by inhibiting several signaling and metabolic pathways (91). Given the dependence of HCV on the secretion of VLDL, this suggests *naringenin could be used to inhibit the production of virus in hepatocytes*.

The molecular mechanism behind naringenin's hypolipidemic effect was studied mainly in HepG2 cells, where naringenin was shown to reduce the secretion of VLDL and LDL (92, 93) through the inhibition of ACAT2 and MTP (92, 94), critical enzymes for VLDL assembly. Allister *et al.* demonstrated that this inhibition is regulated primarily through the mitogen-activated protein kinase pathway, through MEK1/2 and ERK1/2 (94). In addition, naringenin was shown to induce LDL receptor (LDL-R) (95), whose expression in the ER leads to the degradation of ApoB (96, 97). This upregulation of LDL-R transcription was shown to be caused by activation of PI3K upstream of SREBP-1 (95). Naringenin was also shown to inhibit HMGR (98), while activating enzymes important in fatty acid oxidation such as CYP4A11 (99).

Despite the success in describing some of the mechanisms involved in naringenin's effect on VLDL secretion, *these mechanisms are thought to account only for ~50% of the observed inhibition (100), suggesting a deeper understanding of the underlying principals is still lacking.*

1.3.2 Polyphenols interact with nuclear receptors

In recent years, research has elucidated the mechanisms of action of multiple natural products, in particular, plant-derived polyphenolic compounds. A large number of plant-derived compounds have been found to modulate the activities of NRs, notably those of the PPAR, LXR, and FXR families (101). *The myriad effects of naringenin in cells, suggest that the flavonoids may also target nuclear receptors.*

Strengthening this hypothesis is the anecdotal report that naringenin interacts with LXR (95) and more recently that it activates PPARα in U-2OS cells (102). A similar pathway was demonstrated for green tea polyphenols and soy isoflavones which

regulate LXRα and PPARα (101). The understanding that nuclear receptors are regulated to some degree by kinases of the MAPK and PI3K/Akt pathways through phosphorylation could provide a link between previously described mechanisms and a NR-mediated mechanism.

1.3.3 Naringenin pharmacokinetics and toxicity

Following enteral administration, naringin is hydrolyzed to its aglycone form, naringenin, either by gut flora or intestinal enzymes prior to being absorbed in the intestine (103). Intestinal flora has also been shown to degrade naringenin to other metabolites, such as 4-hydroxbenzoic acid (104, 105). Naringenin's low solubility in aqueous environments is thought to contribute to its low bioavailability: in clinical trials, plasma concentrations have not been reported to exceed 6μM (89, 106). The flavonoid is conjugated either in the intestine or in the liver to a glucuronide form (107), and is finally metabolized by the hepatic CYP1A enzyme (108).

Limited information is available regarding naringenin's toxicity. Notably, as a naturally-derived product, the flavonoid is marketed as a food supplement. In rats, its oral LD_{50} has been reported to be >5000 mg/kg (109), and in human studies, naringenin was administered at oral doses of up to 2g without any adverse effects (110). *In vitro* toxicity has been demonstrated to be low in several cell types, with cell growth IC_{50} values of >1mM (89).

1.3.4 Cyclodextrins could improve naringenin's low bioavailability

Naringenin's anti-atherogenic and anti-inflammatory properties, along with its antiviral potential, make it an interesting candidate for clinical application. As with other drugs, however, efficacy depends on the ability to reproducibly deliver the molecule to patients (111). The ability to breakdown naringin to the absorbable naringenin form varies widely between patients, possibly owing to differences in gut flora (106). Thus, a method of enhancing the bioavailability of naringenin itself is required.

Cyclodextrins are a family of cyclical oligosacchrides, composed of varying numbers of glucopyranoside rings that form a three-dimensional toroid structure. The

inner face of the toroid is significantly less hydrophilic than the surrounding water, providing an energetic advantage to the insertion of hydrophobic molecules into the cavity. β-cyclodextrins, specifically, are composed of seven sugar rings, and have been shown to be non-toxic to humans (112). These cyclodextrins are widely used in the food and pharmaceutical industries as excipients to enhance the solubility of hydrophobic molecules.

The potential of β-cyclodextrins to enhance the solubility and gut absorption of flavonoids was demonstrated by Uekama and coworkers (113). The researchers complexed the flavonoid-glycoside, rutin, with HPβCD, and found an >10-fold increase in its solubility in aqueous solution. Plasma concetration, as measured by area-under-the-curve (AUC), increased nearly 3-fold. Several effects could explain an increased rate of transport following complexation with HPβCD, including enhancement of dissolution kinetics, increase in solubility, decrease in degradation kinetics in the gut, change in the properties of the intestinal membrane, and shuttling and enhancement of drug concentration at the intestinal wall (**Figure 6**) (114, 115). Notably, HPβCD, particularly, is known to cause very little irritation to the gut mucosa and is used in multiple preparations (116).

The hydrophobic nature of naringenin, and its structural similarity to the hydrophobic quercetin unit in rutin, suggests that its delivery could similarly be enhanced through complexation with HPβCD.

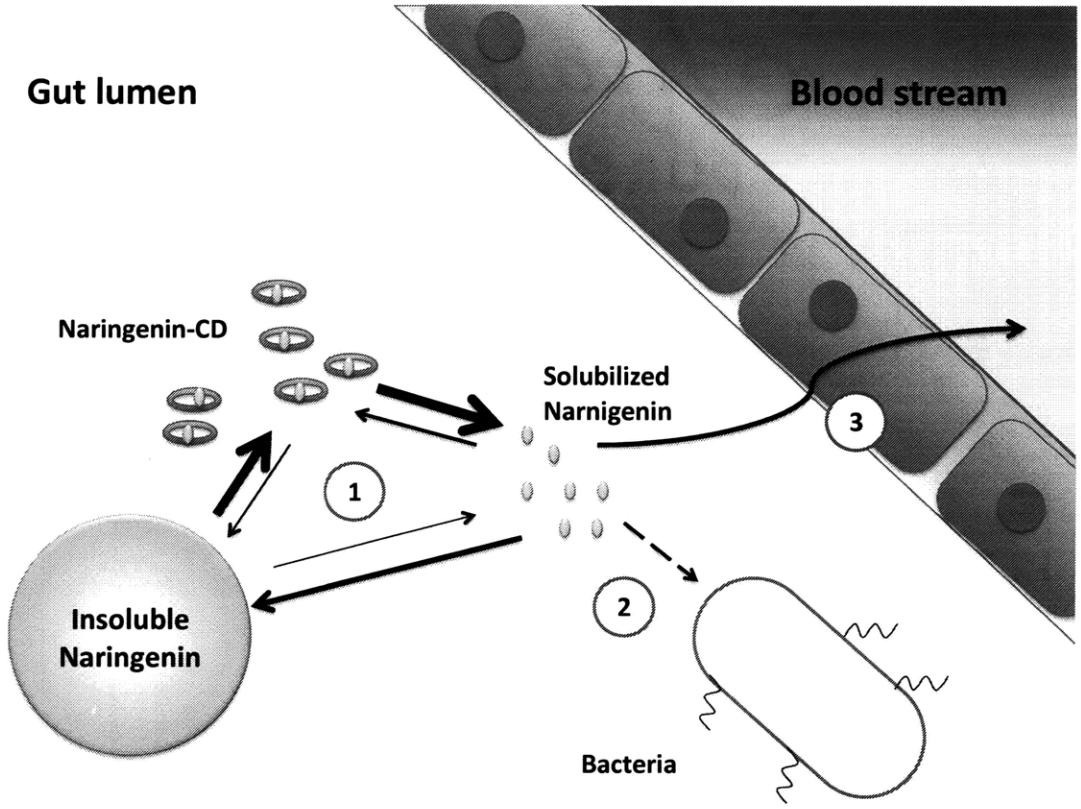

Figure 6 - Enhanced absorption of naringenin in the gut. Complexation of a small, hydrophobic molecule such as naringenin with cyclodextrin (CD) could lead to enhanced absorption by several means. (1) Complexation could shift the thermodynamic balance and enhance the kinetics of dissolution. (2) CD could limit the amount of naringenin that is exposed to degradation by gut microbes. (3) Naringenin could alter the properties of the intestinal wall microenvironment or of the wall itself. CD complexation is not expected to affect post-absorption steps, as CD does not cross the intestinal wall.

1.4 This thesis

The sum of this work suggests that naringenin may be useful in the treatment of HCV. We will first examine the mechanism underlying the flavonoid's effects on HCV production and show it is due to its inhibition of VLDL production. We demonstrate that naringenin blocks the assembly of infectious particles. We then show that naringenin's metabolic, and consequently, anti-viral effects can be attributed to its effect on nuclear receptors. Finally, we demonstrate that through complexation with β-cyclodextrins, the molecule can be delivered in a clinically relevant manner.

1.5 References

1. Dienstag JL, McHutchison JG. American Gastroenterological Association technical review on the management of hepatitis C. Gastroenterology 2006;130:231-264; quiz 214-237.

2. Shepard CW, Finelli L, Alter MJ. Global epidemiology of hepatitis C virus infection. Lancet Infect Dis 2005;5:558-567.

3. McHutchison JG. Understanding hepatitis C. Am J Manag Care 2004;10:S21-29.

4. Rodriguez-Luna H, Douglas DD. Natural history of hepatitis C following liver transplantation. Curr Opin Infect Dis 2004;17:363-371.

5. Choo QL, Kuo G, Weiner AJ, Overby LR, Bradley DW, Houghton M. Isolation of a cDNA clone derived from a blood-borne non-A, non-B viral hepatitis genome. Science 1989;244:359-362.

6. Manns MP, Foster GR, Zeuzem S, Zoulim F. The way forward in HCV treatment - finding the right path. Nat Rev Drug Discov 2007.

7. Ge D, Fellay J, Thompson AJ, Simon JS, Shianna KV, Urban TJ, Heinzen EL, et al. Genetic variation in IL28B predicts hepatitis C treatment-induced viral clearance. Nature 2009;461:399-401.

8. Zeuzem S, Berg T, Moeller B, Hinrichsen H, Mauss S, Wedemeyer H, Sarrazin C, et al. Expert opinion on the treatment of patients with chronic hepatitis C. J Viral Hepat 2009;16:75-90.

9. Manns MP, Wedemeyer H, Cornberg M. Treating viral hepatitis C: efficacy, side effects, and complications. Gut 2006;55:1350-1359.

10. Ye J. Reliance of host cholesterol metabolic pathways for the life cycle of hepatitis C virus. PLoS Pathog 2007;3:e108.

11. De Francesco R, Migliaccio G. Challenges and successes in developing new therapies for hepatitis C. Nature 2005;436:953-960.

12. McGovern BH, Abu Dayyeh BK, Chung RT. Avoiding therapeutic pitfalls: the rational use of specifically targeted agents against hepatitis C infection. Hepatology 2008;48:1700-1712.

13. McHutchison JG, Bartenschlager R, Patel K, Pawlotsky JM. The face of future hepatitis C antiviral drug development: recent biological and virologic advances and their translation to drug development and clinical practice. J Hepatol 2006;44:411-421.

14. Moriishi K, Matsuura Y. Host factors involved in the replication of hepatitis C virus. Rev. Med. Virol. 2007;17:343-354.

15. Goto K, Watashi K, Inoue D, Hijikata M, Shimotohno K. Identification of cellular and viral factors related to anti-hepatitis C virus activity of cyclophilin inhibitor. Cancer Sci 2009;100:1943-1950.

16. Kapadia SB, Barth H, Baumert T, McKeating JA, Chisari FV. Initiation of hepatitis C virus infection is dependent on cholesterol and cooperativity between CD81 and scavenger receptor B type I. J Virol 2007;81:374-383.

17. Liu, Yang, Shen, Turner, Coyne, Wang. Tight Junction Proteins Claudin-1 and Occludin Control Hepatitis C Virus Entry and are Downregulated during Infection to Prevent Superinfection. J Virol 2008.

18. Molina S, Castet, Fournier-Wirth C, Pichard-Garcia L, Avner R, Harats D, Roitelman J, et al. The low-density lipoprotein receptor plays a role in the infection of primary human hepatocytes by hepatitis C virus. Journal of Hepatology 2007;46:411-419.

19. Wünschmann S, Medh JD, Klinzmann D, Schmidt WN, Stapleton JT. Characterization of hepatitis C virus (HCV) and HCV E2 interactions with CD81 and the low-density lipoprotein receptor. J Virol 2000;74:10055-10062.

20. Fraser CS, Doudna JA. Structural and mechanistic insights into hepatitis C viral translation initiation. Nat Rev Microbiol 2007;5:29-38.

21. Penin F, Dubuisson J, Rey FA, Moradpour D, Pawlotsky JM. Structural biology of hepatitis C virus. Hepatology 2004;39:5-19.

22. Giannini C, Brechot C. Hepatitis C virus biology. Cell Death Differ 2003;10 Suppl 1:S27-38.

23. Quinkert D, Bartenschlager R, Lohmann V. Quantitative analysis of the hepatitis C virus replication complex. J Virol 2005;79:13594-13605.

24. Roingeard P, Hourioux C, Blanchard E, Prensier G. Hepatitis C virus budding at lipid droplet-associated ER membrane visualized by 3D electron microscopy. Histochem Cell Biol 2008;130:561-566.

25. Hourioux C, Ait-Goughoulte M, Patient R, Fouquenet D, Arcanger-Doudet F, Brand D, Martin A, et al. Core protein domains involved in hepatitis C virus-like particle assembly and budding at the endoplasmic reticulum membrane. Cell Microbiol 2007;9:1014-1027.

26. Gastaminza, Cheng, Wieland, Zhong, Liao, Chisari. Cellular determinants of hepatitis C virus assembly, maturation, degradation, and secretion. Journal of Virology 2008;82:2120-2129.

27. Serfaty L, Andreani T, Giral P, Carbonell N, Chazouillères O, Poupon R. Hepatitis C virus induced hypobetalipoproteinemia: a possible mechanism for steatosis in chronic hepatitis C. Journal of Hepatology 2001;34:428-434.

28. André, Komurian-Pradel F, Deforges S, Perret M, Berland JL, Sodoyer M, Pol S, et al. Characterization of low- and very-low-density hepatitis C virus RNA-containing particles. Journal of Virology 2002;76:6919-6928.

29. Barba G, Harper F, Harada T, Kohara M, Goulinet S, Matsuura Y, Eder G, et al. Hepatitis C virus core protein shows a cytoplasmic localization and associates to cellular lipid storage droplets. Proc Natl Acad Sci USA 1997;94:1200-1205.

30. Olofsson, Boström, Andersson, Rutberg, Perman, Borén. Lipid droplets as dynamic organelles connecting storage and efflux of lipids. Biochim Biophys Acta 2008.

31. Delang L, Paeshuyse J, Vliegen I, Leyssen P, Obeid S, Durantel D, Zoulim F, et al. Statins potentiate the in vitro anti-hepatitis C virus activity of selective hepatitis C virus inhibitors and delay or prevent resistance development. Hepatology 2009;50:6-16.

32. Ikeda M, Abe K, Yamada M, Dansako H, Naka K, Kato N. Different anti-HCV profiles of statins and their potential for combination therapy with interferon. Hepatology 2006;44:117-125.

33. Ye, Wang, Sumpter, Brown, Goldstein, Gale. Disruption of hepatitis C virus RNA replication through inhibition of host protein geranylgeranylation. Proc Natl Acad Sci USA 2003;100:15865-15870.

34. Wang, Gale, Keller, Huang, Brown, Goldstein, Ye. Identification of FBL2 as a geranylgeranylated cellular protein required for hepatitis C virus RNA replication. Molecular Cell 2005;18:425-434.

35. Su A, Pezacki, Wodicka, Brideau, Supekova L, Thimme, Wieland, et al. Genomic analysis of the host response to hepatitis C virus infection. Proc Natl Acad Sci USA 2002;99:15669-15674.

36. Pietschmann T, Kaul A, Koutsoudakis G, Shavinskaya A, Kallis S, Steinmann E, Abid K, et al. Construction and characterization of infectious intragenotypic and intergenotypic hepatitis C virus chimeras. Proc Natl Acad Sci USA 2006;103:7408-7413.

37. Zhong, Gastaminza, Cheng, Kapadia S, Kato T, Burton DR, Wieland SF, et al. Robust hepatitis C virus infection in vitro. Proc Natl Acad Sci USA 2005;102:9294-9299.

38. Huang, Sun, Owen, Li, Chen, Gale, Ye. Hepatitis C virus production by human hepatocytes dependent on assembly and secretion of very low-density lipoproteins. Proc Natl Acad Sci USA 2007;104:5848-5853.

39. Gastaminza, Kapadia, Chisari. Differential biophysical properties of infectious intracellular and secreted hepatitis C virus particles. Journal of Virology 2006;80:11074-11081.

40. Negro F. Mechanisms and significance of liver steatosis in hepatitis C virus infection. World J Gastroenterol 2006;12:6756-6765.

41. Yang W, Hood BL, Chadwick SL, Liu S, Watkins SC, Luo G, Conrads TP, et al. Fatty acid synthase is up-regulated during hepatitis C virus infection and regulates hepatitis C virus entry and production. Hepatology 2008;48:1396-1403.

42. Park, Jun HJ, Wakita T, Cheong JH, Hwang SB. Hepatitis C virus nonstructural 4B protein modulates SREBP signaling via AKT pathway. J Biol Chem 2009.

43. Moriishi K, Mochizuki R, Moriya K, Miyamoto H, Mori Y, Abe T, Murata S, et al. Critical role of PA28gamma in hepatitis C virus-associated steatogenesis and hepatocarcinogenesis. Proc Natl Acad Sci USA 2007;104:1661-1666.

44. Gronemeyer, Gustafsson, Laudet. Principles for modulation of the nuclear receptor superfamily. Nat Rev Drug Discov 2004;3:950-964.

45. Tsutsumi T, Suzuki T, Shimoike T, Suzuki R, Moriya K, Shintani Y, Fujie H, et al. Interaction of hepatitis C virus core protein with retinoid X receptor alpha modulates its transcriptional activity. Hepatology 2002;35:937-946.

46. Yamaguchi A, Tazuma S, Nishioka T, Ohishi W, Hyogo H, Nomura S, Chayama K. Hepatitis C virus core protein modulates fatty acid metabolism and thereby causes lipid accumulation in the liver. Dig Dis Sci 2005;50:1361-1371.

47. Kim, Kim, Kim, Cheong. Hepatitis B virus X protein induces lipogenic transcription factor SREBP1 and fatty acid synthase through the activation of nuclear receptor LXRalpha. Biochem J 2008;416:219-230.

48. Na, Shin, Roh, Kang, Hong, Oh, Seong, et al. Liver X receptor mediates hepatitis B virus X protein-induced lipogenesis in hepatitis B virus-associated hepatocellular carcinoma. Hepatology 2008.

49. Blasiole, Davis, Attie. The physiological and molecular regulation of lipoprotein assembly and secretion. Molecular BioSystems 2007.

50. Ikonen E. Cellular cholesterol trafficking and compartmentalization. Nat Rev Mol Cell Biol 2008;9:125-138.

51. Gronemeyer H, Gustafsson JA, Laudet V. Principles for modulation of the nuclear receptor superfamily. Nat Rev Drug Discov 2004;3:950-964.

52. Ory DS. Nuclear receptor signaling in the control of cholesterol homeostasis: have the orphans found a home? Circulation Research 2004;95:660-670.

53. Wurtz JM, Bourguet W, Renaud JP, Vivat V, Chambon P, Moras D, Gronemeyer H. A canonical structure for the ligand-binding domain of nuclear receptors. Nat Struct Biol 1996;3:87-94.

54. McKenna, O'Malley. Combinatorial Control of Gene Expression by Nuclear Receptors and Coregulators. Cell 2002.

55. Rochette-Egly. Nuclear receptors: integration of multiple signalling pathways through phosphorylation. Cellular Signalling 2003.

56. Tobin, Steineger, Alberti, Spydevold, Auwerx, Gustafsson, Nebb. Cross-talk between fatty acid and cholesterol metabolism mediated by liver X receptor-alpha. Molecular Endocrinology 2000;14:741-752.

57. Yoshikawa, Ide, Shimano, Yahagi, Amemiya-Kudo, Matsuzaka, Yatoh, et al. Cross-talk between peroxisome proliferator-activated receptor (PPAR) alpha and liver X receptor (LXR) in nutritional regulation of fatty acid metabolism. I. PPARs suppress sterol regulatory element binding protein-1c promoter through inhibition of LXR signaling. Molecular Endocrinology 2003;17:1240-1254.

58. Ide, Shimano, Yoshikawa, Yahagi, Amemiya-Kudo, Matsuzaka, Nakakuki, et al. Cross-talk between peroxisome proliferator-activated receptor (PPAR) alpha and liver X receptor (LXR) in nutritional regulation of fatty acid metabolism. II. LXRs suppress lipid degradation gene promoters through inhibition of PPAR signaling. Molecular Endocrinology 2003;17:1255-1267.

59. Xu HE, Stanley TB, Montana VG, Lambert MH, Shearer BG, Cobb JE, McKee DD, et al. Structural basis for antagonist-mediated recruitment of nuclear co-repressors by PPARalpha. Nature 2002;415:813-817.

60. Reschly EJ, Ai N, Welsh WJ, Ekins S, Hagey LR, Krasowski MD. Ligand specificity and evolution of liver X receptors. J Steroid Biochem Mol Biol 2008;110:83-94.

61. Xu HE, Lambert MH, Montana VG, Plunket KD, Moore LB, Collins JL, Oplinger JA, et al. Structural determinants of ligand binding selectivity between the peroxisome proliferator-activated receptors. Proc Natl Acad Sci U S A 2001;98:13919-13924.

62. Nolte RT, Wisely GB, Westin S, Cobb JE, Lambert MH, Kurokawa R, Rosenfeld MG, et al. Ligand binding and co-activator assembly of the peroxisome proliferator-activated receptor-gamma. Nature 1998;395:137-143.

63. Farnegardh M, Bonn T, Sun S, Ljunggren J, Ahola H, Wilhelmsson A, Gustafsson JA, et al. The three-dimensional structure of the liver X receptor beta reveals a flexible ligand-binding pocket that can accommodate fundamentally different ligands. J Biol Chem 2003;278:38821-38828.

64. Laudet V, H. G, editors. The nuclear receptor factsbook: Academic Press; 2002.

65. Jordan VC. Antiestrogens and selective estrogen receptor modulators as multifunctional medicines. 2. Clinical considerations and new agents. J Med Chem 2003;46:1081-1111.

66. Jordan VC. Antiestrogens and selective estrogen receptor modulators as multifunctional medicines. 1. Receptor interactions. J Med Chem 2003;46:883-908.

67. Chang F, Jaber LA, Berlie HD, O'Connell MB. Evolution of peroxisome proliferator-activated receptor agonists. Ann Pharmacother 2007;41:973-983.

68. Gervois P, Fruchart J, Staels B. Drug Insight: mechanisms of action and therapeutic applications for agonists of peroxisome proliferator-activated receptors. Nature clinical practice Endocrinology & metabolism 2007;3:145-156.

69. Li, Glass. PPAR- and LXR-dependent pathways controlling lipid metabolism and the development of atherosclerosis. The Journal of Lipid Research 2004.

70. Mittra, Bansal, Bhatnagar. From a glucocentric to a lipocentric approach towards metabolic syndrome. Drug Discovery Today 2008.

71. Guillou, Martin, Pineau. Transcriptional regulation of hepatic fatty acid metabolism. Subcell Biochem 2008;49:3-47.

72. Lee, Olson, Evans. Minireview: lipid metabolism, metabolic diseases, and peroxisome proliferator-activated receptors. Endocrinology 2003;144:2201-2207.

73. Martin, Guillou, Lasserre, Déjean, Lan, Pascussi, Sancristobal, et al. Novel aspects of PPARalpha-mediated regulation of lipid and xenobiotic metabolism revealed through a nutrigenomic study. Hepatology 2007;45:767-777.

74. Raalte v, Li, Pritchard, Wasan. Peroxisome proliferator-activated receptor (PPAR)-alpha: a pharmacological target with a promising future. Pharm Res 2004;21:1531-1538.

75. Smith SA. Peroxisome proliferator-activated receptors and the regulation of mammalian lipid metabolism. Biochem Soc Trans 2002;30:1086-1090.

76. Vuppalanchi R, Chalasani N. Nonalcoholic fatty liver disease and nonalcoholic steatohepatitis: Selected practical issues in their evaluation and management. Hepatology 2009;49:306-317.

77. Millatt, Bocher, Fruchart, Staels B. Liver X receptors and the control of cholesterol homeostasis: potential therapeutic targets for the treatment of atherosclerosis. Biochim Biophys Acta 2003;1631:107-118.

78. Mitro, Mak, Vargas, Godio, Hampton, Molteni, Kreusch, et al. The nuclear receptor LXR is a glucose sensor. Nature 2007;445:219-223.

79. Edwards, Kennedy, Mak. LXRs; oxysterol-activated nuclear receptors that regulate genes controlling lipid homeostasis. Vascul Pharmacol 2002;38:249-256.

80. Forman, Ruan, Chen, Schroepfer, Evans. The orphan nuclear receptor LXRalpha is positively and negatively regulated by distinct products of mevalonate metabolism. Proc Natl Acad Sci USA 1997;94:10588-10593.

81. Venkateswaran, Laffitte, Joseph, Mak, Wilpitz, Edwards, Tontonoz. Control of cellular cholesterol efflux by the nuclear oxysterol receptor LXR alpha. Proc Natl Acad Sci USA 2000;97:12097-12102.

82. Yoshikawa, Shimano, Amemiya-Kudo, Yahagi, Hasty, Matsuzaka, Okazaki, et al. Identification of liver X receptor-retinoid X receptor as an activator of the sterol regulatory element-binding protein 1c gene promoter. Molecular and Cellular Biology 2001;21:2991-3000.

83. Pawar, Botolin, Mangelsdorf, Jump. The Role of Liver X Receptor-α in the Fatty Acid Regulation of Hepatic Gene Expression. Journal of Biological Chemistry 2003.

84. Vega RB, Huss JM, Kelly DP. The coactivator PGC-1 cooperates with peroxisome proliferator-activated receptor alpha in transcriptional control of nuclear genes

encoding mitochondrial fatty acid oxidation enzymes. Molecular and Cellular Biology 2000;20:1868-1876.

85. Son YL, Lee YC. Molecular determinants of the interactions between LXR/RXR heterodimers and TRAP220. Biochem Biophys Res Commun 2009;384:389-393.

86. Miyata, McCaw, Patel, Rachubinski, Capone. The orphan nuclear hormone receptor LXR alpha interacts with the peroxisome proliferator-activated receptor and inhibits peroxisome proliferator signaling. J Biol Chem 1996;271:9189-9192.

87. Laffitte, Joseph, Walczak, Pei, Wilpitz, Collins, Tontonoz. Autoregulation of the human liver X receptor alpha promoter. Molecular and Cellular Biology 2001;21:7558-7568.

88. Hu, Li, Wu, Xia, Lala. Liver X receptors interact with corepressors to regulate gene expression. Molecular Endocrinology 2003;17:1019-1026.

89. Wilcox, Borradaile, Huff. Antiatherogenic Properties of Naringenin, a Citrus Flavonoid. Cardiovascular Drug Reviews 1999.

90. Fuhr U, Kummert AL. The fate of naringin in humans: a key to grapefruit juice-drug interactions? Clin Pharmacol Ther 1995;58:365-373.

91. Wilcox LJ, Borradaile NM, Huff MW. Antiatherogenic Properties of Naringenin, a Citrus Flavonoid. Cardiovascular Drug Reviews 1999.

92. Wilcox, Borradaile, Dreu d, Huff. Secretion of hepatocyte apoB is inhibited by the flavonoids, naringenin and hesperetin, via reduced activity and expression of ACAT2 and MTP. J Lipid Res 2001;42:725-734.

93. Borradaile, Dreu d, Barrett, Huff. Inhibition of hepatocyte apoB secretion by naringenin: enhanced rapid intracellular degradation independent of reduced microsomal cholesteryl esters. J Lipid Res 2002;43:1544-1554.

94. Allister, Borradaile, Edwards, Huff. Inhibition of microsomal triglyceride transfer protein expression and apolipoprotein B100 secretion by the citrus flavonoid naringenin and by insulin involves activation of the mitogen-activated protein kinase pathway in hepatocytes. Diabetes 2005;54:1676-1683.

95. Borradaile, Dreu d, Huff. Inhibition of net HepG2 cell apolipoprotein B secretion by the citrus flavonoid naringenin involves activation of phosphatidylinositol 3-kinase, independent of insulin receptor substrate-1 phosphorylation. Diabetes 2003;52:2554-2561.

96. Gillian-Daniel DL, Bates PW, Tebon A, Attie AD. Endoplasmic reticulum localization of the low density lipoprotein receptor mediates presecretory degradation of apolipoprotein B. Proc Natl Acad Sci USA 2002;99:4337-4342.

97. Twisk J, Gillian-Daniel DL, Tebon A, Wang L, Barrett PH, Attie AD. The role of the LDL receptor in apolipoprotein B secretion. Journal of Clinical Investigation 2000;105:521-532.

98. Jeon SM, Kim HK, Kim HJ, Do GM, Jeong TS, Park YB, Choi MS. Hypocholesterolemic and antioxidative effects of naringenin and its two metabolites in high-cholesterol fed rats. Transl Res 2007;149:15-21.

99. Huong DT, Takahashi Y, Ide T. Activity and mRNA levels of enzymes involved in hepatic fatty acid oxidation in mice fed citrus flavonoids. Nutrition (Burbank, Los Angeles County, Calif) 2006;22:546-552.

100. Allister EM, Borradaile NM, Edwards JY, Huff MW. Inhibition of microsomal triglyceride transfer protein expression and apolipoprotein B100 secretion by the citrus flavonoid naringenin and by insulin involves activation of the mitogen-activated protein kinase pathway in hepatocytes. Diabetes 2005;54:1676-1683.

101. Huang TH, Teoh AW, Lin BL, Lin DS, Roufogalis B. The role of herbal PPAR modulators in the treatment of cardiometabolic syndrome. Pharmacol Res 2009;60:195-206.

102. Liu, Shan, Zhang, Ning, Lu, Cheng. Naringenin and hesperetin, two flavonoids derived from Citrus aurantium up-regulate transcription of adiponectin. Phytotherapy research : PTR 2008;22:1400-1403.

103. Crozier A, Jaganath IB, Clifford MN. Dietary phenolics: chemistry, bioavailability and effects on health. Natural product reports 2009;26:1001-1043.

104. Kanaze, Bounartzi, Georgarakis, Niopas. Pharmacokinetics of the citrus flavanone aglycones hesperetin and naringenin after single oral administration in human subjects. Eur J Clin Nutr 2006:6.

105. Winter J, Moore LH, Dowell VR, Bokkenheuser VD. C-ring cleavage of flavonoids by human intestinal bacteria. Appl Environ Microbiol 1989;55:1203-1208.

106. Erlund I, Meririnne E, Alfthan G, Aro A. Plasma kinetics and urinary excretion of the flavanones naringenin and hesperetin in humans after ingestion of orange juice and grapefruit juice. J Nutr 2001;131:235-241.

107. Choudhury R, Chowrimootoo G, Srai K, Debnam E, Rice-Evans CA. Interactions of the flavonoid naringenin in the gastrointestinal tract and the influence of glycosylation. Biochemical and Biophysical Research Communications 1999;265:410-415.

108. Nielsen SE, Breinholt V, Justesen U, Cornett C, Dragsted LO. In vitro biotransformation of flavonoids by rat liver microsomes. Xenobiotica 1998;28:389-401.

109. Ortiz-Andrade RR, Sanchez-Salgado JC, Navarrete-Vazquez G, Webster SP, Binnie M, Garcia-Jimenez S, Leon-Rivera I, et al. Antidiabetic and toxicological evaluations of naringenin in normoglycaemic and NIDDM rat models and its implications on extra-pancreatic glucose regulation. Diabetes Obes Metab 2008;10:1097-1104.

110. Booth AN, Jones FT, Deeds F. Metabolic and glucosuria studies on naringin and phloridzin. J Biol Chem 1958;233:280-282.

111. U.S. Food and Drug Administration C. Guidance for Industry: Bioavailability and Bioequivalence Studies for Orally Administered Drug Products--General Considerations. In: Research USFaDACfDEa, editor.: Office of Training and Communications, Division of Communications Management, Drug Information Branch; 2003.

112. Stella VJ, He Q. Cyclodextrins. Toxicol Pathol 2008;36:30-42.

113. Miyake, Arima, Hirayama, Yamamoto, Horikawa, Sumiyoshi, Noda, et al. Improvement of solubility and oral bioavailability of rutin by complexation with 2-hydroxypropyl-beta-cyclodextrin. Pharmaceutical development and technology 2000;5:399-407.

114. Carrier RL, Miller LA, Ahmed I. The utility of cyclodextrins for enhancing oral bioavailability. J Control Release 2007;123:78-99.

115. Loftsson T, Vogensen SB, Brewster ME, Konrádsdóttir F. Effects of cyclodextrins on drug delivery through biological membranes. Journal of pharmaceutical sciences 2007;96:2532-2546.

116. Challa R, Ahuja A, Ali J, Khar RK. Cyclodextrins in drug delivery: an updated review. AAPS PharmSciTech 2005;6:E329-357.

2 Apolipoprotein B-dependent hepatitis C virus secretion is inhibited by the grapefruit flavonoid naringenin

2.1 Introduction

HCV has long been known to associate with circulating lipoproteins (1), and its interactions with the cholesterol and lipid pathways have been recently described (2). In this work, we demonstrate that HCV is actively secreted by infected cells through a Golgi-dependent mechanism while bound to very low density lipoprotein (VLDL). Silencing apolipoprotein B (ApoB) messenger RNA in infected cells causes a 70% reduction in the secretion of both ApoB-100 and HCV. More importantly, we demonstrate that the grapefruit flavonoid naringenin, previously shown to inhibit VLDL secretion both in vivo and in vitro, inhibits the microsomal triglyceride transfer protein activity as well as the transcription of 3-hydroxy-3-methyl-glutaryl-coenzyme A reductase and acyl-coenzyme A:cholesterol acyltransferase 2 in infected cells. Stimulation with naringenin reduces HCV secretion in infected cells by 80%. Moreover, we find that naringenin is effective at concentrations that are an order of magnitude below the toxic threshold in primary human hepatocytes and in mice.

2.2 Results

2.2.1 Huh7.5.1-Secreted HCV Is Bound to ApoB

Recent evidence suggests that HCV binds to low-density particles prior to virus egress (3) and that viral secretion requires both ApoB expression and VLDL assembly to occur (4). Therefore, HCV secreted by the JFH1/Huh7.5.1 full viral lifecycle model could potentially be secreted while bound to VLDL. To determine if Huh7.5.1-produced HCV is bound to VLDL, we immunoprecipitated the Huh7.5.1-conditioned medium against human ApoB antibodies and detected bound HCV core protein in the eluted sample. The results presented in **Figure 1a** demonstrate that HCV core protein is bound to ApoB-100 in our samples. HCV core could not be detected when the sample was precipitated against irrelevant antibody (control) but was easily detected in the cell medium (JFH1).

2.2.2 HCV Secretion Mirrors That of VLDL

The interaction between HCV and ApoB suggests that the virus is be actively secreted by the cells while bound to VLDL. However, the interaction between these particles might also occur outside the cell. To determine if HCV is being actively secreted by the cells while bound to VLDL, we studied viral secretion in response to oleate and insulin stimulation, which have previously shown to oppositely modulate ApoB secretion in culture (5). **Figure 1b** shows ApoB, HCV core, and HCV-positive strand RNA secretion by Huh7.5.1 cells infected with the JFH-1 virus. As expected, ApoB secretion is significantly up-regulated by oleate ($p=0.002$) and down-regulated by insulin ($p=0.007$) in a dose-dependent manner. Similarly, HCV core protein secretion is significantly up-regulated by oleate ($p=0.007$) and down-regulated by insulin ($p = 0.02$) in a dose-dependent manner. The secretion of HCV-positive strand RNA, measured by qRT-PCR, follows the same path. However, intracellular levels of HCV RNA remained unchanged following both treatments.

Brefeldin A is a commonly used toxin that disrupts communication between the endoplasmic reticulum and the Golgi, inhibiting the active secretion of proteins (5-7). Not surprisingly, the addition of brefeldin A (2.5 g/mL) blocked ApoB secretion ($p=0.0001$). Interestingly, brefeldin A significantly inhibits the secretion of HCV core protein ($p=0.002$) and HCV-positive strand RNA ($p=0.007$). To assess whether the changes in HCV core protein and RNA secretion correlate with changes of viral infectivity in the cell supernatant, we measured the ability of the secreted virus to infect naïve Huh7.5.1 cells. **Figure 1c** shows that the infectivity of the cell supernatant increased following oleate stimulation, decreased because of insulin, and was strongly inhibited following brefeldin A stimulation by 89% ± 10% ($p=0.001$). These results suggest that HCV is being actively secreted by the cells, perhaps while bound to VLDL.

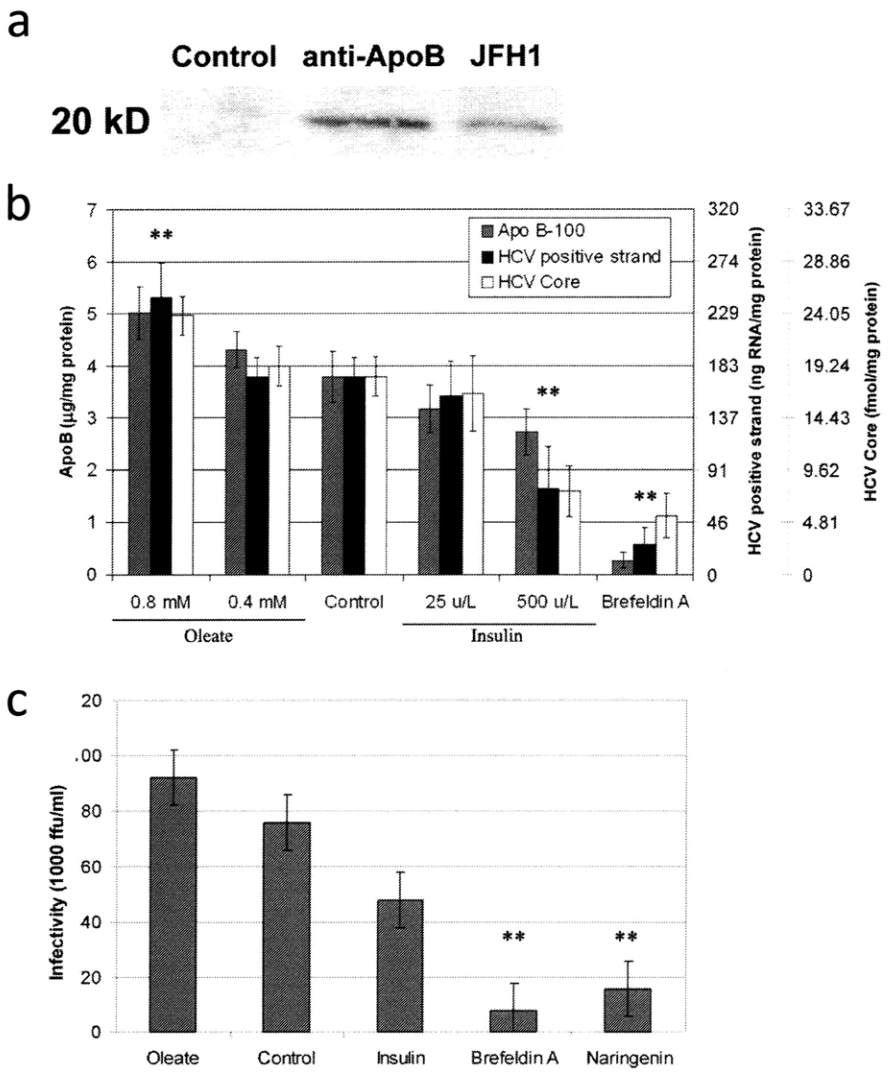

Figure 1 (A) Immunoprecipitation of Huh7.5.1-secreted ApoB followed by anti-HCV core staining (coimmunoprecipitation). (B) Cell culture secretion of ApoB, HCV-positive strand RNA, and HCV core protein in JFH-1-infected Huh7.5.1 cells in response to oleate, insulin, and brefeldin A. The secretions of ApoB, HCV RNA, and HCV core protein are significantly up-regulated by oleate and down-regulated by insulin in a dose-dependent manner. Brefeldin A, which blocks Golgi-dependent secretion of proteins, significantly inhibits the secretion of ApoB, HCV RNA, and HCV core. Cell viability for all conditions was greater than 90%. (C) Infectivity of cell culture supernatant assessed by colony formation on naïve Huh7.5.1 cells: oleate (0.8 mM), insulin (500 U/L), brefeldin A (2.5µg/mL), and naringenin (200µM). **p<0.01

2.2.3 HCV Core Antigen Colocalizes with ApoB

Previously, HCV core protein was shown to associate with ApoAII (8) and lipid droplets in HepG2 cells (9) overexpressing the core protein. Just recently, Huang et al. (4) demonstrated that HCV core protein colocalizes with ApoB in a chromosomally integrated cDNA model of HCV. To ascertain if HCV core protein associates with ApoB in JFH-1 virus-infected Huh7.5.1 cells, we double-stained Huh7.5.1 cells 2 days post infection by immunofluorescence for both viral and native proteins. **Figure 2** demonstrates the colocalization of HCV's core and ApoB100 in infected cells. HCV core protein associates with areas in the cytoplasm that are positive for ApoB100. However, we note that although the proteins appear to be closely associated, we fail to find a one-to-one correspondence between the viral and native proteins in our model of the full viral lifecycle.

The association between ApoB100 and HCV core protein as well as previous data suggests that HCV might be tagging along ApoB secretion. Therefore, silencing ApoB production in the cell might decrease HCV secretion. **Figure 2d** demonstrates a 69% ± 6% decrease in ApoB secretion following transfection with SureSilencing shRNA ($P = 0.0001$). Interestingly, HCV core protein secretion was significantly decreased by 75% ± 4% at the same time ($P = 0.0002$). HCV-positive strand RNA secretion was also significantly decreased by 69% ± 4% ($P = 0.0015$).

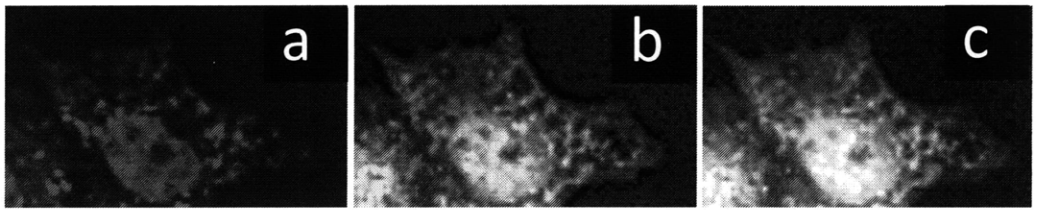

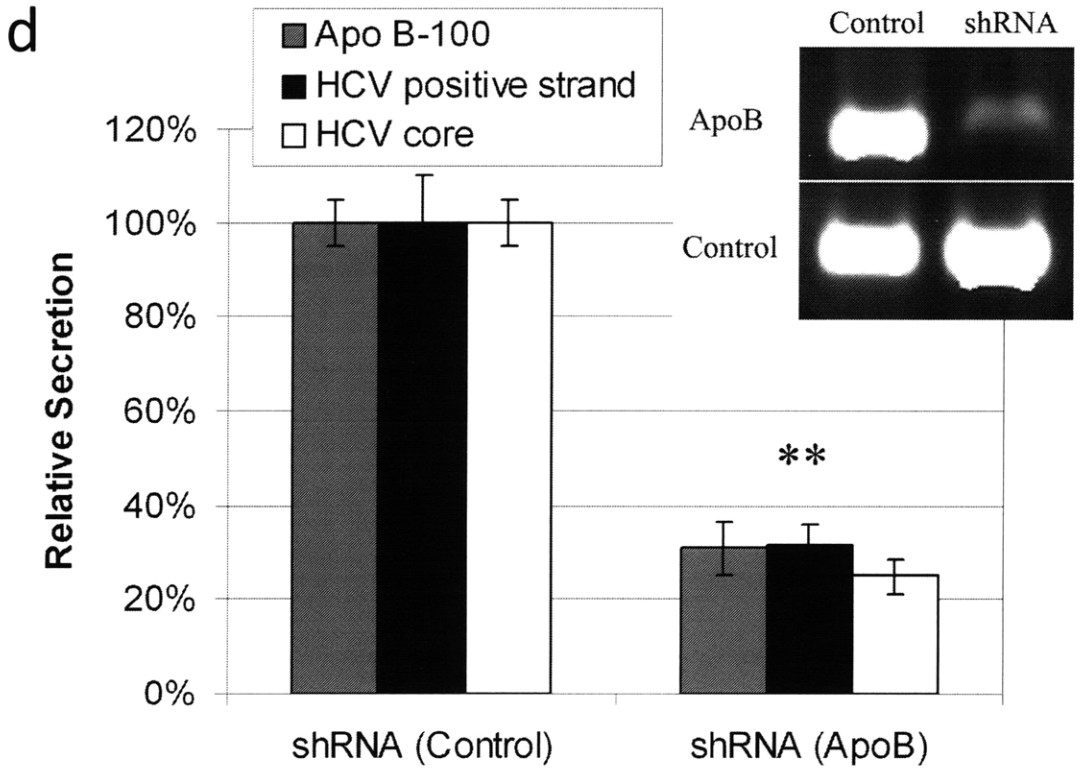

Figure 2 - Double immunofluorescence staining of JFH-1-infected Huh7.5.1 cells. (A) Staining for HCV core protein (red). (B) Staining for ApoB100 (green). (C) Superpositioning of the images demonstrates that HCV core protein associates with ApoB100 in the cytoplasm. (D) Relative secretion of ApoB, HCV-positive strand RNA, and HCV core protein in JFH-1-infected Huh7.5.1 cells following silencing of ApoB100 mRNA by SureSilencing shRNA transfection. **p<0.01.

2.2.4 HCV Secretion Is Inhibited by Naringenin

Naringenin is a grapefruit flavonoid previously shown to reduce cholesterol levels both *in vivo* (10-13) and *in vitro* (14-16). It is thought that naringenin inhibits ApoB secretion by reducing the activity and expression of MTP and ACAT (14, 16). To assess if naringenin inhibits HCV secretion in a similar manner, we cultured infected Huh7.5.1 cells in the presence of naringenin for 24 hours. **Figure 3a** demonstrates that naringenin inhibits the secretion of HCV core ($p=0.0001$) and HCV-positive strand RNA ($p=0.0006$) in a dose-dependent manner. At the concentration of 200μM, naringenin inhibited HCV secretion by 80% ± 10%. Interestingly, intracellular levels of HCV-positive strand RNA (**Figure 3c**) remained unchanged. To assess whether the naringenin-induced inhibition of HCV core protein and RNA secretion correlated with changes of viral infectivity in the cell supernatant, we measured the ability of the secreted virus to infect naïve Huh7.5.1 cells. **Figure 1c** shows that the infectivity of the cell supernatant was strongly inhibited following naringenin stimulation by 79% ± 10% ($p=0.002$).

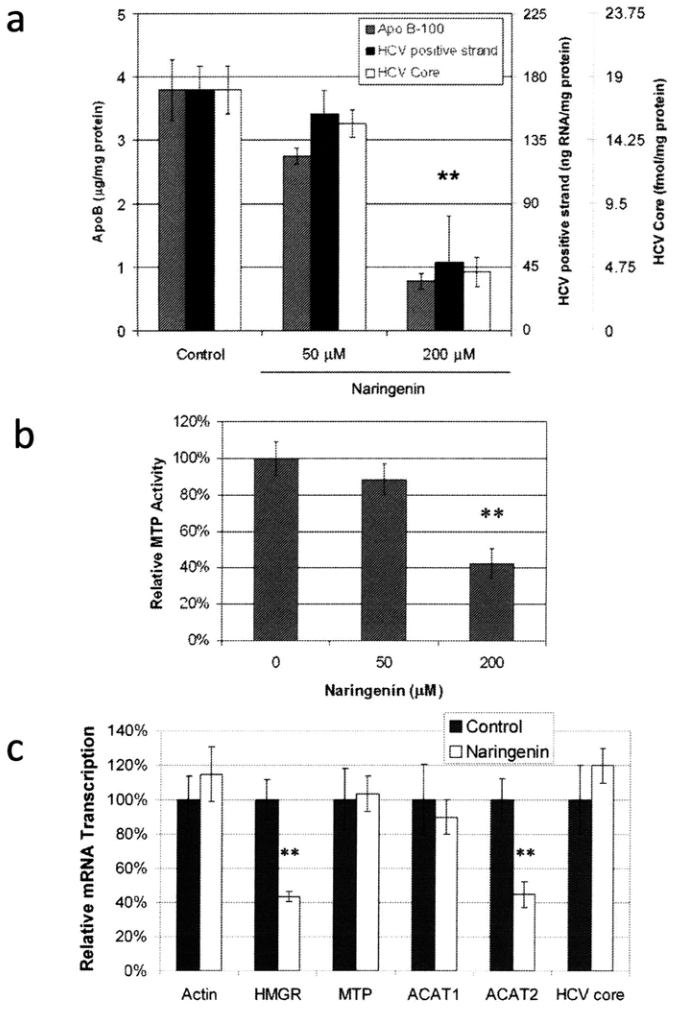

Figure 3 - (a) Inhibition of ApoB, HCV-positive strand RNA, and HCV core protein secretion by the grapefruit flavonoid naringenin. Naringenin significantly inhibits the secretion of HCV core (p=0.0001) and HCV-positive strand RNA (p=0.0006) in a dose-dependent manner. At the concentration of 200µM, naringenin inhibited HCV secretion by 80% ± 10%. Cell viability for all conditions was greater than 90%. **p<0.01. (b) Naringenin inhibits the activity of MTP in a dose-dependent manner. At the concentration of 200µM, MTP activity was reduced by 58% ± 8% (p=0.001). (c) Naringenin induces changes in hepatic gene transcription measured by qRT-PCR. HMGR transcription was reduced by 57% ± 3% (p=0.01), whereas the transcription of ACAT2 was reduced by 55% ± 7% (p=0.016). The mRNA levels of actin, MTP, and ACAT1 remained unchanged. Intracellular RNA levels of HCV core also remained unchanged during the 24 hours of treatment. **p<0.02.

2.2.5 Naringenin Does Not Display Hepatic or In Vivo Toxicity

To assess the potential of naringenin-based treatment, we measured ApoB secretion in primary human hepatocytes following 24 hours of stimulation with naringenin. **Figure 4a** demonstrates a dose-dependent decrease in ApoB secretion following naringenin stimulation. At 200μM naringenin, ApoB secretion was reduced by 60% ± 7% (p=0.007). The viability of primary human hepatocytes exposed to increasing concentrations of naringenin is shown in **Figure 4b**. Human hepatocyte viability was 81% ± 3% at 200μM naringenin and was not judged to be statistically different than that of the control (78% ± 3%). Human hepatocyte viability dropped significantly only at naringenin concentrations greater than 1000μM.

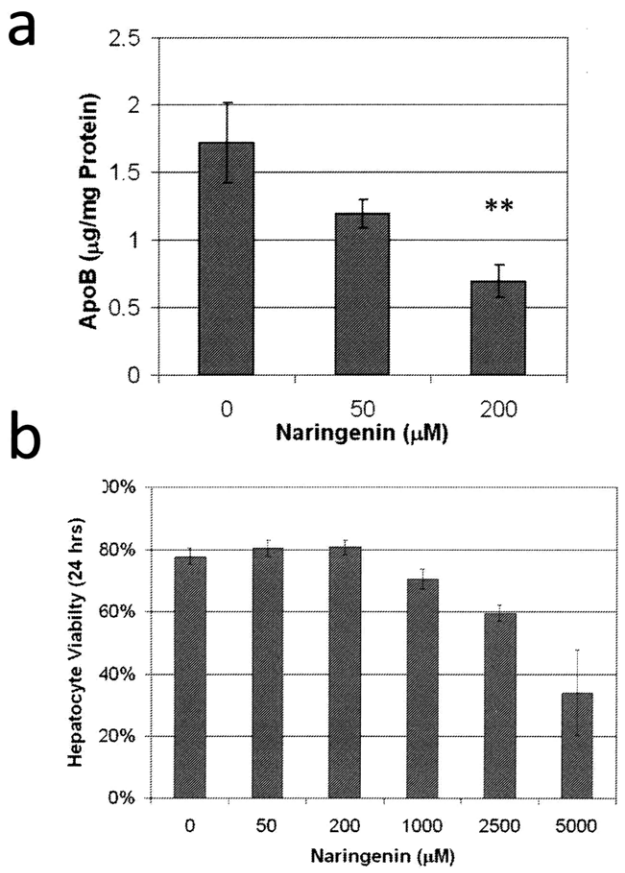

Figure 4 - (a) Naringenin stimulation inhibits ApoB secretion of primary human hepatocytes in a dose-dependent manner. At 200µM naringenin, ApoB secretion was reduced by 60% ± 7% (p=0.007). (b) Viability of freshly isolated human hepatocytes exposed to increasing concentrations of naringenin for 24 hours. Human hepatocyte viability was 81% ± 3% at 200µM naringenin and was not judged to be statistically different than the control (77% ± 3%). Human hepatocyte viability dropped significantly only at naringenin concentrations greater than 1000µM.

To further assess naringenin potential, we delivered naringenin by intraperitoneal injection to 8-week-old male SCID mice at concentrations of 60, 300, and 1500 mg/kg (approximately 200, 1000, and 5000 M). Animal survival was not affected by naringenin at these doses. To discern if liver damage occurred, we measured levels of AST and ALT in the animals' plasma 48 hours following injection. **Figure 5a** demonstrates that there was no elevation of ALT levels under all conditions. AST levels appeared to increase but remained under 100 U/L even at the highest dose. To assess naringenin's ability to reduce circulating VLDL levels, we measured total triglyceride levels in animal plasma. **Figure 5b** demonstrates a decrease in triglycerides following naringenin injection.

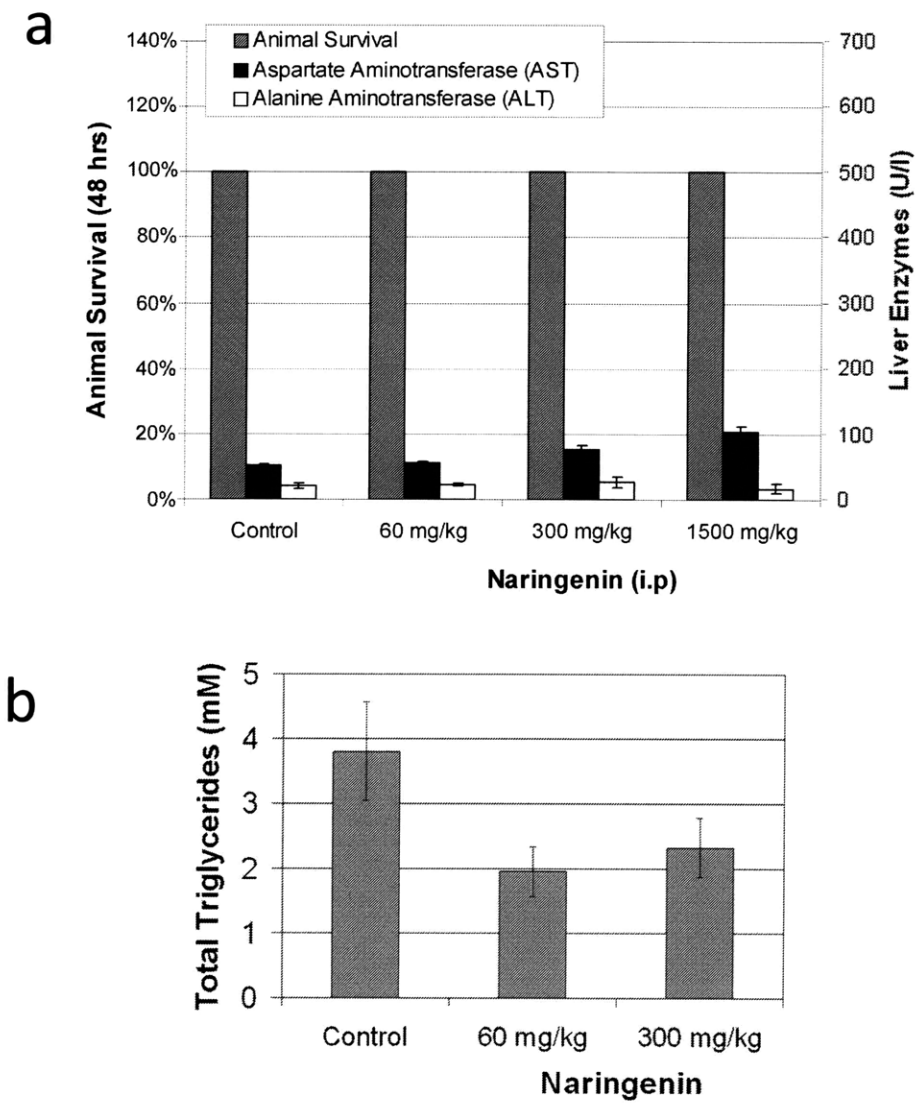

Figure 5 - Animal survival and liver enzyme release following intraperitoneal (i.p.) injection of naringenin into 8-week-old male SCID mice. Animals were injected with naringenin at 60, 300, and 1500 mg/kg of body weight. Animals were sacrificed at 48 hours, at which time liver enzymes (AST and ALT) and total triglycerides were analyzed in the animals' plasma. (a) Animal survival was monitored for several days following injection and was not affected even at the highest dose (1500 mg/kg). The ALT level appeared unchanged over all conditions, whereas AST was found to be slightly elevated at the highest dose. (b) Total triglycerides analyzed in animal plasma 24 hours following injection decreased in response to naringenin.

2.3 Discussion

The recent development of the JFH-1 virus (17) in combination with the Huh7.5.1 cell line (18) has allowed for the efficient infection of cells and the generation of large virus titers in culture. This model allows for the identification of intercellular infectious HCV particles with a higher density than that of their secreted counterparts (3), suggesting the binding of HCV to low-density particles in the endoplasmic reticulum. Just recently, Huang et al. (4) demonstrated that HCV assembled in ApoB and MTP enriched vesicles and that the viral secretion was dependent on both ApoB expression and VLDL assembly in a chromosomally integrated cDNA model of HCV secretion. As the association between HCV and serum lipoproteins (VLDL and LDL) is well known (19), these results strongly suggest that HCV might hitch a ride on the lipoprotein-cholesterol lifecycle. This hypothesis is intriguing as it might explain the presence of HCV in intestinal cells, a second site of lipoprotein production (20). In addition, it might explain HCV uptake by LDL receptor (21, 22), scavenger receptor class B type I (23), and heparin sulfate (24).

Our results strongly support this hypothesis. We demonstrate that HCV produced by the Huh7.5.1 cell line is bound to ApoB and that its secretion is inhibited by brefeldin A, a metabolite of the fungus *Eupenicillium brefeldianum*, which blocks the communication between the endoplasmic reticulum and the Golgi apparatus, effectively inhibiting protein secretion (5-7). We also demonstrate that HCV secretion is up-regulated by the fatty acid oleate and down-regulated by insulin, precisely mirroring ApoB secretion by the cells (5). Moreover, silencing ApoB100 mRNA caused a significant and parallel decrease in HCV core protein secretion. This ApoB-dependent HCV secretion pathway suggests a novel therapeutic approach for the treatment of HCV infection.

The ability of naringenin, or its glycosylated form, to significantly reduce plasma cholesterol levels has been demonstrated both *in vivo* (10-13) and *in vitro* (14-16). Our

results demonstrate that short-term (24-hour) stimulation of infected hepatocytes with 200μM naringenin significantly inhibits HCV secretion by 80% ± 10% and the infectivity of the titer by 79% ± 10%. At the same time, transcription of the viral RNA remains unchanged. We suggest that this is due in part to the inhibition of MTP activity by 58% ± 8% as well as the inhibition of HMGR and ACAT2 transcription. To further demonstrate naringenin as a potential therapy, we show that the compound is nontoxic to freshly isolated human hepatocytes up to concentrations greater than 1000μM. In addition, we demonstrate that naringenin induced a 60% ± 7% decrease in ApoB secretion by primary human hepatocytes.

The concept of supplementing HCV patients' diets with naringenin is appealing. A recent clinical trial in hypercholesterolemic patients demonstrated that a low dose of naringin (400 mg/day) lowered LDL levels by 17% (25). A similar cholesterol-lowering effect of naringenin was demonstrated in rabbits (10, 11) and rats (26). However, it is worth noting that the absorbance of naringenin through the intestinal wall is limited (less than 8%). Prior studies have suggested that the Medium Lethal Dose LD50 for naringenin is >5000 mg/kg for rats by intragastric administration (27). Our results show that doses up to 1500 mg/kg naringenin given by intraperitoneal injection to mice did not cause death or a marked elevation of liver enzymes, suggesting that intravenous administration of naringenin is in the realm of possibility.

The ability of the liver to regenerate in the context of the RNA-based lifecycle of HCV allows for the potential clearance of the viral infection. It is thought that clearance occurs in about 15-25% of HCV-infected patients. The possible reduction of HCV viral load by inhibiting viral secretion could allow uninfected cells to regenerate, potentially increasing the overall rate of viral clearance.

2.4 Materials and methods

Reagents and Antibodies

Fetal bovine serum (FBS), phosphate-buffered saline (PBS), Dulbecco's modified Eagle medium (DMEM), penicillin, streptomycin, and trypsin-ethylene diamine tetraacetic acid (EDTA) were obtained from Invitrogen Life Technologies (Carlsbad, CA). Lipoprotein-free FBS was purchased from Biomedical Technologies (Stoughton, MA). Insulin was obtained from Eli-Lilly (Indianapolis, IN). Oleate, naringenin, and brefeldin A were purchased from Sigma-Aldrich Chemicals (St. Louis, MO). Immunofluorescence-grade paraformaldehyde was purchased from Electron Microscope Sciences (Hatfield, PA). OptiMEM I basal medium and Lipofectamine 2000 were purchased from Invitrogen Life Technologies. The SureSilencing shRNA plasmid kit for human ApoB [green fluorescent protein (GFP)] was purchased from SuperArray (Frederick, MD). An MTP fluorescent activity kit was purchased from Roar Biomedical (New York, NY). Unless otherwise noted, all other chemicals were purchased from Sigma-Aldrich Chemicals. For immunoprecipitation, Protein A-Sepharose was purchased from Invitrogen, whereas horseradish peroxidase-conjugated goat anti-mouse secondary was purchased from Santa Cruz Biotech (Santa Cruz, CA). For immunofluorescence studies, normal donkey serum and secondary F(ab')2 antibody fragments (multiple-labeling [ML] grade) were obtained from Jackson Immunoresearch (Bar Harbor, ME). Mouse anti-HCV core antigen (5 μg/mL) was purchased from US Biological (Swampscott, MA). Goat anti-ApoB (10 μg/mL) was purchased from R&D Systems, Inc. (Minneapolis, MN).

Cells and Viruses

The Huh7.5.1 human hepatoma cell line and a plasmid containing the JFH-1 genome were kindly provided by Dr. Chisari (Scripps Research Institute, La Jolla, CA) and Dr. Wakita (National Institute of Infectious Diseases, Tokyo, Japan), respectively. Huh7.5.1

cells were cultured in DMEM supplemented with 10% FBS, 200 units/mL penicillin, and 200 mg/mL streptomycin in a 5% CO_2-humidified incubator at 37°C. In vitro transcribed genomic JFH-1 RNA was delivered to cells by liposome-mediated transfection as described by Zhong et al. (18) Infected Huh7.5.1 cells were passaged every 3 days and used at passage <15. The presence of HCV in these cells and corresponding supernatants were determined by quantitative, reverse-transcription, polymerase chain reaction (qRT-PCR) and immunofluorescence staining. Primary human hepatocytes were purchased from BD Biosciences (San Jose, CA) and cultured on a collagen-coated 12-well plate in a C+H culture medium composed of DMEM supplemented with 10% heat-inactivated FBS, 200 U/mL penicillin/streptomycin, 7.5 μg/mL hydrocortisone, 20 ng/mL epidermal growth factor (EGF), 14 ng/mL glucagons, and 0.5 U/mL insulin. The medium was supplemented with 2% dimethyl sulfoxide for long-term culture of the primary cells.

HCV Secretion

HCV-infected Huh7.5.1 cells were plated on a 6-well plate at a density of 1×10^5 cells/cm^2 and cultured overnight in the standard medium. Prior to the beginning of the experiment, the cells were washed 3 times with PBS and cultured with DMEM containing 5% lipoprotein-free FBS. Oleate, insulin, naringenin, and brefeldin A were added at this time as described in the text. Following 24 hours of incubation, the plate was gently agitated to release mechanically bound particles, and the medium was collected, filtered to remove cellular debris, and stored at -80°C for further analysis. The attached cells were washed 3 times with PBS, harvested, pelleted, and stored at -80°C for further analysis.

Coimmunoprecipitation

The binding of Huh7.5.1-secreted JFH1 particles to ApoB was assessed with coimmunoprecipitation. Anti-human ApoB-100 antibody (5μg) was bound to 100μL of Protein A-Sepharose on ice. Three milliliters of the JFH1-infected Huh7.5.1 conditioned medium (1×10^6 cells/mL) was added to the mixture, which was subsequently rotated for 4 hours at 4°C. The sample was spun down at 10,000g in a microcentrifuge and washed 3 times with 50 mM trishydroxymethylaminomethane (Tris)-HCl (pH 7.5) containing 5

mM EDTA. Finally, the sample was eluted in 100μL of 10 mM Tris-HCl (pH 8.5) containing sodium dodecyl sulfate. The protein concentration in the eluted buffer was quantified as described later, and 20μg of protein was loaded onto a 7.5% Tris-HCL resolving gel. Resolved proteins were transferred to a polyvinylidene fluoride membrane and stained against HCV core (0.5μg/mL).

HCV Infectivity

The infectivity of the secreted HCV particles was measured as previously described (18). Naïve Huh7.5.1 cells were grown to 80% confluence and exposed to cell culture supernatants diluted 10-fold in the culture medium. Following 1 hour of incubation at 37°C, the medium was replaced, and the cells were cultured for 3 additional days. Levels of HCV infection were determined by immunofluorescence staining for HCV core protein. The viral titer is expressed as focus forming units per milliliter of supernatant.

Human ApoB Enzyme-Linked Immunosorbent Assay (ELISA)

Huh7.5.1-secreted and primary human hepatocyte-secreted ApoB was detected in the medium with the ALerCHEK, Inc. (Portland, ME), total human ApoB ELISA kit. The medium was diluted 1:10 with the specimen diluent, and the assay was carried out according to the manufacturer's directions.

HCV Core Antigen ELISA

Huh7.5.1-secreted HCV core antigen was detected in the medium with the Wako Chemicals (Cambridge, MA) ORTHO HCV antigen ELISA kit. The medium was used as is, and the assay was carried out according to the manufacturer's directions.

Total Protein Assay

The total protein content of the cells was measured with the Bio-Rad Laboratories (Hercules, CA) protein assay based on the Bardford method. Briefly, a cell pellet was lysed in 350μL of 0.1% Triton X-100, and 5μL samples were loaded onto a 96-well plate and incubated for 15 minutes with 250μL of Coomassie Blue reagent at room temperature. Absorbance was measured at 595 nm and compared to a bovine serum albumin standard.

Quantitative, Real-Time, Reverse-Transcription Polymerase Chain Reaction (PCR)

Virus samples collected in each experiment were filtered with a 0.45μm filter, and a volume of 100μL for each sample was heated at 95°C for 45 minutes. The reverse-transcription reaction step was performed on a Mastercycler epgradientS (Eppendorf) instrument using Omniscript and Sensiscript RT kits (Qiagen). Real-time PCR was performed on a Light Cycler LC-24 (Idaho Technology) using SuperScript III Platinum CellsDirect Two-Step qRT-PCR kits (Invitrogen). For the reverse-transcription step, 2μL of a sample without RNA extraction was used. For real-time PCR, 1μL of the reverse-transcription reactions was used. All reactions were performed according to the manufacturer's instructions with the primers detailed in Table 1.

Gene		Primer
HCV 5 untranslated region	Forward	5'-GCAGAAAGCGTCTAGCCATGGCGT-3'
	Reverse	5'-CTCGCAAGCACCCTATCAGGCAGT-3'
MTP	Forward	5'-GAGGTTTCTCTATGCCTGTGGATTT-3'
	Reverse	5'-CCCAGGATTAACTTCTTAGCTTCCA-3'
ACAT1	Forward	5'-CAATACAATGGTGGGTGAAGAGAAG-3'
	Reverse	5'-AAAATCTTTCCTTGTTCTGGAGGTG-3'
HMGR	Forward	5'-GACCCCTTTGCTTAGATGAAAAAGA-3'
	Reverse	5'-GGACTGGAAACGGATATAAAGGTTG-3'
Actin	Forward	5'-GTCGTACCACTGGCATTGTG-3'
	Reverse	5'-CTCTCAGCTGTGGTGGTGAA-3'
ACAT2	Forward	5'-CATGCGGGAGGCTATACAAT-3'
	Reverse	5'-GTAGATGGTGCGGAAATGCT-3

Table 1 – Primers used in qRT-PCR experiments.

Cellular Viability

The viability of both Huh7.5.1 cells and primary human hepatocytes was studied with Thermo Fisher Scientific (Waltham, MA) Infinity aspartate aminotransferase (AST) liquid reagent. Medium samples (15μL/well) were loaded onto a 96-well plate in triplicates and mixed with 150μL of the AST liquid reagent. Absorbance decay was measured at the wavelength of 340 nm with 15-second intervals in a Bio-Rad Benchmark Plus spectrophotometer. Values were normalized to the total amount of AST available per culture, which was determined by total cell lysis induced by 1% Triton X-100 for 20 minutes at room temperature. Cell viability for all conditions reported in the Results section was greater than 90%.

MTP Activity Assay

MTP activity was analyzed with an MTP assay kit as previously described (28). The assay is based on a transfer of a fluorescent signal between donor and acceptor particles due to MTP activity. Briefly, confluent Huh7.5.1 cells were stimulated with naringenin or a carrier control for 24 hours and were then washed with ice-cold PBS and scraped off the dish with a cell scraper. Samples were homogenized by sonication (3 × 5 seconds) in a buffer containing protease inhibitors. The MTP assay was performed by the incubation of 50μg of cellular protein with 10μL of donor and acceptor solutions in 250μL of total buffer (15 mM Tris, pH 7.4; 40 mM NaCl; 1 mM EDTA). The increase in the fluorescent signal was measured over 12 hours at 37°C at the excitation wavelength of 465 nm and emission wavelength of 538 nm.

Animal Studies

Male SCID mice (8 weeks old, 20-25 g) were obtained from Charles River Laboratories (Wilmington, MA). Animals were treated in accordance with National Institutes of Health guidelines and the Massachusetts General Hospital Subcommittee on Research Animal Care. The mice were allowed free access to laboratory chow and water *ad labium*. Naringenin was dissolved in 0.5% Tween 20 diluted in saline and given by intraperitoneal injection. Two days following the treatment, animals were sacrificed,

and blood was withdrawn by cardiac puncture. AST and alanine aminotransferase (ALT) enzyme levels were assessed as described previously. Total triglycerides were measured with a kit purchased from Sigma-Aldrich Chemicals according to the manufacturer's instructions.

Silencing ApoB mRNA

HCV-infected Huh7.5.1 cells were plated in T-25 tissue culture flasks at a density of 1×10^5 cells/cm^2 and cultured overnight in the standard medium. Prior to silencing, the cells were washed 3 times with PBS, and the medium was replaced with OptiMEM basal medium. SureSilencing shRNA (GFP) plasmids against human ApoB100 as well as shRNA plasmid control (500 ng/mL) were combined with Lipofectamine 2000 in OptiMEM and incubated with the cells overnight. SureSilencing shRNA plasmids code for GFP, which was used to sort the transfected Huh7.5.1 cells with FACSAria (BD Biosciences) located at the Partners AIDS Research Center. Transfected cells (10% of the total population) were sorted directly into a 12-well plate and allowed to adhere overnight. The culture medium was conditioned by the transfected cells for 24 hours and analyzed as described previously.

Immunofluorescence Microscopy

Huh7.5.1 cells were washed 3 times with PBS and fixed in 4% electron microscopy-grade paraformaldehyde for 10 minutes at room temperature. Slides were then washed with PBS and incubated in 100 mmol/L glycine for 15 minutes to saturate reactive groups. Samples were permeabilized for 15 minutes with 0.1% Triton X-100, blocked for 30 minutes with 1% bovine serum albumin and 5% donkey serum at room temperature, and stained with primary antibodies overnight at 4°C. After additional washes with PBS, samples were stained with fluorescently tagged secondary antibodies for 45 minutes at room temperature.

2.5 References

1. André, Komurian-Pradel F, Deforges S, Perret M, Berland JL, Sodoyer M, Pol S, et al. Characterization of low- and very-low-density hepatitis C virus RNA-containing particles. Journal of Virology 2002;76:6919-6928.
2. Ye. Reliance of host cholesterol metabolic pathways for the life cycle of hepatitis C virus. PLoS Pathog 2007;3:e108.
3. Gastaminza, Kapadia, Chisari. Differential biophysical properties of infectious intracellular and secreted hepatitis C virus particles. Journal of Virology 2006;80:11074-11081.
4. Huang, Sun, Owen, Li, Chen, Gale, Ye. Hepatitis C virus production by human hepatocytes dependent on assembly and secretion of very low-density lipoproteins. Proc Natl Acad Sci USA 2007;104:5848-5853.
5. Dixon JL, Ginsberg HN. Regulation of hepatic secretion of apolipoprotein B-containing lipoproteins: information obtained from cultured liver cells. J Lipid Res 1993;34:167-179.
6. Misumi Y, Miki K, Takatsuki A, Tamura G, Ikehara Y. Novel blockade by brefeldin A of intracellular transport of secretory proteins in cultured rat hepatocytes. J Biol Chem 1986;261:11398-11403.
7. Fujiwara T, Oda K, Yokota S, Takatsuki A, Ikehara Y. Brefeldin A causes disassembly of the Golgi complex and accumulation of secretory proteins in the endoplasmic reticulum. J Biol Chem 1988;263:18545-18552.
8. Sabile A, Perlemuter G, Bono F, Kohara K, Demaugre F, Kohara M, Matsuura Y, et al. Hepatitis C virus core protein binds to apolipoprotein AII and its secretion is modulated by fibrates. Hepatology 1999;30:1064-1076.
9. Barba G, Harper F, Harada T, Kohara M, Goulinet S, Matsuura Y, Eder G, et al. Hepatitis C virus core protein shows a cytoplasmic localization and associates to cellular lipid storage droplets. Proc Natl Acad Sci USA 1997;94:1200-1205.
10. Lee CH, Jeong TS, Choi YK, Hyun BH, Oh GT, Kim EH, Kim JR, et al. Anti-atherogenic effect of citrus flavonoids, naringin and naringenin, associated with

hepatic ACAT and aortic VCAM-1 and MCP-1 in high cholesterol-fed rabbits. Biochemical and Biophysical Research Communications 2001;284:681-688.

11. Kurowska EM, Borradaile, Spence JD. Hypocholesterolemic effects of dietary citrus juices in rabbits. Nutrition Research 2000.

12. Jeon SM, Kim HK, Kim HJ, Do GM, Jeong TS, Park YB, Choi MS. Hypocholesterolemic and antioxidative effects of naringenin and its two metabolites in high-cholesterol fed rats. Transl Res 2007;149:15-21.

13. Mulvihill EE, Allister EM, Sutherland BG, Telford DE, Sawyez CG, Edwards JY, Markle JM, et al. Naringenin prevents dyslipidemia, apoB overproduction and hyperinsulinemia in LDL-receptor null mice with diet-induced insulin resistance. Diabetes 2009.

14. Allister, Borradaile, Edwards, Huff. Inhibition of microsomal triglyceride transfer protein expression and apolipoprotein B100 secretion by the citrus flavonoid naringenin and by insulin involves activation of the mitogen-activated protein kinase pathway in hepatocytes. Diabetes 2005;54:1676-1683.

15. Borradaile, Dreu d, Huff. Inhibition of net HepG2 cell apolipoprotein B secretion by the citrus flavonoid naringenin involves activation of phosphatidylinositol 3-kinase, independent of insulin receptor substrate-1 phosphorylation. Diabetes 2003;52:2554-2561.

16. Wilcox, Borradaile, Dreu d, Huff. Secretion of hepatocyte apoB is inhibited by the flavonoids, naringenin and hesperetin, via reduced activity and expression of ACAT2 and MTP. J Lipid Res 2001;42:725-734.

17. Wakita T, Pietschmann T, Kato T, Date T, Miyamoto M, Zhao Z, Murthy K, et al. Production of infectious hepatitis C virus in tissue culture from a cloned viral genome. Nat Med 2005;11:791-796.

18. Zhong, Gastaminza, Cheng, Kapadia S, Kato T, Burton DR, Wieland SF, et al. Robust hepatitis C virus infection in vitro. Proc Natl Acad Sci USA 2005;102:9294-9299.

19. Thomssen R, Bonk S, Propfe C, Heermann KH, Kochel HG, Uy A. Association of hepatitis C virus in human sera with beta-lipoprotein. Med Microbiol Immunol 1992;181:293-300.

20. Deforges S, Evlashev A, Perret M, Sodoyer M, Pouzol S, Scoazec JY, Bonnaud B, et al. Expression of hepatitis C virus proteins in epithelial intestinal cells in vivo. J Gen Virol 2004;85:2515-2523.

21. Nahmias Y, Casali M, Barbe L, Berthiaume F, Yarmush ML. Liver endothelial cells promote LDL-R expression and the uptake of HCV-like particles in primary rat and human hepatocytes. Hepatology 2006;43:257-265.

22. Agnello V, Abel G, Elfahal M, Knight GB, Zhang QX. Hepatitis C virus and other flaviviridae viruses enter cells via low density lipoprotein receptor. Proc Natl Acad Sci U S A 1999;96:12766-12771.

23. Kapadia SB, Barth H, Baumert T, McKeating JA, Chisari FV. Initiation of hepatitis C virus infection is dependent on cholesterol and cooperativity between CD81 and scavenger receptor B type I. J Virol 2007;81:374-383.

24. Barth H, Schnober EK, Zhang F, Linhardt RJ, Depla E, Boson B, Cosset FL, et al. Viral and cellular determinants of the hepatitis C virus envelope-heparan sulfate interaction. J Virol 2006;80:10579-10590.

25. Jung UJ, Kim HJ, Lee JS, Lee MK, Kim HO, Park EJ, Kim HK, et al. Naringin supplementation lowers plasma lipids and enhances erythrocyte antioxidant enzyme activities in hypercholesterolemic subjects. Clinical nutrition (Edinburgh, Scotland) 2003;22:561-568.

26. Kim SY, Kim HJ, Lee MK, Jeon SM, Do GM, Kwon EY, Cho YY, et al. Naringin time-dependently lowers hepatic cholesterol biosynthesis and plasma cholesterol in rats fed high-fat and high-cholesterol diet. Journal of medicinal food 2007;9:582-586.

27. Ortiz-Andrade RR, Sanchez-Salgado JC, Navarrete-Vazquez G, Webster SP, Binnie M, Garcia-Jimenez S, Leon-Rivera I, et al. Antidiabetic and toxicological evaluations of naringenin in normoglycaemic and NIDDM rat models and its implications on extra-pancreatic glucose regulation. Diabetes Obes Metab 2008;10:1097-1104.

28. Perlemuter G, Sabile A, Letteron P, Vona G, Topilco A, Chrétien Y, Koike K, et al. Hepatitis C virus core protein inhibits microsomal triglyceride transfer protein

activity and very low density lipoprotein secretion: a model of viral-related steatosis. FASEB J 2002;16:185-194.

3 Naringenin Inhibits the Assembly and Long-Term Production of Infectious Hepatitis C Virus Particles Through a PPAR-Mediated Mechanism

3.1 Introduction

Hepatitis C virus (HCV) infection affects around 2% of the world population and is the leading cause of chronic liver disease worldwide (1). The current standard of care, a combination treatment of pegylated-interferon α and ribavirin, is effective in only 50% of the patients, is poorly tolerated, and is associated with significant side effects and the emergence of resistant strains (2). Therefore, there is a pressing need for the development of alternative treatment strategies to combat HCV infection. Recently, our group and others demonstrated that the HCV lifecycle is critically dependent on host lipid metabolism (3-6). We have shown that HCV production is metabolically modulated and suggested that the grapefruit flavonoid naringenin could prove to be an effective inhibitor of HCV production (3). Here we demonstrate that naringenin dose-dependently inhibits HCV production without affecting intracellular levels of the viral RNA or protein. We further demonstrate that naringenin blocks the assembly of intracellular infectious viral particles, upstream of viral egress. We show that this antiviral effect is mediated by the inhibition of MTP coupled with the activation of the nuclear receptors PPARα and PPARγ, leading to a decrease in VLDL production without causing lipid accumulation in the cells. Finally, long-term treatment with naringenin leads to a rapid 1.4 log reduction in secreted HCV, not significantly different than 1000 I.U. of interferon. However, during the washout period, HCV levels returned to normal, consistent with our proposed mechanism of action. The data strongly supports further investigation of naringenin in the management and care of HCV infection. The combination of naringenin with STAT-C agents could potentially bring

a rapid reduction in HCV levels during the early treatment phase, which has been associated with a better long-term outcome (7).

3.2 Results

3.2.1 Naringenin inhibits the production of ApoB and HCV

Recently, our group and others demonstrated that HCV secretion in dependent on the assembly and secretion of ApoB through an MTP mediated mechanism (3, 4). We have recently demonstrated that naringenin, a grapefruit flavonoid with demonstrated anti-inflammatory, and hypolipidemic properties blocks the production of HCV in JFH1-infected Huh7.5.1 cells (3) (8). To further characterize naringenin's antiviral activity we treated JFH1-infected Huh7.5.1 cells with increasing concentrations of naringenin for 24 hours. **Figure 1a** shows that naringenin led to a dose-dependent decrease in the secretion of ApoB and viral RNA, with an EC_{50} of 109 μM. Maximal inhibition of secretion of both ApoB and HCV RNA was 74±4% at a concentration of 200 μM. Interestingly, no change in intracellular HCV RNA was noted up to 200 μM suggesting the compound does not affect viral replication. To further explore the effects of naringenin on viral components, infected cells were treated with 200 μM naringenin for 24 hours. Treatment did not lead to an accumulation of viral core protein or viral RNA in cells (**Figure 1b**).

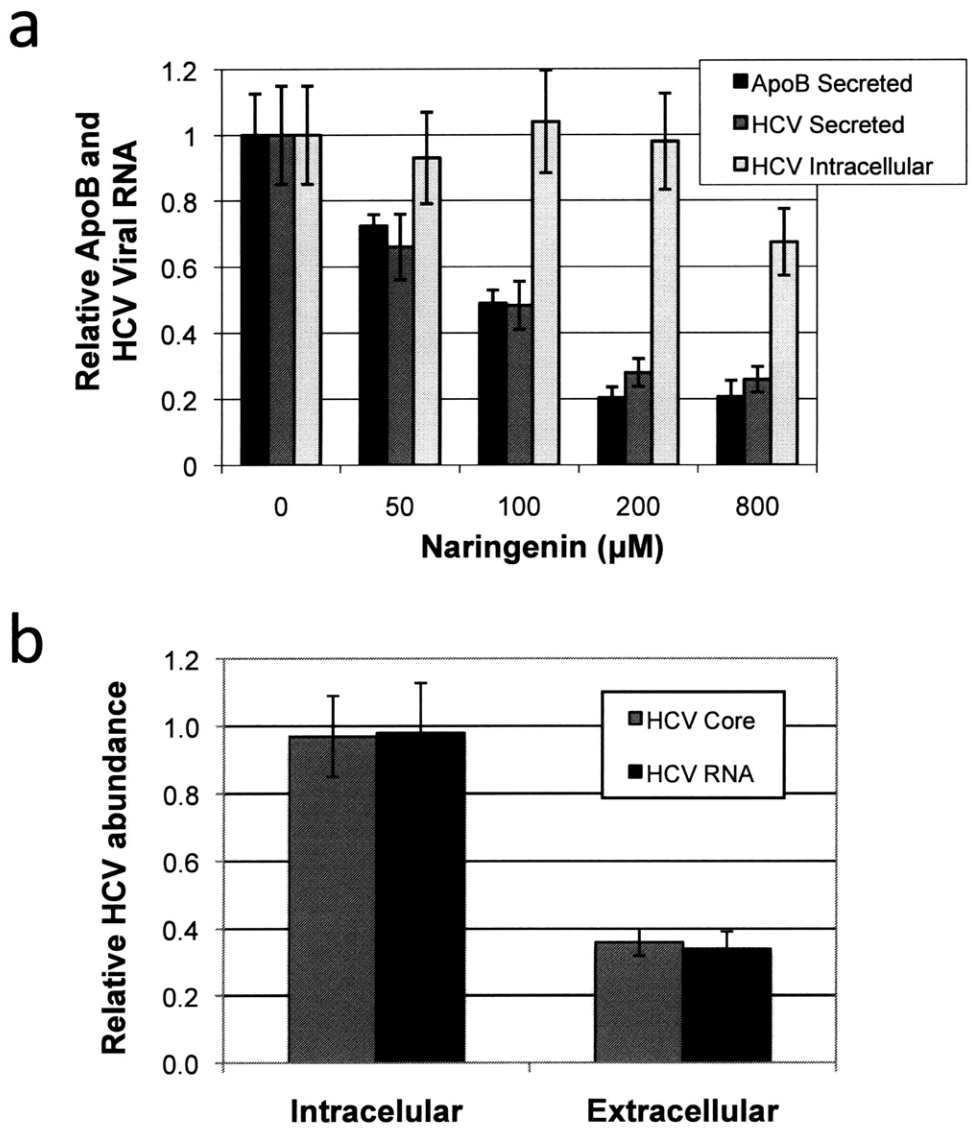

Figure 1 – (a) Naringenin dose-dependently inhibits ApoB-100, HCV RNA, and HCV core protein secretion from JFH1-infected Huh7.5.1 cells. ApoB and viral RNA were reduced by 80% and 72%, respectively. Viral RNA did not accumulate in cells. (b) Chronically infected cells were treated with naringenin. Naringenin treatment decreased the secretion of virus into the media, but did not change the amount of viral RNA or core protein inside cells. Values are normalized to untreated controls.

3.2.2 Naringenin blocks the assembly of HCV infectious particles

We next wished to determine whether naringenin blocks the assembly of HCV prior to viral egress. Cells were first treated with 0.1 μg/mL brefeldin A (BFA), a toxin known to disrupt Golgi-dependent export (3, 4). BFA treatment had previously shown to cause the accumulation of intracellular infectious HCV particles in Huh7.5.1 infected cells (4). Co-treatment of cells with BFA and the MTP-inhibitor, BMS-200150, had previously been shown to block the accumulation of intracellular infectious HCV particles, suggesting MTP is required for HCV assembly (4). As naringenin was previously shown to inhibit MTP activity, we explored if the compounds similarly blocks HCV assembly.

JFH1-infected Huh7.5.1 cells were treated with 0.1 μg/mL BFA and co-treated for 5 hours with 10 μM BMS-200150 or 200 μM naringenin. The production of extracellular infectious particles (**Figure 2b**) was significantly reduced when cells were treated with either BMS-200150 or naringenin (45% and 68%, respectively, $p<0.02$) and abolished entirely when cells were treated with BFA ($p<0.001$). Expectedly, BFA treatment which blocked the production of extracellular infectious particles, lead to the accumulation of infectious HCV particles within the cells (**Figure 2a**). Co-treatment with BMS-200150 decreased the accumulation of infectious particles by 46% ($p<0.05$) compared to BFA-only controls. Importantly, co-treatment with naringenin decreased the accumulation of infectious particles by 42% ($p<0.05$) compared to BFA-only controls (**Figure 2a**) suggesting the flavonoid inhibits the assembly of HCV lipo-viral particles (9).

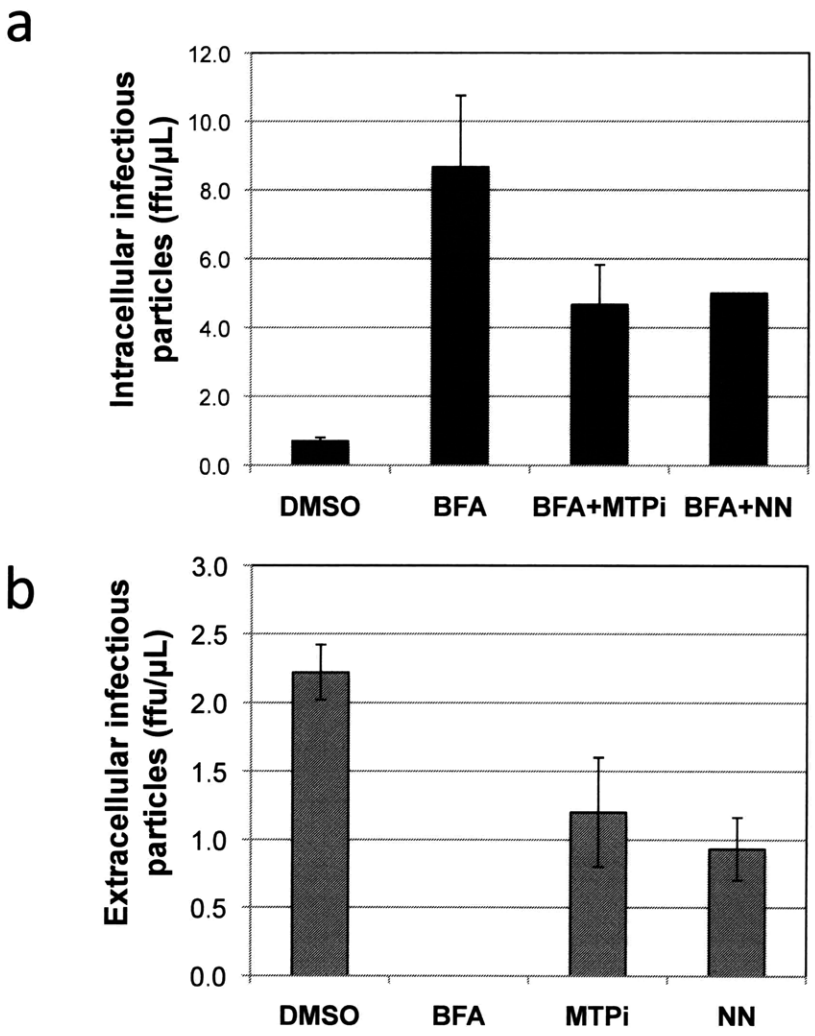

Figure 2 - Naringenin (NN) blocks the assembly intracellular infectious virus particles. (a) Infected cells were treated with 0.1 µg/mL BFA and co-treated with either 10 µM BMS-200150, a known MTP inhibitor (MTPi), or with 200 µM naringenin. Cells were lysed by freeze-thaw and virus-containing supernatant was used in an infectivity titer assay. BFA treatment led to accumulation of infectious virus in cells. BMS-200150 treatment prevented the accumulation of infectious virus in cells, leading to a 46% ($p<0.05$) decrease in infectious particle accumulation. Naringenin had a similar effect to that of the MTP inhibitor, leading to a 42% ($p<0.05$) decrease in infectious particle accumulation. (b) Extracellular infectivity was similarly inhibited by both BMS-200150 and naringenin, by 45% and 68%, respectively ($p<0.02$). *Conducted by our collaborator, Dr. Steve Polyak of University of Washington.*

3.2.3 Naringenin inhibits MTP activity while inducing PPAR activity

Naringenin has been previously shown to inhibit MTP, a critical enzyme in VLDL assembly, in HepG2 cells (10, 11). More recently, the compound was shown to induce PPRE activity in U-2OS cells (12). To explore if naringenin inhibits MTP activity in infected and uninfected Huh7.5.1 cells, cells were treated with 200 μM of naringenin for 24 hours. Cells were subsequently lysed and assayed for MTP activity as previously described (3). Naringenin inhibited MTP activity by 58%±4% in infected cells and 67%±12% in uninfected cells compared to DMSO-treated controls (**Figure 3a**). Previous reports have indicated that MTP inhibition can lead to lipid accumulation and steatosis. To test if naringenin leads to lipid accumulation, primary rat hepatocytes were treated with naringenin for 24 hours and cellular lipids were quantified by Oil-Red-O staining as previously described (13). Oil-Red-O staining showed no significant accumulation of lipids in cells treated with 200 or 400 μM naringenin (**Figure 3b**).

Cellular lipid metabolism is controlled by several nuclear receptors, members of a family of ligand-activated transcription factors (14). Activation of PPARα specifically, has been shown to induce β-oxidation and a reduction in lipogenesis and VLDL secretion (15). Such activation could explain the lack of lipid accumulation. To examine if naringenin induces PPAR activation we used the HG5LN-PPARα reporter cell line (16). In this cell line, the PPARα ligand binding domain (LBD) is fused to a GAL4 DNA binding domain. Activation of PPARα-LBD allows GAL4 to bind its UAS response element transcribing luciferase. **Figure 3c** shows that naringenin treatment enhanced the activity of the PPARα-LBD 2.4-fold ($p<0.001$).

To examine if the activation PPARα-LBD in the reporter cell line correlates with PPRE activity in JFH1-infected Huh7.5.1 cells, we transfected infected cells with the pAOx(X2)luc reporter plasmid which contains two tandem repeats of the AOX PPAR response element (PPRE) upstream of the firefly luciferase reporter gene (17). Renilla luciferase expression was used as control. As shown in **Figure 3d,** naringenin led to a dose-dependent increase in PPRE activity, reaching 23% ± 7% ($p=0.015$) compared to DMSO-treated control. To verify that PPARα activation could indeed reduce ApoB and virus production in our system, we treated Huh7.5.1 cells with classical PPARα agonist, WY-14,643. Cells treated with the agonist produced only 67%

and 37% of the amount of ApoB and HCV RNA, respectively, compared to DMSO-treated controls, a reduction similar to that observed in naringenin-treated cells (**Figure 3E**).

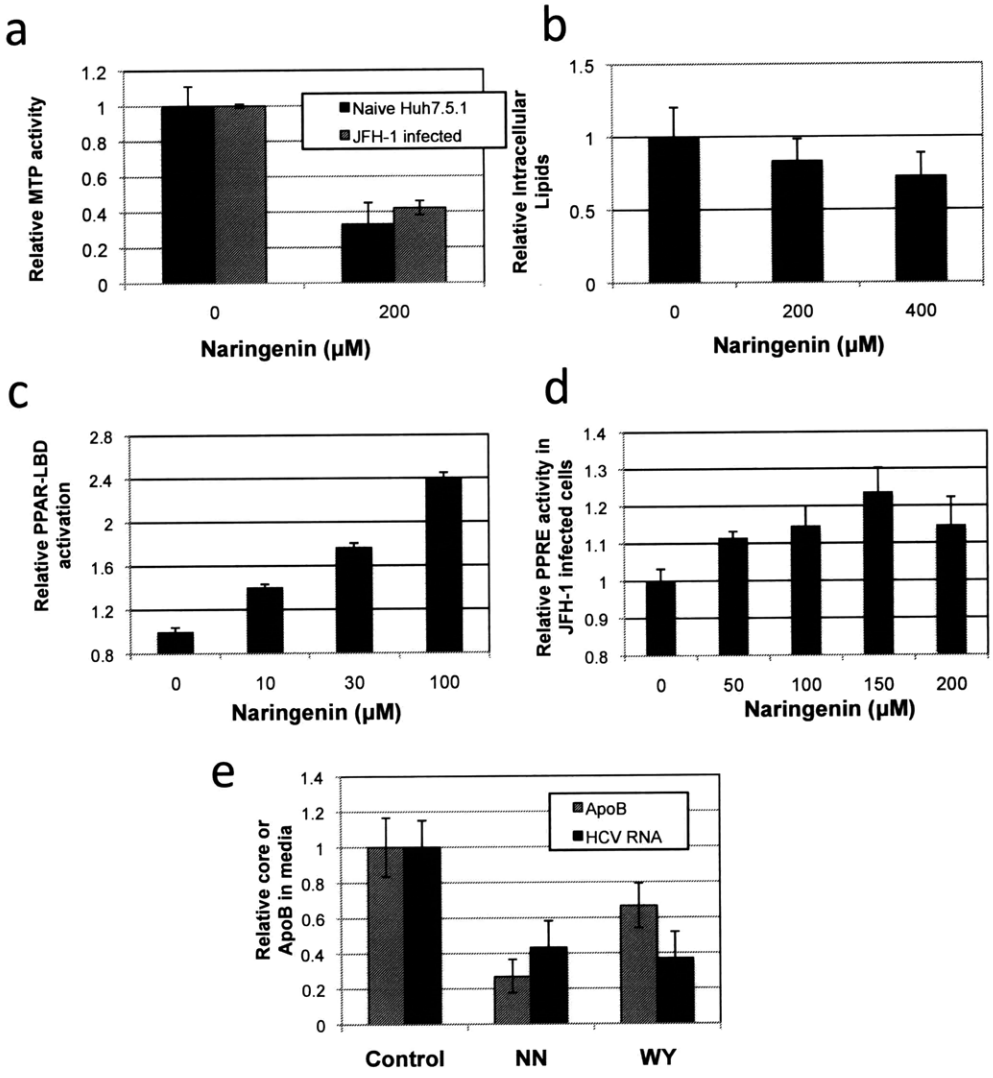

Figure 3. Naringenin (NN) enhances PPAR and inhibits MTP activity in infected cells. (a) Naringenin decreased MTP activity by 33% and 42% for uninfected and infected cells, respectively, without leading to accumulation of lipids in cells (b). (c) HG5LN-PPARα cells were treated with varying amounts of naringenin. Naringenin enhanced PPARα-LBD activity by 140% ± 5% ($p<0.001$) *Conducted by our collaborator, Dr. Patrick Balaguer of Univ Montpellier I, France.* (d) Chronically infected cells were co-transfected with pAOx(X2)Luc and pRL-TK overnight and then treated with naringenin for 24 hours. Naringenin dose-dependently enhanced PPRE activity by up to 24% ± 7% ($p=0.015$). (e) Cells were treated with either 200μM naringenin (NN) or 10μM WY14,643 (WY). Both treatments led to similar decreases in secreted ApoB and viral RNA.

3.2.4 Long-term inhibition of HCV production

Given our observations that 24-hour treatment with naringenin significantly decreases viral secretion, we were interested in exploring the flavonoid's effect on viral production over a period of several days. We therefore treated chronically infected Huh7.5.1 cells with 200μM naringenin over a course of 4 days (treatment). As a positive control, cells were treated with 1000 i.u of IFNα, a concentration previously shown to abolish viral production (18). On days 5-7, treatment was removed from all cells (washout).

As expected, our results showed that ApoB secretion was decreased by naringenin treatment (86%±1%, $p<0.01$), but not by IFNα that showed a 16%±3% increase. Importantly, naringenin treatment caused a rapid 1.2 log reduction in HCV RNA and a 60% reduction in HCV core ($p<0.05$). This inhibition in HCV production was similar to IFNα which showed a maximal 1.7 log reduction in HCV RNA and a 70% reduction in HCV Core (**Figure 4**). Interestingly, during the washout period, HCV levels in naringenin treated cells returned to normal suggesting that the compound did not affect viral replication.

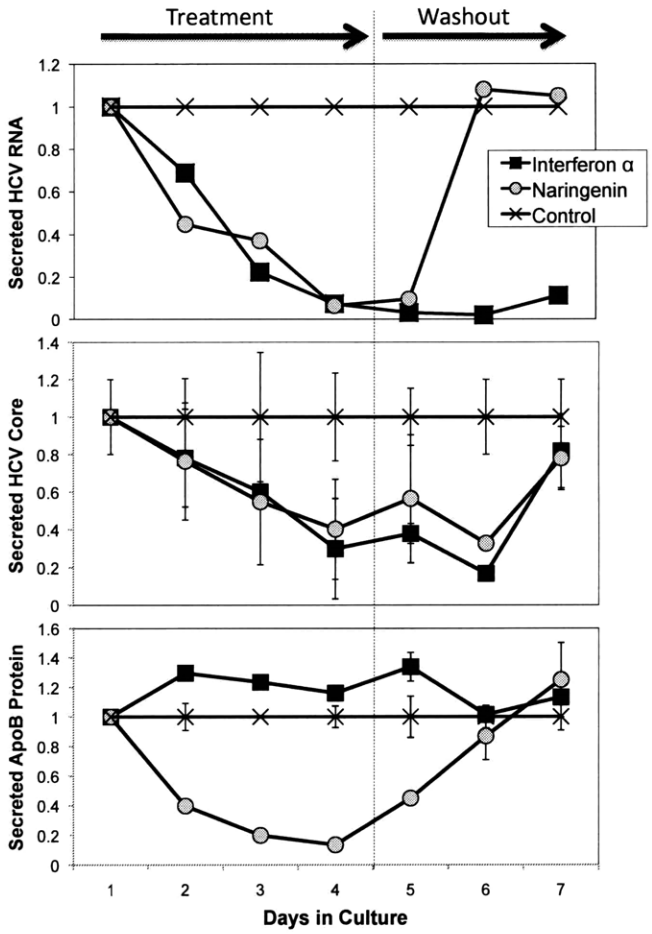

Figure 4 - Naringenin causes a rapid inhibition of HCV production during long-term treatment. Cells were treated for 4 days with 200 μM naringenin or 1000 i.u IFNα, culture media was replaced daily. During the 3 day washout period, all wells were treated with media without treatment. (a) Viral RNA release into media decreased during treatment, down to 6% with naringenin and 2% with IFNα compared to controls. During washout phase, naringenin-treated samples contained RNA levels similar to controls, suggesting viral replication was unchanged. (b) HCV core levels in media decreased during treatment for naringenin and IFNα. For naringenin-treated cells on days 4, core in the media was reduced to 40%±26%. Core accumulation was partly restored during the last day of washout in both naringenin and IFNα-treated samples 78% ± 17%, 82% ± 20%, respectively. C) ApoB secretion declined during treatment with naringenin. On days 4, ApoB secretion in naringenin-treated cells decreased to 13%±1%.

3.3 Discussion

HCV is a global public health problem affecting close to 3% of the world population. The current standard of care consists of pegylated IFNα and ribavirin. Despite the high incidence of adverse effects, this combination therapy is only effective in approximately half of the patients, and is associated with the emergence of resistant strains (19, 20). While protease and polymerase inhibitors developed in the context of STAT-C are showing a remarkable potential, similar indications of resistant strains have already been reported in clinical trials. A complimentary approach is to target a host pathway, such as VLDL assembly, on which the virus depends. HCV would require numerous mutations and a significant alteration of its lifecycle to escape, essentially becoming a different virus.

HCV is a positive-strand RNA virus, a member of the *Flaviviridae* family. The viral life cycle begins upon entry into the host cell. The process of cell entry has yet to be clarified completely, but may involve several cell-surface receptors, including the LDL receptor (LDLR) (21, 22). Following entry, viral proteins are translated and accumulate in the cellular ER, inducing morphological changes in the cell with the formation of a membranous web, where viral replication has been reported to occur in ER-associated lipid droplets (23-26). Viral assembly is thought to occur in the ER, where the virus attaches to either nascent or mature VLDL particles (27, 28). Finally, the virus is exported out of the cell in a Golgi-dependent manner (**Figure 5**) (4).

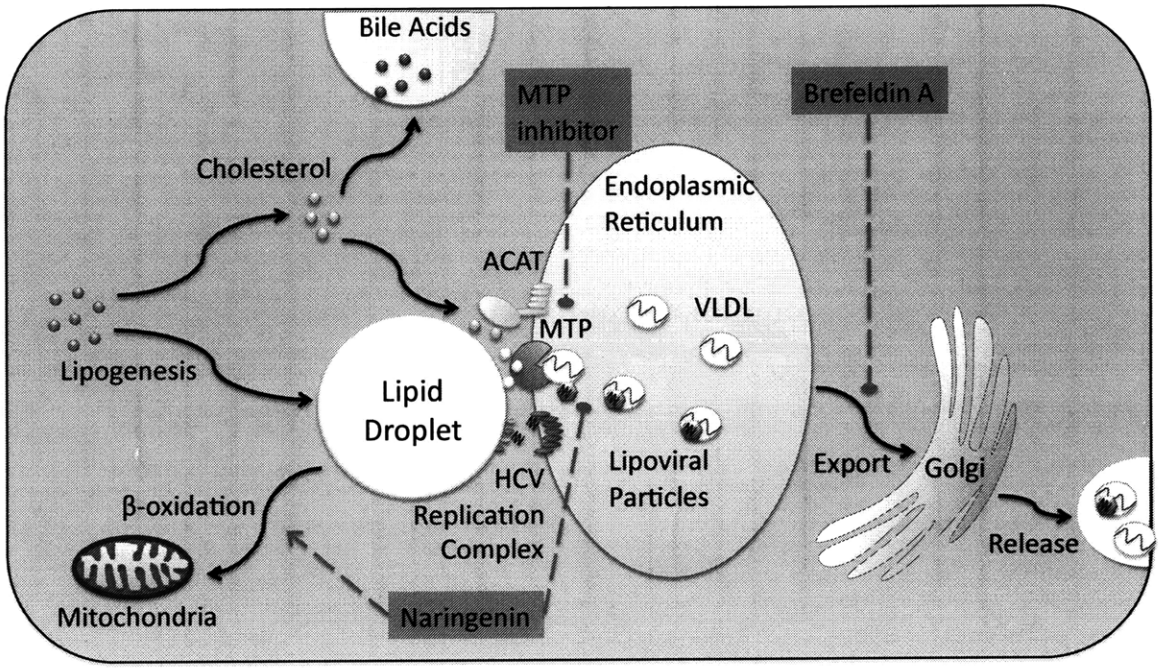

Figure 5 – Lipid metabolism affects the HCV viral lifecycle. The availability of lipids, including triglycerides and cholesterol, in the cell are essential for several steps in the viral lifecycle. Viral replication complexes are known to associate with lipid droplets, and geranylgeranylation has been shown to be crucial for viral replication. Our group and others have demonstrated the dependence of infectious particle assembly on the assembly and export of VLDL from cells. Decreasing lipid production and inhibition of VLDL assembly in the ER are potential new approaches to combating HCV infection. ACAT – acyl-CoA cholesteryl acyl transferase, MTP – microsomal triglyceride transfer protein, VLDL – very low-density lipoprotein.

The link between the virus and lipid metabolism has been suggested by both observational and experimental studies (29). The viral life cycle depends heavily on lipid metabolism, and both we and others have shown that HCV replication is inhibited by statins and enhanced by the addition of fatty acids (30, 31). Recently, Gastaminza *et al*. demonstrated the existence of high density intracellular HCV infected particles suggesting the virus binds to low density particles in the ER (28). Using a similar system, Huang *et al.* demonstrated that HCV assembled in vesicles enriched in ApoB, ApoE, and MTP the main components required for VLDL assembly (27). Lastly, our group and others demonstrated that HCV is actively secreted while bound to (VLDL) (3, 4) and that its production can be metabolically modulated.

Our group has previously suggested that naringenin, a grapefruit flavonoid aglycone, could be effective in inhibiting HCV production (3). Naringenin has been shown to possess antioxidative and normolipidemic effects both *in vitro* and *in vivo* (8). The flavonoid has been reported to be an MTP and ACAT inhibitor (29), and a regulator of cytochrome P4503A and 4A activity (30, 31).

In this study, we first showed that naringenin induced a dose-dependent inhibition of HCV RNA and core protein secretion, down to 28% of untreated controls (**Figure 1**). The reduction in viral RNA and protein production correlated with inhibition of HCV infectivity (**Figure 2**). On the other hand, intracellular HCV RNA and protein levels showed no change in response to naringenin treatment, suggesting naringenin was inhibiting a step downstream of viral replication. Nonetheless, given the reduction in viral secretion, the lack of intracellular viral RNA and protein accumulation may suggest a concurrent inhibition of viral replication or enhanced viral degradation.

Assembly of infectious HCV particles has been previously demonstrated to be dependent on MTP activity, and enzyme critical to VLDL assembly. The accumulation of infectious viral particles in cells treated with BFA, a toxin which disrupts the Golgi network (32, 33), is consistent with our own findings (3) and the observations of Chisari and coworkers (4). Here we showed that naringenin, like MTP inhibitor BMS-200150, blocks the accumulation of infectious particles in BFA-treated cells up to 42% ($p<0.05$) suggesting that the flavonoid blocks the assembly of infectious viral particles. Consistent with this observation, we showed naringenin inhibited MTP activity by 58%±4% in infected cells and 67%±12% in uninfected cells, consistent

with the observations of Huff and colleagues in HepG2 cells (10). In a recent clinical study Cuchel and colleagues showed that while the MTP inhibitor BMS-201038 (now AEGR-733) lowered LDL values, it was associated with steatosis and elevated ALT levels, leading to an early termination of the study (34). To test if naringenin leads to a similar level of lipid accumulation, cellular lipids were quantified following naringenin treatment. We show there was no significant accumulation of lipids in cells treated with 200 or 400 μM naringenin (**Figure 3b**).

Our observations and those of other groups' regarding naringenin's ability to modulate the expression of genes important in fatty acid oxidation, led us to examine the effects of naringenin on the nuclear receptor PPARα. We demonstrate that naringenin has a direct effect on PPARα ligand binding domain in the HG5LN-PPARα reporter cell line (16). Consistently, naringenin showed a dose-dependent increase in PPRE activity in JFH1-infected Huh7.5.1 cells. These results are consistent with recent observations of Liu *et al.* in U-2OS osteosarcoma cells (12). Furthermore, Huh7.5.1 cells chronically infected with HCV treated with the PPARα agonist, WY 16,463, showed a 67% decrease in ApoB secretion and a 37% decrease in HCV RNA secretion (**Figure 3d**), supporting the hypothesis that PPARα induction contributes to narigenin's inhibition of HCV production in hepatocytes.

Finally, we wished to demonstrate that naringenin could inhibit viral accumulation in media over a period of several days (**Figure 4**). As expected, naringenin reduced the secretion of ApoB by 86%. This effect was not observed in IFNα-treated cells. When media was examined for viral core and RNA content, both naringenin and IFNα significantly reduced the secretion of HCV RNA by 1.2 and 1.7 log, respectively. Importantly, naringenin's effect on viral secretion was reversible, as viral secretion rebounded during washout, consistent with a mechanism of action that does not eliminate intracellular replication of the virus.

Our results suggest that naringenin blocks the assembly of infectious HCV particles. The tight link between HCV and VLDL assembly, described as lipo-viral particles, suggests a new approach for combating the virus. We expect that targeting host metabolism rather than viral structural elements will decrease the development of resistant strains. The application of naringenin or other PPAR alpha agonists with STAT-C agents could bring a rapid reduction in HCV levels during

the early treatment phase, which has been associated with a better long-term outcome. Our work strongly supports further investigation of naringenin in the management of HCV infections.

3.4 Methods

Reagents

Lipoprotein-free FBS was purchased from Biomedical Technologies (Stoughton, MA). Naringenin, WY14,643, Brefeldin A (BFA), and Oil-Red-O were purchased from Sigma-Aldrich Chemicals (St. Louis, MO). Ciglitazone was purchased from Cayman Chemical (Ann Arbor, MI). Immunofluorescence-grade paraformaldehyde was purchased from Electron Microscope Sciences (Hatfield, PA). All other chemicals were purchased from Invitrogen Life Technologies (Carlsbad, CA) unless otherwise noted. An MTP fluorescent activity kit was purchased from Roar Biomedical (New York, NY). Unless otherwise noted, all other chemicals were purchased from Sigma-Aldrich Chemicals. BMS-200150, a small molecule inhibitor of MTP was synthesized as described (35), and solubilized in DMSO. The compound was provided by Pablo Gastaminza and Francis Chisari.

Cell Culture and Viruses

The Huh7.5.1 human hepatoma cell line and a plasmid containing the JFH-1 genome were kindly provided by Dr. Chisari (Scripps Research Institute, La Jolla, CA) and Dr. Wakita (National Institute of Infectious Diseases, Tokyo, Japan), respectively. Huh7.5.1 cells were cultured in DMEM supplemented with 10% FBS, 200 units/mL penicillin, and 200 mg/mL streptomycin in a 5% CO2-humidified incubator at 37°C. In vitro transcribed genomic JFH-1 RNA was delivered to cells by liposome-mediated transfection as described by Zhong *et al.* (36). Infected Huh7.5.1 cells were passaged every 3 days and used at passage <15.

HCV Secretion

HCV-infected Huh7.5.1 cells were plated on a 6-well plate at a density of 1×10^5 cells/cm^2 and cultured overnight in the standard medium. Prior to the beginning of the experiment, the cells were washed 3 times with PBS and cultured with DMEM containing 5% lipoprotein-free FBS. Naringenin was added at this time as described in the text. Following 24 hours of incubation, the plate was gently agitated to release mechanically bound particles, and the medium was collected, filtered to remove cellular debris, and stored at -80°C for further analysis. The

attached cells were washed 3 times with PBS, harvested, pelleted, and stored at -80°C for further analysis.

Hepatocyte Isolation and Culture

Rat hepatocytes were harvested from adult female Lewis rats (Charles River Laboratories, Boston, MA) weighing 150-200 g by way of a two-step in situ collagenase perfusion technique modified by Dunn et al. (37). Hepatocyte viability after the harvest was greater than 90% based on trypan blue exclusion. All animals were treated in accordance with National Research Council guidelines, and the study was approved by the Subcommittee on Research Animal Care at Massachusetts General Hospital. Hepatocyte purity was greater than 95%.

Hepatocytes were seeded directly on 6-well, collagen gel-coated plates at a density of 100,000 cells/cm2. Culture medium consisted of Hepatocyte Culture Medium (HCM) supplemented with SingleQuots (Lonza, Walkersville, MD), and cultures were maintained in a 10% CO_2-humidified incubator at 37°C.

Intracellular and Extracellular HCV Infectivity

The infectivity of HCV particles was measured as previously described (3). Briefly, naïve Huh7.5.1 cells were grown to 80% confluence and exposed to cell culture supernatants diluted 10-fold in the culture medium. Following 1 hour of incubation at 37°C, the medium was replaced, and the cells were cultured for 3 additional days. Levels of HCV infection were determined by immunofluorescence staining for HCV core protein. The viral titer is expressed as focus forming units (FFU) per milliliter of supernatant. To evaluate infectivity of intracellular particles, cells were scraped into PBS and lysed by freeze-thawing as previously described (4), diluted and used to assess infectivity as above.

GAL4-PPAR activation assays

PPAR activation was examined as previously described using the HGLN5 PPARα and PPARγ cell line (16). Briefly, HGLN5 cells were seeded at a density of 100,000 cells/cm^2, test compounds were added 8 hours later and incubated for 16 hours. Following treatment, cells were washed with PBS and lysed in 25 mM Tris buffer (pH 7.8). Protein concentration was calculated using

the Bradford assay and used to normalize the luciferase activity. Finally, activation of PPARα and PPARγ reporters is presented as percent of maximal activation by the known agonists GW7647 and BRL49653, respectively.

PPRE activation in JFH1-infected Huh7.5.1 cells

The pAOx(X2)luc plasmid which contains two tandem repeats of the AOX PPAR response element (PPRE) upstream of the firefly luciferase reporter gene (17) was a kind gift of Dr. John P. Capone (McMaster University, Canada). The pRL-TK plasmid containing the renilla luciferase reporter under the control of a constitutive thymidine kinase promoter was purchased from Promega Corporation (Madison, WI). JFH1-infected Huh7.5.1 cells were transiently transfected with the pAOx(X2)luc and pRL-TK plasmids using Lipofectamine 2000 according to manufacturer's directions. Following 24 hours incubation with naringenin, cells were lysed and assayed using a Dual-Luciferase Reporter Assay System (Promega, Madison, WI) according to the manufacturer's instructions. All measurements were done in triplicate and data are shown as values normalized to renilla luciferase internal controls.

Human ApoB Enzyme-Linked Immunosorbent Assay (ELISA)

Huh7.5.1-secreted ApoB-100 was detected in the medium with the ALerCHEK, Inc. (Portland, ME), total human ApoB-100 ELISA kit. The medium was diluted 1:10 with the specimen diluent, and the assay was carried out according to the manufacturer's directions.

HCV Core ELISA

Huh7.5.1-secreted HCV core antigen was detected in the medium with the Wako Chemicals (Cambridge, MA) ORTHO HCV antigen ELISA kit. The medium was used as is, and the assay was carried out according to the manufacturer's directions.

MTP Activity Assay

MTP activity was measured using a commercially available fluorescence assay using a commercial kit (Roar Biomedical, Inc., New York, NY). Huh7.5.1 cells were treated with compounds added in fresh media as described above. After 24 hours, cells were scraped into

PBS on ice, centrifuged at 600g for 3min at 4°C to pellet the cells, and resuspended in manufacturer homogenization buffer supplemented with protease inhibitor cocktail (Thermo Scientific). Cell suspensions were then sonicated on ice 3 times for 3 seconds each. 100 μg cell lysates were combined with 10 μL of donor and acceptor particles in 220 μL assay buffer, and incubated at 37°C. Increase in fluorescence was measured using spectra MAX Gemini plate reader with excitation of 465 nm and emission of 538 nm, with 530 nm cutoff. Finally, MTP activity was normalized to sample protein content.

Quantitative, Real-Time, Reverse-Transcription Polymerase Chain Reaction (qRT-PCR)

Virus samples were purified using a QIAamp Viral RNA Mini Kit (Qiagen, Valencia, CA). The reverse-transcription reaction step was performed on a Mastercycler epgradientS (Eppendorf) instrument using a High Capacity cDNA Reverse Transcription Kit (Applied Biosystems, Foster City, CA). Real-time PCR was performed on a MyiQ Real-Time PCR Detection System using iScript One-Step RT-PCR Kit With SYBR Green (Bio-Rad, Hercules, CA), according to the manufacturers' instructions. HCV detection primers used in qRT-PCR were Forward 5'-GGGAAGACTGGGTCCTTTCTTGGAT-3' and Reverse 5'- CGACGGTTGGTGTTTCTTTTGGTTT-3' (Integrated DNA Technologies, Coralville, IA).

Lipid Measurements

Intracellular lipids were measured by Oil-Red-O staining. Cells were washed with PBS and fixed in 10% pH-buffered formalin for 10 minutes, washed in 60% isoprpanol and dried for 15 minutes. Oil-Red-O working solution was added to cells and incubated at room temperature for 10 minutes. Cells were extensively washed visually inspected. Finally, intracellular Oil-Red-O was eluted from cells by incubation in 100% isopropanol for 10 minutes, and quantified at 510nm.

Long-term Treatments

JFH1-infected Huh7.5.1 cells were grown over a course of 7 days in OptiMEM culture medium. Media was collected every 24 hours and stored at -80°c for analysis. On Days 1-4 ("treatment"),

media contained 200μM naringenin, 1000U/mL IFNα, or DMSO. On Days 5-7 ("washout"), all wells were cultured in standard media without treatment.

Statistics

Data are expressed as the mean ± standard deviation. Statistical significance was determined by a one-tailed Student's t-test. A *P*-value of 0.05 was used for statistical significance.

3.5 References

1. Shepard CW, Finelli L, Fiore AE, Bell BP. Epidemiology of hepatitis B and hepatitis B virus infection in United States children. Pediatr Infect Dis J 2005;24:755-760.

2. Manns MP, Foster GR, Zeuzem S, Zoulim F. The way forward in HCV treatment - finding the right path. Nat Rev Drug Discov 2007.

3. Nahmias, Goldwasser, Casali, Poll v, Wakita, Chung, Yarmush M. Apolipoprotein B-dependent hepatitis C virus secretion is inhibited by the grapefruit flavonoid naringenin. Hepatology 2008;47:1437-1445.

4. Gastaminza, Cheng, Wieland, Zhong, Liao, Chisari. Cellular determinants of hepatitis C virus assembly, maturation, degradation, and secretion. Journal of Virology 2008;82:2120-2129.

5. Roingeard P, Hourioux C, Blanchard E, Prensier G. Hepatitis C virus budding at lipid droplet-associated ER membrane visualized by 3D electron microscopy. Histochem Cell Biol 2008;130:561-566.

6. Moriishi K, Matsuura Y. Host factors involved in the replication of hepatitis C virus. Rev. Med. Virol. 2007;17:343-354.

7. Maheshwari A, Ray S, Thuluvath PJ. Acute hepatitis C. Lancet 2008;372:321-332.

8. Wilcox, Borradaile, Huff. Antiatherogenic Properties of Naringenin, a Citrus Flavonoid. Cardiovascular Drug Reviews 1999.

9. André P, Perlemuter G, Budkowska A, Bréchot C, Lotteau V. Hepatitis C virus particles and lipoprotein metabolism. Semin Liver Dis 2005;25:93-104.

10. Wilcox, Borradaile, Dreu d, Huff. Secretion of hepatocyte apoB is inhibited by the flavonoids, naringenin and hesperetin, via reduced activity and expression of ACAT2 and MTP. J Lipid Res 2001;42:725-734.

11. Allister, Borradaile, Edwards, Huff. Inhibition of microsomal triglyceride transfer protein expression and apolipoprotein B100 secretion by the citrus flavonoid naringenin and by insulin involves activation of the mitogen-activated protein kinase pathway in hepatocytes. Diabetes 2005;54:1676-1683.

12. Liu, Shan, Zhang, Ning, Lu, Cheng. Naringenin and hesperetin, two flavonoids derived from Citrus aurantium up-regulate transcription of adiponectin. Phytotherapy research : PTR 2008;22:1400-1403.

13. Ramirez-Zacarias JL, Castro-Munozledo F, Kuri-Harcuch W. Quantitation of adipose conversion and triglycerides by staining intracytoplasmic lipids with Oil red O. Histochemistry 1992;97:493-497.

14. Gronemeyer, Gustafsson, Laudet. Principles for modulation of the nuclear receptor superfamily. Nat Rev Drug Discov 2004;3:950-964.

15. Spann NJ, Kang S, Li AC, Chen AZ, Newberry EP, Davidson NO, Hui ST, et al. Coordinate transcriptional repression of liver fatty acid-binding protein and microsomal triglyceride transfer protein blocks hepatic very low density lipoprotein secretion without hepatosteatosis. J Biol Chem 2006;281:33066-33077.

16. Seimandi, Lemaire, Pillon, Perrin, Carlavan, Voegel, Vignon, et al. Differential responses of PPARalpha, PPARdelta, and PPARgamma reporter cell lines to selective PPAR synthetic ligands. Anal Biochem 2005;344:8-15.

17. Marcus, Miyata, Zhang, Subramani, Rachubinski, Capone. Diverse peroxisome proliferator-activated receptors bind to the peroxisome proliferator-responsive elements of the rat hydratase/dehydrogenase and fatty acyl-CoA oxidase genes but differentially induce expression. Proc Natl Acad Sci USA 1993;90:5723-5727.

18. Dash S, Hazari S, Garry RF, Regenstein F: Mechanisms of Interferon Action and Resistance in Chronic Hepatitis C Virus Infection: Lessons Learned from Cell Culture Studies. In: Hepatitis C Virus Disease, 2008; 16-38.

19. Ghany MG, Strader DB, Thomas DL, Seeff LB. Diagnosis, management, and treatment of hepatitis C: an update. Hepatology 2009;49:1335-1374.

20. Taylor DR, Shi ST, Lai MM. Hepatitis C virus and interferon resistance. Microbes Infect 2000;2:1743-1756.

21. Molina S, Castet V, Fournier-Wirth C, Pichard-Garcia L, Avner R, Harats D, Roitelman J, et al. The low-density lipoprotein receptor plays a role in the infection of primary human hepatocytes by hepatitis C virus. J Hepatol 2007;46:411-419.

22. Wunschmann S, Medh JD, Klinzmann D, Schmidt WN, Stapleton JT. Characterization of hepatitis C virus (HCV) and HCV E2 interactions with CD81 and the low-density lipoprotein receptor. J Virol 2000;74:10055-10062.

23. André, Lotteau. Hepatitis C virus assembly: when fat makes it easier. Journal of Hepatology 2008;49:153-155.

24. Roingeard P, Hourioux C. Hepatitis C virus core protein, lipid droplets and steatosis. Journal of Viral Hepatitis 2008;15:157-164.

25. Shavinskaya A, Boulant S, Penin F, McLauchlan J, Bartenschlager. The lipid droplet binding domain of hepatitis C virus core protein is a major determinant for efficient virus assembly. J Biol Chem 2007;282:37158-37169.

26. Miyanari Y, Atsuzawa K, Usuda N, Watashi K, Hishiki T, Zayas M, Bartenschlager R, et al. The lipid droplet is an important organelle for hepatitis C virus production. Nat Cell Biol 2007;9:1089-1097.

27. Huang, Sun, Owen, Li, Chen, Gale, Ye. Hepatitis C virus production by human hepatocytes dependent on assembly and secretion of very low-density lipoproteins. Proc Natl Acad Sci USA 2007;104:5848-5853.

28. Gastaminza, Kapadia, Chisari. Differential biophysical properties of infectious intracellular and secreted hepatitis C virus particles. Journal of Virology 2006;80:11074-11081.

29. Ye. Reliance of host cholesterol metabolic pathways for the life cycle of hepatitis C virus. PLoS Pathog 2007;3:e108.

30. Kapadia, Chisari. Hepatitis C virus RNA replication is regulated by host geranylgeranylation and fatty acids. Proc Natl Acad Sci USA 2005;102:2561-2566.

31. Kim, Peng, Lin, Choe, Sakamoto, Kato, Ikeda, et al. A cell-based, high-throughput screen for small molecule regulators of hepatitis C virus replication. Gastroenterology 2007;132:311-320.

32. Misumi Y, Miki K, Takatsuki A, Tamura G, Ikehara Y. Novel blockade by brefeldin A of intracellular transport of secretory proteins in cultured rat hepatocytes. J Biol Chem 1986;261:11398-11403.

33. Fujiwara T, Oda K, Yokota S, Takatsuki A, Ikehara Y. Brefeldin A causes disassembly of the Golgi complex and accumulation of secretory proteins in the endoplasmic reticulum. J Biol Chem 1988;263:18545-18552.

34. Cuchel M, Bloedon LT, Szapary PO, Kolansky DM, Wolfe ML, Sarkis A, Millar JS, et al. Inhibition of microsomal triglyceride transfer protein in familial hypercholesterolemia. N Engl J Med 2007;356:148-156.

35. Jamil H, Gordon DA, Eustice DC, Brooks CM, Dickson JK, Jr., Chen Y, Ricci B, et al. An inhibitor of the microsomal triglyceride transfer protein inhibits apoB secretion from HepG2 cells. Proc Natl Acad Sci U S A 1996;93:11991-11995.

36. Zhong, Gastaminza, Cheng, Kapadia S, Kato T, Burton DR, Wieland SF, et al. Robust hepatitis C virus infection in vitro. Proc Natl Acad Sci USA 2005;102:9294-9299.

37. Dunn JC, Tompkins RG, Yarmush ML. Long-term in vitro function of adult hepatocytes in a collagen sandwich configuration. Biotechnol Prog 1991;7:237-245.

4 Naringenin is a PPARα and PPARγ agonist and inhibits LXRα

4.1 Introduction

Dysregulation of lipid and carbohydrate homeostasis has been implicated in multiple disease processes, such as atherogenesis, insulin resistance, and hypermetabolism (2, 3). Naringenin has been recently suggested as a potential normolipidemic agent: in a recent clinical trial, naringenin was shown to reduce circulating levels of low-density lipoprotein (LDL) by 17% in hypercholesterolemic patients (7). Similarly, the cholesterol-lowering effects of naringenin have been demonstrated in rabbits (8, 9) and rats (10).

Naringenin's *in vitro* ability to reduce cellular secretion of very-low density lipoprotein (VLDL) and LDL (11, 12) through the inhibition of ACAT2 (11) and MTP (13, 14), along with its inhibition of HMG CoA reductase (HMGR) and activation of enzymes important in fatty acid oxidation such as CYP4A1 (15) suggest that the flavonoid may be targeting transcriptional regulation of metabolism through nuclear receptors (NRs), a family of ligand-activated transcription factors which respond to and regulate cellular metabolism.

In this study, we demonstrate that naringenin is an agonist of the NRs PPARα and PPARγ, and an antagonist of LXRα. We show that naringenin induces the activation of PPARα and PPARγ ligand-binding domains in GAL4-fusion protein reporters, and induces PPAR response element (PPRE) activity in Huh7.5.1 human hepatoma cells. Concomitantly, naringenin inhibits the activation of the LXRα ligand-binding domain in a GAL4-fusion protein reporter in the presence of the LXRα agonist TO901317. In an *in vitro* TR-FRET assay, this effect is shown to be at least partly mediated by the inhibition of the binding of the Trap220/Drip-2 co-activator peptide to a recombinant LXRα ligand-binding domain. Naringenin also inhibits LXRα response elemenet (LXRE) activity in Huh7.5.1 cells. Lastly, we show the effects of naringenin on PPARα and LXRα-

driven gene transcription, and that naringenin decreases the secretion of ApoB in Huh7.5.1 cells and reduces production of triglycerides and bile salts in primary rat hepatocytes.

4.2 Results

Naringenin's manifold effects on cells, including the induction of β-oxidation, gluconeogenesis (19), and anti-inflammatory (5) properties, suggest an underlying transcriptional mechanism of action, similar to the activities of PPARα and PPARγ agonists such as fibrates or thiazolidinediones (TZDs) (20, 21). Therefore, naringenin's effects on the activation of PPARα and PPARγ were investigated using the previously described HeLa-based reporter cell lines, HG_5LN GAL4-PPARα and HG_5LN GAL4-PPARγ. In these cells, the PPAR ligand binding domain (LBD) linked to a GAL4 DNA binding domain is expressed constitutively. Upon binding to an agonist, the PPAR-GAL4 fusion protein activates a luciferase reporter driven by a pentamer of GAL4 recognition sequences (22).

Naringenin dose-dependently activated PPARα reaching 24%±0.2% induction at 240 μM ($P<0.001$) relative to 1 μM of the PPARα agonist GW7647 (**Figure 1a)**. Furthermore, naringenin activated PPARγ up to 57% ± 0.3% at 80 μM ($P<0.005$) relative to the PPARγ agonist 1 μM BRL49653 (**Figure 1b**).

To further characterize the interaction between PPARα and naringenin, a LanthaScreen time-resolved fluorescence resonance energy transfer (TR-FRET) assay was performed. This cell-free system measures the ability of a compound to enhance the binding of a recombinant PPARα LBD to a PGC1α co-activator peptide, as measured by an increase in TR-FRET signal. While GW7647 showed a clear dose-dependent increase (EC_{50}=2.5nM) in the binding of PGC1α to PPARα, as expected (**Figure 1d**), the binding of PGC1α to PPARα did not increase in the presence of naringenin (**Figure 1c**), suggesting that naringenin's ability to activate PPARα does not directly involve enhancement of PPARα binding to PGC1α.

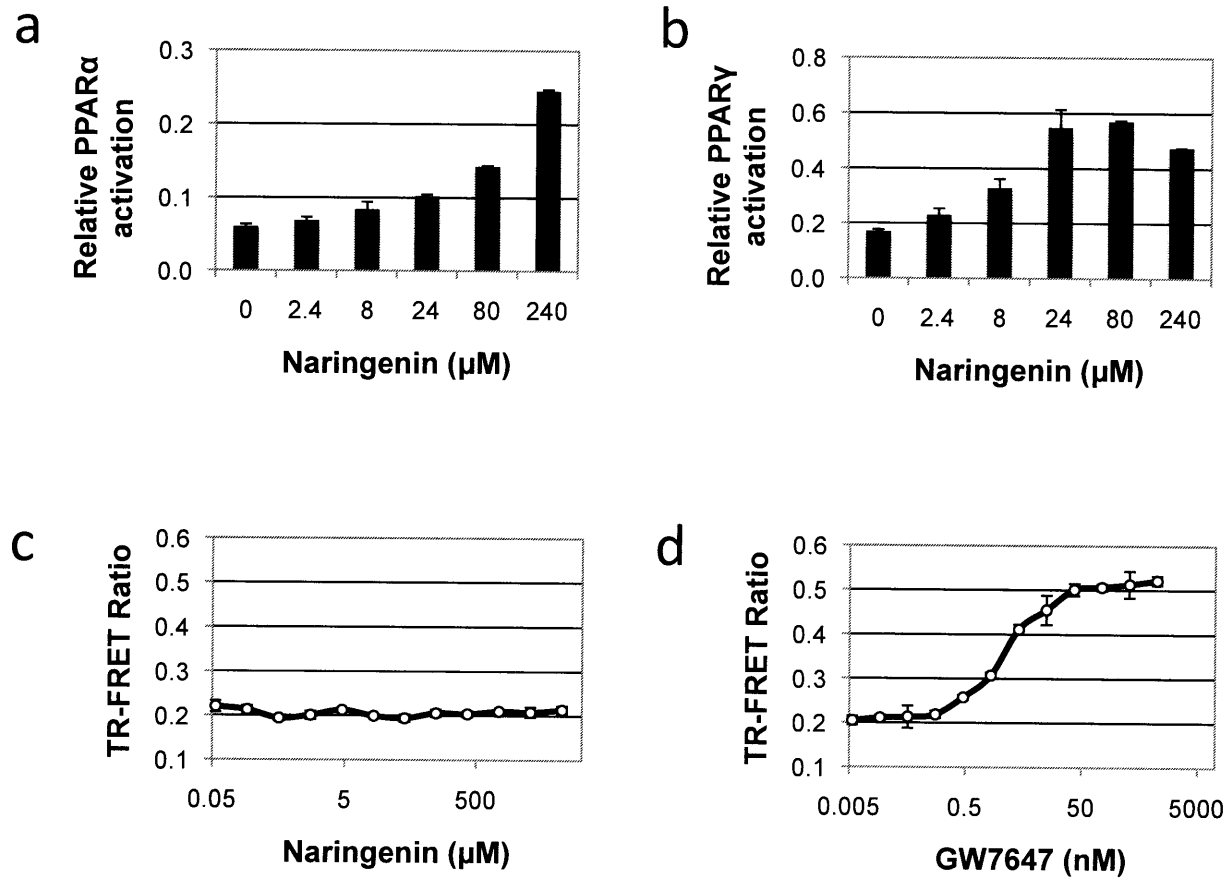

Figure 1 – Naringenin induces PPARα and PPARγ activation through a PGC1α independent mechanism. HG_5LN reporter cells expressing GAL4-PPARα (a) and GAL4-PPARγ (b) reporters were treated with increasing concentrations of naringenin. Naringenin dose-dependently activated PPARα reaching 24%±0.2% induction at 240 μM ($P<0.001$) relative to 1 μM of the PPARα agonist GW7647; and PPARγ up to 57% ± 0.3% at 80 μM ($P<0.005$) relative to the PPARγ agonist 1 μM BRL49653. Data is presented as percent activation relative to 1 μM GW7647 or 1μM BRL49653, respectively. (c) LanthaScreen TR-FRET assay, demonstrating that naringenin did not affect the binding of the PGC1α co-activator peptide to recombinant PPARα LBD. (d) In contrast, the classical PPARα agonist GW7647 induces a dose-dependent binding of PGC1α to PPARα in the same assay. (a-b) *Conducted by our collaborator, Dr. Patrick Balaguer of Univ Montpellier I, France.*

4.2.2 Naringenin inhibits LXRα activity via weak partial agonism

Some of naringenin's hypolipidemic effects may be mediated through inhibition of the activity of the lipogenic LXRα NR. Furthermore, previous research has suggested that naringenin binds LXRα *in vitro* (23). To test naringenin's capacity to function as an LXRα antagonist, LXR-alpha-UAS-bla HEK 293T cells were stimulated with 4.7nM TO901317 (corresponding to the molecule's EC_{80} in this system) and then treated with increasing concentrations of naringenin. Naringenin dose-dependently inhibited LXRα activity, reaching 28.4% ± 0.4% ($p<0.01$) and 39.1% ± 9.4% ($p<0.05$) at concentrations of 126μM and 400μM, respectively (**Figure 2a**).

The interaction between LXRα and naringenin was further characterized using a Lanthascreen TR-FRET assay. Naringenin enhanced the binding of the LXRα LBD to the Trap 220/Drip-2 co-activator moderately, yet significantly, in a dose-dependent manner reaching 38.0% ± 2.8% activation (**Figure 2b**) compared to the well-studied LXRα agonist, TO901317 (**Figure 2c**). Notably, in the presence of 250nM TO901317 (corresponding to the agonist's EC80, as measured in this system), naringenin dose-dependently inhibited the binding of the Trap 220/Drip-2 co-activator to the LXRα LBD, reaching 15.0% ± 4.1% inhibition ($p<0.01$) at 133μM (**Figure 2d**), consistent with its partial agonism of the receptor.

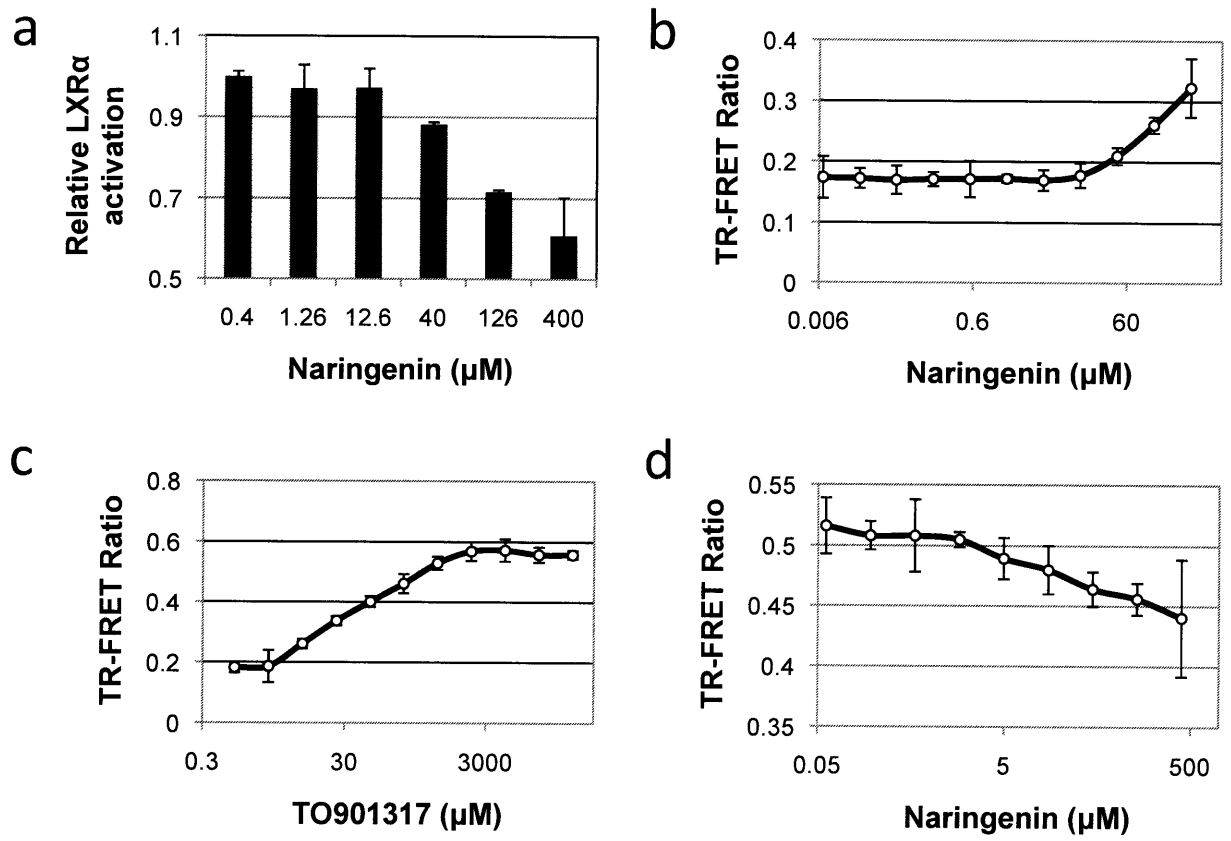

Figure 2 – Naringenin inhibits *in vitro* LXRα reporters through weak agonism. (a) LXR-alpha-UAS-bla HEK 293T cells were stimulated with 4.7nM TO901317 and exposed to increasing concentrations of naringenin. Naringenin dose-dependently inhibited LXRα activity, reaching 28.4% ± 0.4% ($p<0.01$) and 39.1% ± 9.4% ($p<0.05$) at concentrations of 126μM and 400μM, respectively. (b-d) A Lanthascreen LXRα assay was used to assess the ability of naringenin to enhance binding of the Trap 220/Drip-2 co-activator to the LXRα LBD. *Conducted by our collaborator, Dr. Patrick Balaguer of Univ Montpellier I, France.* (b) Naringenin behaved as a weak agonist, enhancing the binding of the LXRα LBD to the Trap 220/Drip-2 co-activator moderately, yet significantly, in a dose-dependent manner reaching 38.0% ± 2.8% activation. (c) The known LXRα agonist TO901317 strongly enhanced co-activator binding. (d) When treated with 250nM TO901317, increasing concentrations of naringenin led to an inhibition of the TR-FRET signal, reaching 15.0% ± 4.1% inhibition ($p<0.01$) at 133μM.

4.2.3 Naringenin enhances activity of PPAR and LXRα-driven reporters

To explore the effect of naringenin on PPAR activation more specifically in hepatocytes, we examined whether the compound would enhance the expression of a PPRE-driven reporter gene in a hepatoma cell line, Huh7.5.1. First, cells were transfected with a plasmid encoding the firefly luciferase gene under control of the acyl-CoA oxidase (AOX) PPRE. Renilla luciferase was used to control for transfection efficiency. Cells were then treated with either increasing concentrations of naringenin, 10μM WY14,643, a known PPARα agonist, or 10μM ciglitazone, a PPARγ agonist. Naringenin treatment significantly and dose-dependently enhanced luciferase expression, reaching 17% ± 7% ($p<0.05$) at 200μM (**Figure 3a**). Notably, similar levels of activation were observed when cells were exposed to the known PPAR agonists, WY14,643 (10% ± 5%) and ciglitazone (24% ± 5%).

To test the ability of naringenin to inhibit LXRα-driven gene expression, Huh7.5.1 cells were transfected with a plasmid carrying the firefly luciferase gene under control of an LXRE. Renilla luciferase was used to control for transfection efficiency. Naringenin treatment significantly and dose-dependently decreased the expression of luciferase, reaching a 50.3% ± 2.6% inhibition at 150μM ($p<0.001$; **Figure 3b**). Interestingly, at 200μM, LXRE activity was inhibited by 37% ± 5% ($p=0.002$). By comparison, one of the few published LXRα-specific antagonist, 5CPPS5 did not produce a significant decrease in LXRE activity in our hands (**Figure 3c**) and led to significant toxicity at higher doses (data not shown).

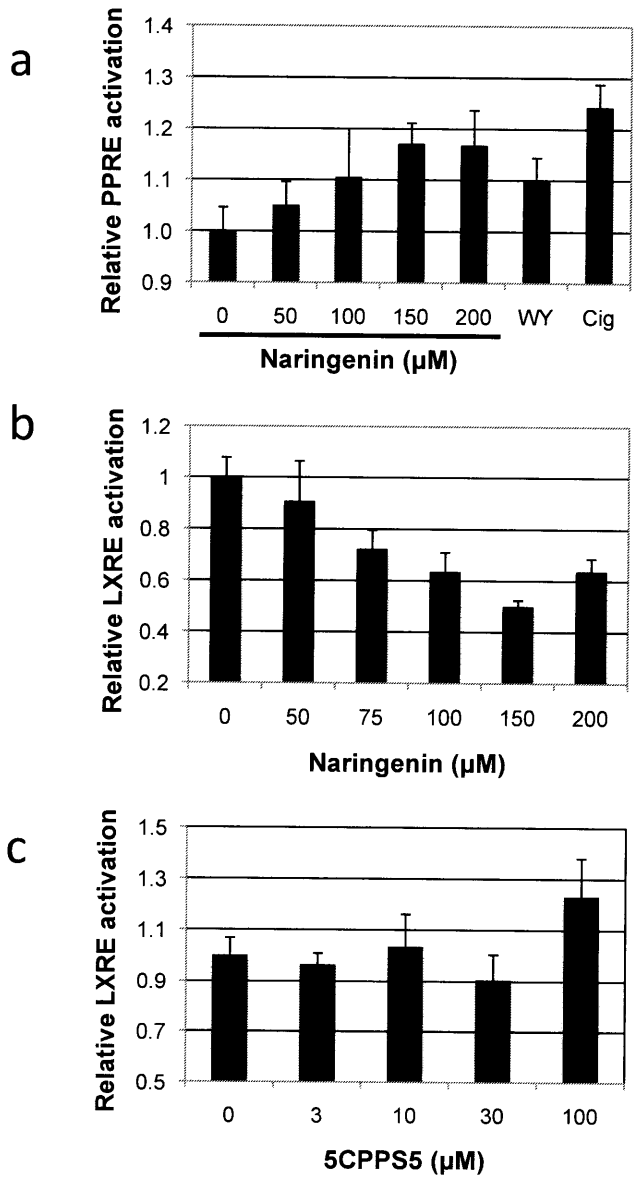

Figure 3 – Naringenin activates PPRE-driven and inhibits LXRE-driven gene expression. (a) In Huh7.5.1 cells transiently transfected with a PPRE-driven luciferase reporter, naringenin dose-dependently enhanced expression of luciferase reaching 17% ± 7% ($p<0.05$) at 200μM,similar to the PPAR agonists WY14,643 and ciglitazone. (b) In Huh7.5.1 cells transiently transfected with an LXRE-driven luciferase reporter, naringenin dose-dependently suppressed expression of luciferase controlled by LXRE, reaching a 50.3% ± 2.6% ($p<0.001$) inhibition at 150μM .(c) 5CPPS5 led to no change in LXRE activity. In all experiments, Renilla luciferase was used to account for variability in transfection efficiencies. *5CPPS5 was a kind gift of Dr. Yuichi Hashimoto, University of Tokyo, Japan.*

4.2.4 Naringenin enhances PPARα-regulated genes and decreases lipid secretion

Given our observations regarding naringenin's effects on NRs, we wished to examine its effects on PPAR- and LXR-regulated gene expression. Prior to measurement of PPARα-regulated mRNA abundance, cells were grown to confluence and incubated with OptiMEM low-serum media overnight. Cells were then treated with 200 μM naringenin for 24 hours and RNA was isolated for analysis by qRT-PCR (**Figure 4a,b**). Naringenin induced PPARα-regulated genes CYP4A11/22, ACOX, and ApoAI by 68%, 31%, and 25%, respectively. Naringenin also reduced the expression of LXRα-regulated genes ABCA1, LXRα, and ABCG1 by 92%, 60%, and 27%, respectively. Interestingly, naringenin also modulated the expresssion of other transcription factors, such as SREBP1 and PPARγ (**Figure 4c**).

We have previously shown that naringenin treatment reduces the secretion of VLDL (24). As our results suggest that naringenin exerts its effects partly through activation of PPARs, we next examined the effects of the PPARα and PPARγ agonists, WY14,643 and ciglitazone, on the secretion of ApoB. Huh7.5.1 cells were stimulated for 24 hours with 200μM naringenin, 10μM WY14,643, or 10μM ciglitazone, and media was collected and analyzed (**Figure 4d**). Predictably, naringenin treatment led to a 73% ± 9% ($p<0.001$) reduction in ApoB production. This compared with a 33% ± 12% ($p<0.01$) reduction produced by treatment with WY14,643. Treatment with cigilitazone did not lead to a significant change in VLDL production.

Lastly, we wished to examine naringenin's effects on several key metabolites. Specifically, we predicted that naringenin treatment would reduce the secretion of triglycerides from cells and that bile acid production would be reduced due to suppression of the LXRα pathway (25, 26). Primary rat hepatocytes were stimulated with 200μM and media was analyzed for urea, triglycerides, and bile salts content (**Figure 4e**). Naringenin treatment led to a 61% ± 19% ($p<0.001$) reduction in triglyceride accumulation in the medium and a 32% ± 11% ($p=0.005$) reduction in bile salt production. Urea accumulation in the media did not change significantly, however.

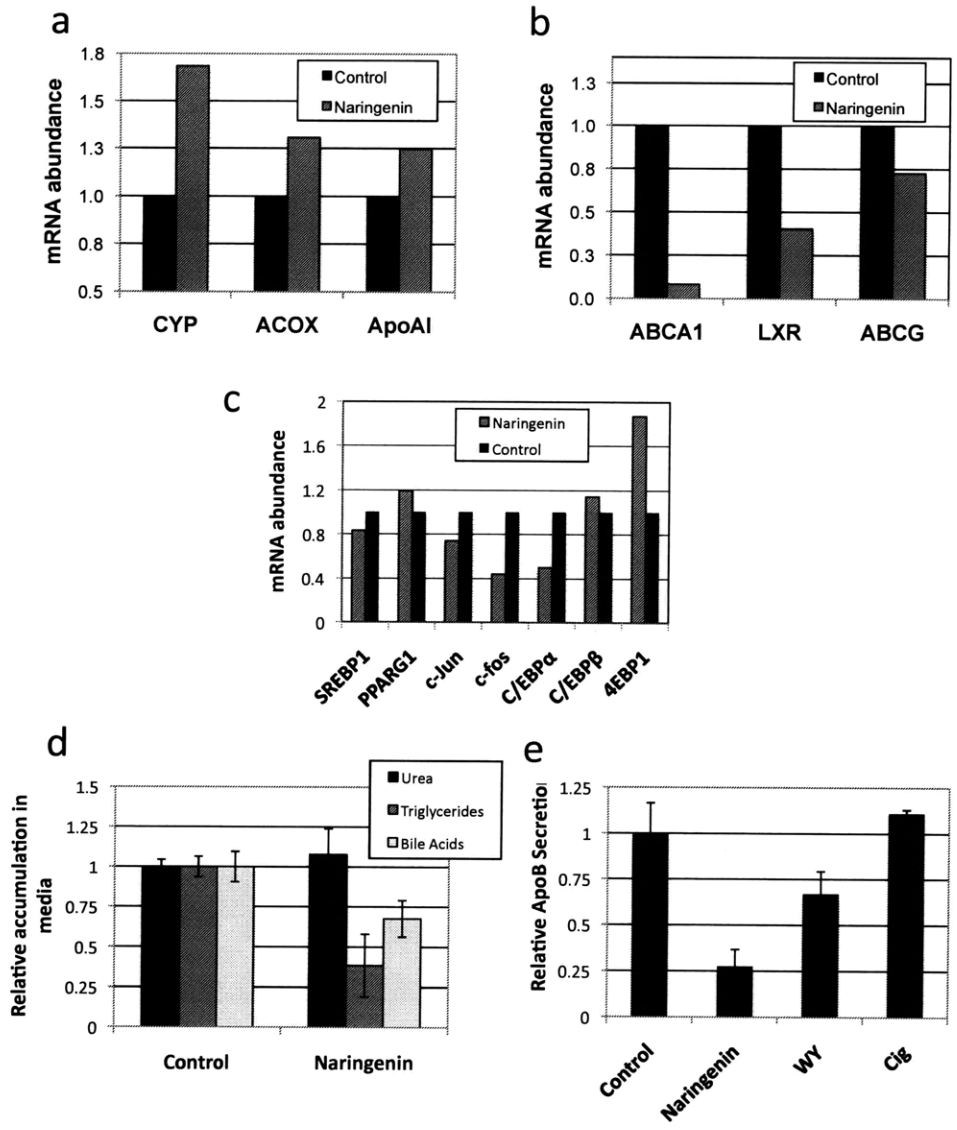

Figure 4 – Naringenin regulates PPARα- and LXRα-controlled genes and inhibts lipid secretion. Cells were treated with 200 μM naringenin for 24 hours as described and RNA was isolated for analysis by qRT-PCR. (a) Naringenin induced PPARα-regulated genes. CYP4A11/22, ACOX, and ApoAI were induced 68%, 31%, and 25%, respectively. (b) Naringenin reduced the expression of LXRα-induced genes. ABCA1, LXRα, and ABCG1 were downregulated by 92%, 60%, and 27%, respectively. (c) Huh7.5.1 cells were stimulated for 24 hours with 200μM naringenin, 10μM WY14,643, or 10μM ciglitazone, and media was collected and analyzed. Naringenin treatment led to a 73% ± 9% ($p<0.001$) reduction in ApoB production, while WY14,643 led to a 33% ± 12% ($p<0.01$) reduction. Treatment with cigilitazone did not lead to a significant change in VLDL production. (d) Primary rat hepatocytes were stimulated with 200μM and media was analyzed for urea, triglycerides, and bile salts. Naringenin treatment led to a 61% ± 19% ($p<0.001$) reduction in triglyceride accumulation and a 32% ± 11% ($p=0.005$) reduction in bile salt production. Urea accumulation in the media did not change significantly.

4.3 Discussion

Dysregulation of lipid and carbohydrate homeostasis is associated with multiple disease states, including metabolic, inflammatory, and infectious disorders (27). Metabolic regulation is achieved in mammals through an intricate mechanism that responds to multiple physiological cues. The response to dietary glucose, for example, is highly dependent on secretion of insulin and inhibition of glucagon secretion by pancreatic alpha and beta cells (28). In hepatocytes, both insulin and glucose metabolites induce expression of genes encoding glucose transporters and glycolytic and lipogenic enzymes, such as the L-type pyruvate kinase (L-PK), acetyl-CoA carboxylase (ACC), and fatty acid synthase (FASN) (29). Concomitantly, genes of the gluconeogenic pathway, such as the phosphoenolpyruvate carboxykinase gene, are downregulated (28, 30).

In recent years, several NRs have emerged as key regulators of cellular metabolism (26, 31, 32), with specific metabolites shown to be their natural ligands: LXRs respond to oxysterols and glucose (33, 34), the farnesoid X receptor (FXR) which responds to bile acids (35), and PPARs, which respond to fatty acids (36).

The PPAR family of NRs includes PPARα, PPARγ, and PPARδ. The prevalence of these receptor subtypes varies in different tissues, with PPARα being the most prevalent subtype in the liver, and PPARγ the most abundant in adipose tissue (20). PPARα is activated by fatty acids released in a physiological *fasting* state, leading to increased β-oxidation and gluconeogenesis (37, 38). In clinical practice, PPARα agonists (fibrates) are used to treat hyperlipidemia, whereas PPARγ agonists (TZDs) are used to increase insulin sensitivity (21, 39).

The LXR family of NRs includes both LXRα and LXRβ (33, 34, 40). The latter is ubiquitously expressed, while the former is found primarily in the liver, adipose tissue, and macrophages and is activated by the abundance of glucose and sterols (41), typical of a physiological *fed* state. In the liver, following activation by its ligands, LXRα activates lipogenic and glycolytic genes partly through activation of SREBP-1c (42, 43). Several of these genes are involved in the production of VLDL and its secretion by hepatocytes (44).

Following the binding of a ligand, both PPARs and LXRs become activated and heterodimerize with another NR, the retinoid X receptor (RXR) (31). The activated heterodimer then binds conserved response elements in specific genes, while recruiting other co-regulatory molecules, such as the co-activators PGC1α (45) and Trap220 (46) for PPARα and LXRα, respecitvely. The requirement of both LXR and PPAR for the RXR binding partner leads to competitive inhibition at the level of receptor activation, offering a transcriptional layer of control over fasted-to-fed transition (18, 47, 48). The existence of both a PPRE and an LXRE in the regulatory region of the LXRα gene (49, 50) suggests further levels of cross-regulation. Lastly, other coactivators, corepressors and kinases, such as PI3K and ERK, can regulate nuclear receptor activity by non-transcriptional mechanisms (51-53).

Naringin is an abundant citrus flavonoid responsible for the bitter taste in grapefruit. Naringin is hydrolyzed to its aglycone form, naringenin, prior to being absorbed in the intestine. Naringenin has been reported to be an antioxidant with demonstrated hypolipidemic, anti-carcinogenic and anti-inflammatory properties (5). The molecular mechanism behind naringenin's hypolipidemic effect has been studied mainly in HepG2 cells, where naringenin was shown to reduce the secretion of VLDL and LDL (54, 55) through the inhibition of ACAT2 and MTP (54, 56), critical enzymes for VLDL assembly. Allister *et al.* demonstrated that this inhibition is regulated primarily through the mitogen-activated protein kinase pathway, through MEK1/2 and ERK1/2 (56). In addition, naringenin was shown to upregulate LDL receptor (LDL-R) (23), whose expression in the ER leads to the degradation of ApoB (57, 58). This induction of LDL-R transcription was shown to be caused by activation of PI3K upstream of SREBP-1 (23). Naringenin has also been shown to inhibit HMGR (59), while activating enzymes important in fatty acid oxidation such as CYP4A1 (60). These myriad effects suggest that the flavonoid's target might be at the nuclear receptor level. Strengthening this hypothesis is the anecdotal report that naringenin interacts with LXR (23) and, more recently, that it activates PPARα in U-2OS cells (61). A similar pathway was demonstrated for green tea polyphenols, soy isoflavones, and the citrus flavone tangeretin, which regulate LXRα and PPARα (62, 63).

In vivo studies provide further evidence of naringenin's hypolipidemic effects. In a recent clinical trial, a daily 400 mg dose of naringenin was shown to reduce circulating LDL levels by 17% in hypercholesterolemic patients (7). Similar cholesterol lowering effects of naringenin have been demonstrated in rabbits (8, 9) and rats (10).

In our study, we first showed that naringenin functioned as a PPARα and PPARγ agoinst in a reporter cell line. In this system, a previously described HeLa cell line was used, in which either the PPARα or PPARγ LBD attached to a GAL4 DNA binding domain was being constitutively expressed (22). Luciferase expression was driven by a GAL4 upstream activating sequence (UAS_G) in response to the activity of agonists on the NR LBD. Our results demonstrate that naringenin significantly activated both PPARα and PPARγ compared to known agonists.

Next, a LanthScreen time-resolved fluorescence resonance energy transfer (TR-FRET) assay was used to explore further the direct effect of naringenin on the PPARα LBD. In this cell-free assay, a donor fluorophore is attached to PGC1α, a PPARα co-activator, while an acceptor flurophore is attached to the LBD of PPARα. A conformational shift induced by agonist binding increases the affinity of the co-activator for the LBD, and leads to enhanced binding and an increase in FRET. In this assay, while increasing concentrations of GW7647, a known PPARα agonist, led to an increase in FRET signal, no such increase was observed in response to naringenin up to a concentration of 133μM, suggesting that PPARα activation does not occur through a direct enhancement of PPARα's affinity for the PGC1a co-activator.

To examine the ability of naringenin to drive PPRE-regulated gene expression, we transiently transfected Huh7.5.1 cells, a heptoma-derived cell line, with a previously described PPRE-driven reporter plasmid (17). This plasmid encodes two copies of the AOX PPRE upstream of the firefly luciferase reporter, and has been demonstrated to respond to PPAR agonists. We showed that naringenin significantly increased the expression of the PPRE-driven luciferase. Furthermore, PPRE activation was statistically similar to that obtained using both WY14,643 and ciglitazone. In our hands, PPRE activation by naringenin was critically dependent on culture conditions: when cells were seeded at low density or were not serum-starved prior to stimulation, naringenin's effect on PPRE activation was either abolished or reversed (data not shown),

suggesting that naringenin's effect on PPAR induction is dependent on the metabolic state of the cell. This phenomenon is currently under further investigation.

We next tested the ability of naringenin to inhibit LXRα, as the inhibition of LXRα activity would be expected to lead to a decrease in VLDL secretion. First, as in the case of PPAR, the effect of naringenin on activation of an LXRα-GAL4 chimera was examined in a reporter cell line. GeneBlazer LXR-alpha-UAS-bla HEK 293T cells were treated with TO901317 at the agonist's EC80 (250nM) and increasing concentrations of naringenin, and the resulting signal was quantified. Naringenin inhibited LXRα activity in this system significantly. Given these results, we continued to explore the mechanism of LXRα inhibtion using a LanthaScreen LXRα TR-FRET assay. Analogously to the PPARα LanthaScreen assay, this assay measures the FRET between a donor flurophore bound to the Trap-220 co-activator and the LXRα LBD. At concentrations higher than 100μM, naringenin increased the FRET signal moderately, but significantly, consistent with the behavior of a weak agonist of LXRα. This suggested that when co-applied with TO901317, naringenin would act as an antagonist. Indeed, we observed a reduction in the FRET signal when increasing concentrations of naringenin were added in the presence of TO901317. These results suggest the naringenin's inhibitory effect on LXRα could in part be the result of competitive inhibition with the NR's natural ligands.

To examine the ability of naringenin to inhibit the activity of an LXRE-driven gene expression, Huh7.5.1 cells were transiently transfected with an LXRE-driven reporter plasmid (18) and treated with increasing concentrations of naringenin in the presence of TO901317. Naringenin dose-dependently inhibited luciferase expression, reaching 50.3% at 150μM. Interestingly, mirroring the decreased activation of PPARγ observed in the PPARγ-GAL4 system at higher concentrations, LXRE activity was also higher at 200μM than at 150μM.

We next wished to examine the effects of naringenin on gene transcription and metabolism. Huh7.5.1 cells were treated with naringenin and analyzed for changes in mRNA abundance by qRT-PCR. Genes involved in β-oxidation and reverse cholesterol transport, CYP4A11/22, ACOX, and ApoAI increased by 68%, 31%, and 25%, respectively. Naringenin also reduced the

expression of LXRα-regulated genes involved in glucose transport and lipogenesis, ABCA1, LXRα, and ABCG1 by 92%, 60%, and 27%, respectively.

Naringenin's effects on NRs and their downstream genes led us to hypothesize that cells treated with the flavonoid would produce less triglycerides and bile salts, specifically in rat hepatocytes, as LXRα activation has been shown to drive lipid and bile synthesis in rats (25, 26). Primary rat hepatocytes treated with naringenin indeed secreted less triglycerides and bile salts than untreated controls. Importantly, urea secretion was maintained, suggesting naringenin' effects were not simply a result of cell death or loss of function.

Lastly, we examined the effects of other PPAR agonists on ApoB production. Huh7.5.1 cells were treated with naringenin, WY16,463 (PPARα agonist) or ciglitazone (PPARγ agonist). Naringenin and WY16,463 treatment led to significant reductions in ApoB secretion. Notably, naringenin's effect was significantly more pronounced than that of the PPARα agonist's. Furthermore, the PPARγ agonist, ciglitazone, did not change the production of ApoB significantly. These results suggest that in Huh7.5.1 cells, naringenin's PPARα activation is more important than its PPARγ activation in blocking VLDL production; and that other mechanisms, such as LXRα inhibition are likely contributing to the observed reduction, as well.

Several other investigations have analyzed the effects of small molecules on PPAR- and LXRα-driven gene activation. While many of these have demonstrated significant changes in response to suggested ligands, most have involved the over-expression of one or more nuclear receptors. While this has the obvious advantage of increasing signal-to-noise ratios, over-expression of receptors could result in a distortion of the cellular network of interacting NRs. We therefore chose not to over-express NRs, and rather to study the effects of naringenin in a heptoma cell line that contains limited amounts of these nuclear receptors.

Other mechanisms of naringenin's effect on lipid production and mobilization have been proposed. Huff and colleagues have extensively characterized the effects of naringenin on both insulin and MAPK signaling pathways. Specifically, naringenin was shown to inhibit the activity of MTP, the rate-limiting enzyme in VLDL assembly, through the activation of MAPK signaling,

leading to a decrease in VLDL secretion in HepG2 cells (56). Furthermore, naringenin activates PI3K signaling, leading to the upregulation of LDL-R expression (23), which has been shown in a separate study to lead to a degradation of ApoB in the ER (57, 58). While our observations are generally consistent with these previous studies, some minor discrepancies could be explained by differences in experimental conditions, such as cell types that were used and time scales that were examined. The relationship between naringenin's previously described mechanisms of action and its effects on nuclear receptor signaling – whether causative, associative, or independent – remains to be established.

Naringenin's ability to decrease VLDL secretion by hepatocytes could lead to benefits in treating varied disease states, including atherogenic processes and infectious disease. The antiatherogenic effects of naringenin have been widely explored, most recently in mice (19). The ability of the molecule to agonize both the PPARα and PPARγ receptors, suggest it could have both anti-lipogenic effects and insulin-sensitzing properties, as has been clinically demonstrated by the fibrate (PPARα agonist) and TZD (PPARγ agonist) classes of drugs, respectively. Indeed, dual PPARα and PPARγ agonists have recently been investigated as normoglycemic and antiatherogenic agents (64).

Recently, our group has shown that naringenin inhibits the secretion of ApoB from HCV-infected Huh7.5.1 cells, and that inhibition of VLDL secretion from hepatocytes leads to a decrease in HCV particle accumulation in media (24). Other groups have demonstrated similar reductions in virus secretion in response to inhibition of VLDL production and secretion (65, 66). We are currently conducting a clinical trial to explore the possible effects of short-term naringenin treatment in non-responsive HCV patients. Recently, it has been demonstrated that lipogenic changes observed in hepatitis B (HBV)-associated hepatic steatosis are mediated by the induction of LXR and its target genes by the viral HBx protein (67, 68). Due to naringenin's inhibitory effects on LXR, the molecule could prove useful in abating the steatotic process associated with HBV infection.

Lastly, there is increasing evidence for the link between metabolic, inflammatory, and infectious disease (69). Atherosclerosis is known to be mediated by inflammatory processes,

and recent evidence suggests that drugs designed to mitigate atherogenesis, such as statins, exert part of their clinical benefits through their anti-inflammatory effects (70). Similarly, a large body of work has demonstrated the detrimental effects of inflammation on the liver in the context of viral hepatitis, steatosis, and the development of hepatocellular carcinoma (71). Naringenin's anti-oxidant, anti-inflammatory, anti-thrombotic, and vasodilatory effects, could increase the potential of the molecule's therapeutic potential.

4.4 Materials and Methods

Reagents

Fetal bovine serum (FBS), phosphate-buffered saline (PBS), Dulbecco's modified Eagle medium (DMEM), penicillin, streptomycin, trypsin-ethylene diamine tetraacetic acid (EDTA), OptiMEM basal medium, and Lipofectamine 2000 were obtained from Invitrogen Life Technologies (Carlsbad, CA). Insulin was obtained from Eli-Lilly (Indianapolis, IN). Dual luciferase assay kit was purchased from Promega (Madison, WI). Unless otherwise noted, all other chemicals were purchased from Sigma-Aldrich Chemicals (St. Louis, MO).

Cell culture

The Huh7.5.1 human hepatoma cell line was kindly provided by Dr. Chisari (Scripps Research Institute, La Jolla, CA) and Dr. Wakita (National Institute of Infectious Diseases, Tokyo, Japan), respectively. Huh7.5.1 cells were cultured in DMEM supplemented with 10% FBS, 200 units/mL penicillin, and 200 mg/mL streptomycin in a 5% CO_2-humidified incubator at 37°C. Huh7.5.1 cells were passaged every 3 days and used at passage <15.

GAL4-nuclear receptor activation assays

PPAR activation was examined as previously described using the HGLN5 cell line. Briefly, HeLa cells were stably transfected with the p(GAL4RE)5-βGlob-Luc-SVNeo plasmid, encoding the firefly luciferase gene driven by a pentamer of yeast activator GAL4 binding sites in front of β-globin promoter. Cells were subsequently stably transfected with either pGAL4-PPARα-puro, or pGAL4-PPARγ-puro, encoding amino acids 1-147 of GAL4, followed by a short linker and the ligand binding domain of either PPARα or PPARγ, resecitvely. HGLN5 cells were treated with varying amounts of ethanol-dissolved naringenin and luciferase activity was compared to that of known agonists of PPARα and PPARγ, GW7647 or BRL49653, respectively.

LXRα activation was investigated using the GeneBLAzer Beta-lactamase reporter technology (Invitrogen SelectScreen Cell-Based Nuclear Receptor Profiling Service, Madison, WI). LXR-alpha-UAS-bla HEK 293T cells were thawed and resuspended in Assay Media (DMEM phenol red free, 2% CD-treated FBS, 0.1 mM NEAA, 1 mM Sodium Pyruvate, 100 U/mL/100 µg/mL

Pen/Strep) to a concentration of 312,500 cells/mL. The control agonist TO901317 at the pre-determined EC80 concentration (4.7 nM) was added to wells containing variable concentrations of naringenin. The plate was incubated for 16-24 hours at 37ºC/5% CO_2 in a humidified incubator. Substrate Loading Solution was added to each well and the plate is incubated for 2 hours at room temperature. The plate is read on a fluorescence plate reader. Results for each concentration (n=4) are reported as percent activation of TO901317-stimulated, naringenin-free controls.

TR-FRET Assays

LanthaScreen TR-FRET Coactivator Assays were used to identify agonists and/or antagonists of PPARα and of LXRα. In these cell-free assays, ligands are identified by their ability to bind the LBD of the respective receptor and induce a conformational change that results in recruitment of a fluorescein-labeled coactivator peptide. A purified, glutathione S-transferase (GST)-tagged PPAR alpha or LXRα ligand-binding domain (LBD) is indirectly labeled using a terbium-labeled anti-GST tag antibody. Recruitment of fluorescein-labeled coactivator peptide – PGC1a for PPARα or Trap220 for LXRα – is measured by monitoring fluorescence resonance energy transfer (FRET) from the terbium-labeled antibody to the fluorescein on the peptide, resulting in a high TR-FRET ratio (520 nm:490 nm emission). Test compounds were diluted in 100% DMSO, and assays were run per the manufacturer's instructions. Briefly, to test the ability of a molecule to function as an NR agonist, increasing concentrations of either naringenin or a control agonist were added to wells containing NR LBD and co-activator peptide solutions. To test the ability of a molecule to function as an LXRα antgonist, a similar protocol was followed, but 250nM TO901317 (EC80 of the agonist, as measured in this assay) was added to all wells. In both agonist and antagonist modes, following 1 to 2 hour incubation at room temperature, the 520/490 TR-FRET ratio was measured with a PerkinElmer Envision fluorescent plate reader with TRF laser excitation using the following filter set: excitation 330 nm, emission 495 nm, and emission 520 nm. A 100 µs delay followed by a 200 µs integration time was used to collect the time-resolved signal. Results are displayed as percent activation compared to maximal activation of positive control.

PPAR and LXRα response element luciferase reporter assays

To examine the ability of naringenin to drive luciferase expression from a PPRE- or LXRE response element reporter, Huh7.5.1 cells were transiently transfected with one of two previously described reporter plasmids, pAOx(x2)luc or pDR4(X2)luc, respectively (17, 18). The pRL-TK plasmid (Promega, Madison, WI), which constitutively expresses renilla luciferase under the control of the thymidine kinase promoter, was co-transfected to control for transfection efficiency. To examine PPRE-driven expression, pAOx(x2)luc was transfected into Huh7.5.1 cells, which were kept in OptiMEM for 22hrs following transfection. Media was then replaced by DMEM supplemented with 10% FBS, 200 units/mL penicillin, and 200 mg/mL streptomycin along with variable concentrations of naringenin, the known PPARα agonist WY14,643, or the known PPARγ agonist, ciglitizone. After 24 hours, cells were lysed in Passive Lysis Buffer (Promega). The ratio of firefly luciferase to renilla luciferase luminescence was quantified using a Dual Luciferase Assay kit (Promega) following the manufacturer's instructions on a FB12 Single Tube Luminometer (Berthold Technologies USA, Oak Ridge, TN). To examine LXRE-driven expression, cells were similarly transfected and treated with 1μM TO901317 along with varying concentrations of naringenin. Lysis and signal quantification were carried out as above. Naringenin was dissolved in DMSO. DMSO levels were equal in all samples and never exceeded 0.5%. Results are reported as percent activation compared to untreated (DMSO-only) controls.

qRT-PCR

Following a 4-hour stimulation, cells were lysed with RLT Plus buffer containing β-mercaptoethanol and RNA was isolated using RNeasy Mini Kit on a QIACube device (Qiagen, Valencia, CA). Total RNA was quantified on a ND-1000 spectrophotometer (NanoDrop Technologies, Rockland, Del.) and mRNA transcript abundance was measured on a MyiQ Real-Time PCR Detection System using iScript One-Step RT-PCR Kit With SYBR Green (Bio-Rad, Hercules, CA), according to the manufacturers' instructions. Primers used in these reactions (Integrated DNA Technologies, Coralville, IA) were designed using the PRIMER-BLAST program and appear in Table 1. The Insulin Signaling Pathway PCR Array from SABiosciences was used

with a RT^2 First Strand Kit for reverse transciption and RT^2 qPCR Master Mix (Frederick, MD) on a Strategene Mx3000 cycler.

Gene	Primers
CYP4A11/22	ACT GGC TCT TCG GGC ACA TC
	ACA CGA ACT TTG CCT CCC CA
ACOX	TGG CAC ATA CGT GAA ACC GC
	CGC TGT ATC GGA TGG CAA TG
ApoAI	AAA GCT GCG GTG CTG ACC TT
	CGC TGT CTT TGA GCA CAT CCA
LXRa	GCT CCT TTT CTG ACC GGC TT
	TGA ATT CCA CTT GCA GCC CT
ABCA1	TCT GGA AAG CTC TGA AGC CG
	TGA GTT CCT CCC ACA TGC CT
ABCG1	ACC GGG GAA AAG TCT GCA AT
	TCA CCA GCC GAC TGT TCT GA

Table 1 – List of primers used for qRT-PCR analysis.

ApoB secretion analysis

Huh7.5.1 cells were incubated overnight in OptiMEM I media. Cells were then treated with media containing naringenin for 24 hours, and then media was collected and analyzed. ApoB was quantified in the medium using the ALerCHEK, Inc. (Portland, ME), total human ApoB ELISA kit. Media was diluted 1:10 with the specimen diluent, and the assay was carried out according to the manufacturer's directions.

Metabolite assays

To assess the amount of triglycerides that were produced by the cultured hepatocytes, Triglyceride Reagent and the Free Glycerol Reagent were used. The two reagents were combined into a working stock solution by creating a 4 to 1 mixture of Triglyceride Reagent and Free Glycerol Reagent, respectively. Briefly, in the assay, triglycerides are broken down into glycerol backbones and hydrocarbon chains. The glycerol backbone then reacts with the Free Glycerol Reagent and is read at 540 nm on a spectrophotometer. 2μl of media were added in a

96 well plate to 200 μl of working stock solution and allowed to incubate at 37ºC for 5 minutes. After incubation, the amount of glycerol in the solution was assayed on a spectrophotometer plate reader at 540 nm.

4.5 References

1. McGarry JD, Foster DW. Regulation of hepatic fatty acid oxidation and ketone body production. Annu Rev Biochem 1980;49:395-420.

2. Gastaldelli A, Kozakova M, Hojlund K, Flyvbjerg A, Favuzzi A, Mitrakou A, Balkau B. Fatty liver is associated with insulin resistance, risk of coronary heart disease, and early atherosclerosis in a large European population. Hepatology 2009;49:1537-1544.

3. Buchman A, Korenblatt K, Klein S: Nutrition and the Liver. In: Schiff ER, Sorrell MF, Maddrey WC, eds. Schiff's diseases of the liver, 2006.

4. Hogan P, Dall T, Nikolov P, Association AD. Economic costs of diabetes in the US in 2002. Diabetes Care 2003;26:917-932.

5. Wilcox, Borradaile, Huff. Antiatherogenic Properties of Naringenin, a Citrus Flavonoid. Cardiovascular Drug Reviews 1999.

6. Crozier A, Jaganath IB, Clifford MN. Dietary phenolics: chemistry, bioavailability and effects on health. Natural product reports 2009;26:1001-1043.

7. Jung UJ, Kim HJ, Lee JS, Lee MK, Kim HO, Park EJ, Kim HK, et al. Naringin supplementation lowers plasma lipids and enhances erythrocyte antioxidant enzyme activities in hypercholesterolemic subjects. Clinical Nutrition 2003;22:561–568.

8. Kurowska E, Borradaile N, Spence JD, Carroll KK. Hypocholesterolemic effects of dietary citrus juices in rabbits. Nutr. Res. 2000;20:121-129.

9. Lee C-H, Jeong T-S, Choi Y-K, Hyun B-H, Oh G-T, Kim E-H, Kim J-R, et al. Anti-atherogenic effect of citrus flavonoids, naringin and naringenin, associated with hepatic ACAT and aortic VCAM-1 and MCP-1 in high cholesterol-fed rabbits. Biochem Biophys Res Commun 2001;284:681-688.

10. Kim S-Y, Kim H-J, Lee M-K, Jeon S-M, Do G-M, Kwon E-Y, Cho Y-Y, et al. Naringin time-dependently lowers hepatic cholesterol biosynthesis and plasma cholesterol in rats fed high-fat and high-cholesterol diet. J Med Food 2006;9:582-586.

11. Wilcox LJ, Borradaile NM, Dreu LEd, Huff MW. Secretion of hepatocyte apoB is inhibited by the flavonoids, naringenin and hesperetin, via reduced activity and expression of ACAT2 and MTP. Journal of Lipid Research 2001;42:725-734.

12. Kurowska EM, Manthey JA, Casaschi A, Theriault AG. Modulation of HepG2 Cell Net Apolipoprotein B Secretion by the Citrus Polymethoxyflavone, Tangeretin. Lipids 2004;39:143–151.

13. Borradaile NM, Dreu LEd, Barrett PHR, Huff MW. Inhibition of hepatocyte apoB secretion by naringenin: enhanced rapid intracellular degradation independent of reduced microsomal cholesteryl esters. Journal of Lipid Research 2002;43.

14. Borradaile NM, Dreu LEd, Huff MW. Inhibition of Net HepG2 Cell Apolipoprotein B Secretion by the Citrus Flavonoid Naringenin Involves Activation of Phosphatidylinositol 3-Kinase, Independent of Insulin Receptor Substrate-1 Phosphorylation. Diabetes 2003;52:2554-2561.

15. Huong DT, Takahashi Y, Ide T. Activity and mRNA levels of enzymes involved in hepatic fatty acid oxidation in mice fed citrus flavonoids. Nutrition 2006;22:546-552.

16. Liu L, Shan S, Zhang K, Ning Z-Q, Lu X-P, Cheng Y-Y. Naringenin and Hesperetin, Two Flavonoids Derived from Citrus aurantium Up-regulate Transcription of Adiponectin. Phytotherapy Research 2008;22:1400-1403.

17. Marcus, Miyata, Zhang, Subramani, Rachubinski, Capone. Diverse peroxisome proliferator-activated receptors bind to the peroxisome proliferator-responsive elements of the rat hydratase/dehydrogenase and fatty acyl-CoA oxidase genes but differentially induce expression. Proc Natl Acad Sci USA 1993;90:5723-5727.

18. Miyata, McCaw, Patel, Rachubinski, Capone. The orphan nuclear hormone receptor LXR alpha interacts with the peroxisome proliferator-activated receptor and inhibits peroxisome proliferator signaling. J Biol Chem 1996;271:9189-9192.

19. Mulvihill EE, Allister EM, Sutherland BG, Telford DE, Sawyez CG, Edwards JY, Markle JM, et al. Naringenin prevents dyslipidemia, apoB overproduction and hyperinsulinemia in LDL-receptor null mice with diet-induced insulin resistance. Diabetes 2009.

20. Lee, Olson, Evans. Minireview: lipid metabolism, metabolic diseases, and peroxisome proliferator-activated receptors. Endocrinology 2003;144:2201-2207.

21. Gervois P, Fruchart J, Staels B. Drug Insight: mechanisms of action and therapeutic applications for agonists of peroxisome proliferator-activated receptors. Nature clinical practice Endocrinology & metabolism 2007;3:145-156.

22. Seimandi, Lemaire, Pillon, Perrin, Carlavan, Voegel, Vignon, et al. Differential responses of PPARalpha, PPARdelta, and PPARgamma reporter cell lines to selective PPAR synthetic ligands. Anal Biochem 2005;344:8-15.

23. Borradaile, Dreu d, Huff. Inhibition of net HepG2 cell apolipoprotein B secretion by the citrus flavonoid naringenin involves activation of phosphatidylinositol 3-kinase, independent of insulin receptor substrate-1 phosphorylation. Diabetes 2003;52:2554-2561.

24. Nahmias, Goldwasser, Casali, Poll v, Wakita, Chung, Yarmush M. Apolipoprotein B-dependent hepatitis C virus secretion is inhibited by the grapefruit flavonoid naringenin. Hepatology 2008;47:1437-1445.

25. Gupta S, Pandak WM, Hylemon PB. LXR alpha is the dominant regulator of CYP7A1 transcription. Biochem Biophys Res Commun 2002;293:338-343.

26. Fabiani D. Lipid-activated nuclear receptors: from gene transcription to the control of cellular metabolism. Eur. J. Lipid Sci. Technol 2004.

27. Mittra, Bansal, Bhatnagar. From a glucocentric to a lipocentric approach towards metabolic syndrome. Drug Discovery Today 2008.

28. Saltiel AR, Kahn CR. Insulin signalling and the regulation of glucose and lipid metabolism. Nature 2001;414:799-806.

29. Gregori C, Guillet-Deniau I, Girard J, Decaux JF, Pichard AL. Insulin regulation of glucokinase gene expression: evidence against a role for sterol regulatory element binding protein 1 in primary hepatocytes. FEBS Letters 2006;580:410-414.

30. Vaulont, Vasseur-Cognet, Kahn. Glucose Regulation of Gene Transcription. Journal of Biological Chemistry 2000.

31. Gronemeyer, Gustafsson, Laudet. Principles for modulation of the nuclear receptor superfamily. Nat Rev Drug Discov 2004;3:950-964.

32. Ory. Nuclear receptor signaling in the control of cholesterol homeostasis: have the orphans found a home? Circulation Research 2004;95:660-670.

33. Mitro, Mak, Vargas, Godio, Hampton, Molteni, Kreusch, et al. The nuclear receptor LXR is a glucose sensor. Nature 2007;445:219-223.

34. Edwards, Kennedy, Mak. LXRs; oxysterol-activated nuclear receptors that regulate genes controlling lipid homeostasis. Vascul Pharmacol 2002;38:249-256.

35. Sinal CJ, Tohkin M, Miyata M, Ward JM, Lambert G, Gonzalez FJ. Targeted disruption of the nuclear receptor FXR/BAR impairs bile acid and lipid homeostasis. Cell 2000;102:731-744.

36. Gottlicher M, Widmark E, Li Q, Gustafsson JA. Fatty acids activate a chimera of the clofibric acid-activated receptor and the glucocorticoid receptor. Proc Natl Acad Sci U S A 1992;89:4653-4657.

37. Martin, Guillou, Lasserre, Déjean, Lan, Pascussi, Sancristobal, et al. Novel aspects of PPARalpha-mediated regulation of lipid and xenobiotic metabolism revealed through a nutrigenomic study. Hepatology 2007;45:767-777.

38. Raalte v, Li, Pritchard, Wasan. Peroxisome proliferator-activated receptor (PPAR)-alpha: a pharmacological target with a promising future. Pharm Res 2004;21:1531-1538.

39. Vuppalanchi R, Chalasani N. Nonalcoholic fatty liver disease and nonalcoholic steatohepatitis: Selected practical issues in their evaluation and management. Hepatology 2009;49:306-317.

40. Millatt, Bocher, Fruchart, Staels B. Liver X receptors and the control of cholesterol homeostasis: potential therapeutic targets for the treatment of atherosclerosis. Biochim Biophys Acta 2003;1631:107-118.

41. Forman, Ruan, Chen, Schroepfer, Evans. The orphan nuclear receptor LXRalpha is positively and negatively regulated by distinct products of mevalonate metabolism. Proc Natl Acad Sci USA 1997;94:10588-10593.

42. Yoshikawa, Shimano, Amemiya-Kudo, Yahagi, Hasty, Matsuzaka, Okazaki, et al. Identification of liver X receptor-retinoid X receptor as an activator of the sterol regulatory element-binding protein 1c gene promoter. Molecular and Cellular Biology 2001;21:2991-3000.

43. Pawar, Botolin, Mangelsdorf, Jump. The Role of Liver X Receptor-α in the Fatty Acid Regulation of Hepatic Gene Expression. Journal of Biological Chemistry 2003.

44. Venkateswaran, Laffitte, Joseph, Mak, Wilpitz, Edwards, Tontonoz. Control of cellular cholesterol efflux by the nuclear oxysterol receptor LXR alpha. Proc Natl Acad Sci USA 2000;97:12097-12102.

45. Vega RB, Huss JM, Kelly DP. The coactivator PGC-1 cooperates with peroxisome proliferator-activated receptor alpha in transcriptional control of nuclear genes encoding mitochondrial fatty acid oxidation enzymes. Molecular and Cellular Biology 2000;20:1868-1876.

46. Son YL, Lee YC. Molecular determinants of the interactions between LXR/RXR heterodimers and TRAP220. Biochem Biophys Res Commun 2009;384:389-393.

47. Ide, Shimano, Yoshikawa, Yahagi, Amemiya-Kudo, Matsuzaka, Nakakuki, et al. Cross-talk between peroxisome proliferator-activated receptor (PPAR) alpha and liver X receptor (LXR) in nutritional regulation of fatty acid metabolism. II. LXRs suppress lipid degradation gene promoters through inhibition of PPAR signaling. Molecular Endocrinology 2003;17:1255-1267.

48. Yoshikawa, Ide, Shimano, Yahagi, Amemiya-Kudo, Matsuzaka, Yatoh, et al. Cross-talk between peroxisome proliferator-activated receptor (PPAR) alpha and liver X receptor (LXR) in nutritional regulation of fatty acid metabolism. I. PPARs suppress sterol regulatory element binding protein-1c promoter through inhibition of LXR signaling. Molecular Endocrinology 2003;17:1240-1254.

49. Laffitte, Joseph, Walczak, Pei, Wilpitz, Collins, Tontonoz. Autoregulation of the human liver X receptor alpha promoter. Molecular and Cellular Biology 2001;21:7558-7568.

50. Tobin, Steineger, Alberti, Spydevold, Auwerx, Gustafsson, Nebb. Cross-talk between fatty acid and cholesterol metabolism mediated by liver X receptor-alpha. Molecular Endocrinology 2000;14:741-752.

51. Hu, Li, Wu, Xia, Lala. Liver X receptors interact with corepressors to regulate gene expression. Molecular Endocrinology 2003;17:1019-1026.

52. Rochette-Egly. Nuclear receptors: integration of multiple signalling pathways through phosphorylation. Cellular Signalling 2003.

53. McKenna, O'Malley. Combinatorial Control of Gene Expression by Nuclear Receptors and Coregulators. Cell 2002.

54. Wilcox, Borradaile, Dreu d, Huff. Secretion of hepatocyte apoB is inhibited by the flavonoids, naringenin and hesperetin, via reduced activity and expression of ACAT2 and MTP. J Lipid Res 2001;42:725-734.

55. Borradaile, Dreu d, Barrett, Huff. Inhibition of hepatocyte apoB secretion by naringenin: enhanced rapid intracellular degradation independent of reduced microsomal cholesteryl esters. J Lipid Res 2002;43:1544-1554.

56. Allister, Borradaile, Edwards, Huff. Inhibition of microsomal triglyceride transfer protein expression and apolipoprotein B100 secretion by the citrus flavonoid naringenin and by insulin involves activation of the mitogen-activated protein kinase pathway in hepatocytes. Diabetes 2005;54:1676-1683.

57. Gillian-Daniel DL, Bates PW, Tebon A, Attie AD. Endoplasmic reticulum localization of the low density lipoprotein receptor mediates presecretory degradation of apolipoprotein B. Proc Natl Acad Sci USA 2002;99:4337-4342.

58. Twisk J, Gillian-Daniel DL, Tebon A, Wang L, Barrett PH, Attie AD. The role of the LDL receptor in apolipoprotein B secretion. Journal of Clinical Investigation 2000;105:521-532.

59. Jeon SM, Kim HK, Kim HJ, Do GM, Jeong TS, Park YB, Choi MS. Hypocholesterolemic and antioxidative effects of naringenin and its two metabolites in high-cholesterol fed rats. Transl Res 2007;149:15-21.

60. Huong DT, Takahashi Y, Ide T. Activity and mRNA levels of enzymes involved in hepatic fatty acid oxidation in mice fed citrus flavonoids. Nutrition (Burbank, Los Angeles County, Calif) 2006;22:546-552.

61. Liu, Shan, Zhang, Ning, Lu, Cheng. Naringenin and hesperetin, two flavonoids derived from Citrus aurantium up-regulate transcription of adiponectin. Phytotherapy research : PTR 2008;22:1400-1403.

62. Kurowska, Manthey, Casaschi, Theriault. Modulation of HepG2 cell net apolipoprotein B secretion by the citrus polymethoxyflavone, tangeretin. Lipids 2004;39:143-151.

63. Huang TH, Teoh AW, Lin BL, Lin DS, Roufogalis B. The role of herbal PPAR modulators in the treatment of cardiometabolic syndrome. Pharmacol Res 2009;60:195-206.

64. Chang F, Jaber LA, Berlie HD, O'Connell MB. Evolution of peroxisome proliferator-activated receptor agonists. Ann Pharmacother 2007;41:973-983.

65. Gastaminza, Cheng, Wieland, Zhong, Liao, Chisari. Cellular determinants of hepatitis C virus assembly, maturation, degradation, and secretion. Journal of Virology 2008;82:2120-2129.

66. Huang, Sun, Owen, Li, Chen, Gale, Ye. Hepatitis C virus production by human hepatocytes dependent on assembly and secretion of very low-density lipoproteins. Proc Natl Acad Sci USA 2007;104:5848-5853.

67. Kim, Kim, Kim, Cheong. Hepatitis B virus X protein induces lipogenic transcription factor SREBP1 and fatty acid synthase through the activation of nuclear receptor LXRalpha. Biochem J 2008;416:219-230.

68. Na, Shin, Roh, Kang, Hong, Oh, Seong, et al. Liver X receptor mediates hepatitis B virus X protein-induced lipogenesis in hepatitis B virus-associated hepatocellular carcinoma. Hepatology 2008.

69. Sheikh M, Choi J, Qadri I, Friedman J, Sanyal A. Hepatitis C virus infection: molecular pathways to metabolic syndrome. Hepatology 2008;47:2127-2133.

70. Montecucco F, Mach F. Update on statin-mediated anti-inflammatory activities in atherosclerosis. Semin Immunopathol 2009;31:127-142.

71. Mahmood S, Togawa K, Kawanaka M, Niiyama G, Yamada G. An Analysis of Risk Factors for Developing Hepatocellular Carcinoma in a Group of Hepatitis C Patients with Stage 3 Fibrosis following Interferon Therapy. Cancer Inform 2008;6:381-387.

5 Enhancement of Naringenin Bioavailability by Complexation with Hydroxypropoyl-β-cyclodextrin

5.1 Introduction

The ability of naringenin to significantly reduce plasma cholesterol levels has been demonstrated both in vivo and in vitro (1-3). Naringenin's clinical relevance is limited, however, by low solubility and bioavailability owing in part to its largely hydrophobic ring structure. In this study, β-cyclodextrins were examined as potential excipients to enhance the solubility and enteral uptake of the flavonoid. Cyclodextrins are a family of cyclic oligosaccharides that create a 3-dimensional toroid structure, providing a cavity that can accommodate small hydrophobic molecules. Cyclodextrins can therefore be used as excipients to improve the solubility of hydrophobic drugs and other molecules (4, 5). Specifically, the bioavailability of rutin, a flavonoid-glycoside similar in structure to naringin, was significantly enhanced by complexation with 2-hydroxypropyl-β-cyclodextrin (HPβCD) (6).

Here, we demonstrate that 2-hydroxypropyl-β-cyclodextrin (HPβCD), enhances the solubility of naringenin, its transport across a Caco-2 model of human gut epithelium, and its plasma concentrations following oral administration to Sprague-Dawley rats. Combined with HPβCD's strong safety record, our results suggest that naringenin-HPβCD complexes could be used to achieve clinically relevant doses of the flavonoid in patients for the treatment of dyslipidemia and HCV infection.

5.2 Results

5.2.1 β-Cyclodextrins increase the solubility of naringenin

Molecules similar to naringenin in structure and size were previously shown to be solubilized by complexation with β-cyclodextrin (7). To explore if naringenin is similarly solublized we generated complexes with β-cyclodextrin (βCD), methyl β-cyclodextrin (mβCD), and 2-hydroxypropyl-β-cyclodextrin (HPβCD). UV analysis indicated that complexation with cyclodextrins resulted in a very small shift in naringenin's absorption spectrum (**Figure 1B**). Concentrations of naringenin were then extrapolated from the previously obtained standard curve (**Figure 1C**). As expected, naringenin solubility in water was 36μM ± 1μM, consistent with previously observed results (8). Upon complexation with cyclodextrins, the amount of solubilized naringenin increased considerably, as summarized in **Table 1**. The three βCDs solubilized naringenin in decreasing order mβCD > HPβCD > βCD resulting in a significant 526, 437, and 132-fold, enhancement in solubility respectively ($p < 0.001$).

	Max. Naringenin Conc. (mM)	Corresponding CD Conc. (mM)	Fold increase in solubility	K_{eq}
βCD	4.8 ± 0.3	20 ± 1	132	6025
mβCD	19 ± 0.9	50 ± 2.5	526	9975
HPβCD	15.8 ± 1.4	50 ± 2.5	437	8203

Table 1 – Naringenin solubility in cyclodextrin solutions.

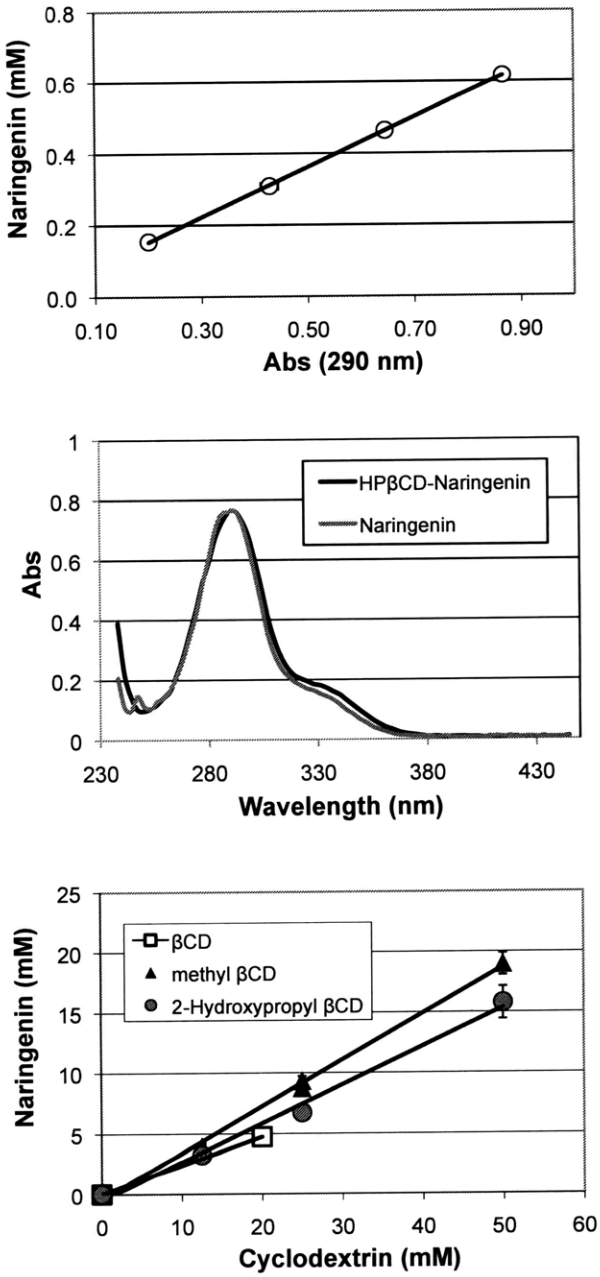

Figure 1 – Cyclodextrins enhance the solubility of naringenin in aqueous solution. (a) A standard curve of naringenin concentration vs. its absorption peak at a wavelength of 290nm (b) Cyclodextrin solutions saturated with naringenin were analyzed by UV absorbance. Complexation with cyclodextrins resulted in a very small shift in naringenin's absorption spectrum. (c) Naringenin concentrations were extrapolated from the previously obtained standard curve. Naringenin solubility in water was 36μM ± 1μM, whereas the amount of solubilized naringenin increased considerably with addition of βCD, mβCD, or HPβCD (132-, 526-, 437-fold, respectively). (a,c) *Conducted by Carolyn Lee-Parsons of Northeastern University.*

5.2.2 HPβCD enhances the transport of naringenin across a Caco-2 monolayer

While mβCD was most effective in enhancing the solubility of naringenin, its use is associated with soft tissue and kidney damage due to its detergent-like effect on membranes (9). On the other hand, HPβCD does not cause hemolysis or irritation due to its low surface tension, and is has been approved as an excipient by the FDA (10). We therefore examined the ability of HPβCD to enhance the transport of naringenin across a monolayer of Caco-2 cells, an established model for drug transport across the human gut epithelium.

Caco-2 cells were grown for 21 days on collagen-coated 24 mm diameter porous transwell membranes (3 μm pores) on which cells form differentiated monolayers, expressing major tight junction proteins, microvilli, and drug transporters (**Figure 2A**) (80, 81). Epithelial integrity and maturity of the monolayers was evaluated by measuring the transport of Lucifer yellow across the monolayer. 11mM naringenin, either alone or in a complex form with 45mM HPβCD, was added to the top assay chamber. Samples were taken from both the top, apical chamber and the bottom, basal chamber at different time intervals and assayed for concentrations of naringenin (**Figure 2B**). The integrity of the Caco-2 monolayer was verified at the end of the experiment by measuring the transport of Lucifer yellow. In the presence of HPβCD, the concentration of naringenin at the basal chamber was increased from 0.04μM ± 0.02μM to 0.51μM ± 0.07μM, representing an 11-fold enhancement of transport across the Caco-2 monolayer. The integrity of the monolayer prior to and following the experiment was similar to controls for both treatments.

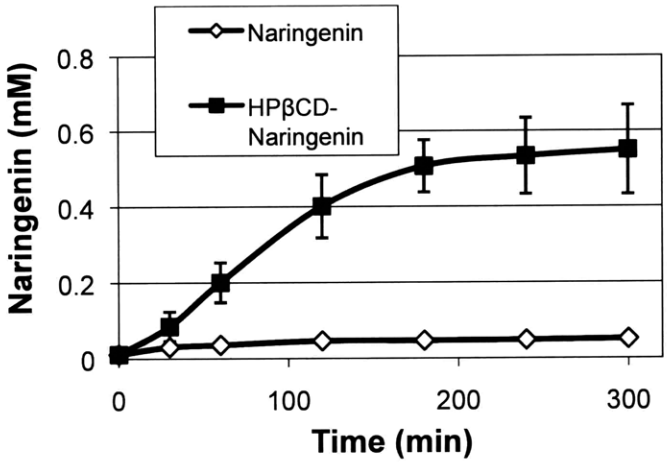

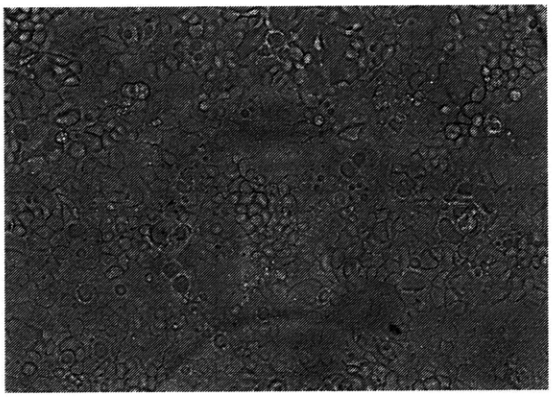

Figure 2 – HPβCD enhances transport of naringenin across Caco-2 cell monolayer. (a) Caco-2 cells were grown for 21 days on collagen-coated 24 mm diameter porous transwell membranes, forming a monolayer. (b) 11mM naringenin, either alone or in a complex form with 45mM HPβCD, was added to the top assay chamber. In the presence of HPβCD, the concentration of naringenin was increased in the basal side from 0.04μM ± 0.02μM to 0.51μM ± 0.07μM, representing an 11-fold enhancement of transport across the Caco-2 monolayer. *Conducted by Ofra Benny of Harvard Medical School, Boston.*

5.2.3 HPβCD enhances the bioavailability of naringenin in rats

To test whether cyclodextrin would enhance the oral bioavailability of naringenin, adult Sprague-Dawley rats were fed 20mg/kg body weight naringenin either alone, or as a 1:16 (wt/wt) HPβCD-naringenin complex, using an oral gavage. Blood samples were collected sequentially at 0, 15, 30, 60, 120, 240, 360, 510, and 600 min from the carotid artery using the previously placed catheter into tubes containing heparin. Immediately after collection, plasma was separated and stored at -80°C for further analysis. At the conclusion of the experiment, all animals were sacrificed, and liver, kidney, and bowel specimens were collected for histology. In an additional experiment, animals were placed in metabolic cages and urine was collected and pooled for the duration of the experiment. Total naringenin (flavonoid and glycoside) was determined by LC-MS as described above.

The complexation of HPβCD with naringenin significantly affected the plasma concentration versus time profile of the flavonoid (**Figure 3a**). Complexation with HPβCD significantly increased the $AUC_{0\text{-}10}$ of naringenin from 2.0 ± 0.5 hr*μg/mL to 15.0 ± 4.9 hr*μg/mL representing a 7.4-fold increase in bioavailability (p=0.005 n=3). Naringenin's maximal concentration, C_{max}, increased from 0.3 ± 0.1 μg/mL to 4.3 ± 1.2 μg/mL representing a 14.6-fold increase (p=0.002 n=3). The calculated half-life for naringenin in plasma was 2.28 hours, consistent with values previously reported in humans (11) and rats (28). Finally, analysis of urine samples in two animals demonstrated renal clearance of 4.2 ± 1%.

Naringenin concentrations in plasma were fitted to a two-compartment pharmacokinetic model (**Figure 3b**). This model suggests that naringenin is transported from the lumen into plasma over 4000-fold the rate than when it is not complexed with cyclodextrin ($k_{1,complexed}$ = 74.6834s^{-1} vs. $k_{1,uncomplexed}$ = 0.0177 s^{-1}). The k_2 clearance parameter was assumed to be constant, and calculated to equal 0.3138 s^{-1}.

5.2.4 Oral administration of HPβCD-naringenin was not associated with adverse effects

Lastly, we wished to examine if the administration of the HPβCD-naringenin complex was associated with tissue or organ damage. Liver, kidneys and intestine were removed 10 hrs following oral administration of the complex and showed no gross pathological changes (data not shown). Histological characterization by a blind observer demonstrated that the small intestine, kidney, and liver sections showed no evidence of tissue injury or inflammation in both groups. Liver sections showed no evidence of hepatocyte damage or neutrophil infiltration to the portal area, while kidney and intestine sections show no tubular/glomerular damage, edema or epithelial damage, respectively (**Figure 4**). One intestine section in a single rat showed a localized small infiltrate, which did not appear to be related to the experiment.

Serum samples were taken from the rats 10 hours after the treatment with HPβCD-naringenin complex, naringenin alone as well as rats treated with saline as a control. The biochemical examination of BUN, ALT/AST, total protein and glucose as parameters of renal and liver function showed no statistical difference between these three groups (**Table 2**). Together with the histological and pathological analysis these results suggest that oral administration of HPβCD-naringenin complex was not associated with any adverse effects.

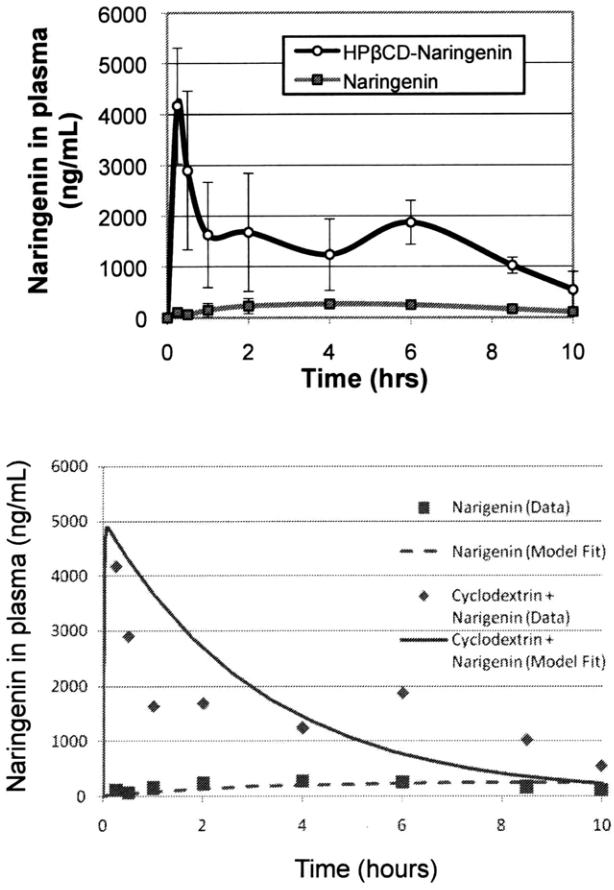

Figure 3 – HPβCD enhances oral bioavailability of naringenin in rats. (a) Male Sprague-Dawley rats were fed 20mg/kg body weight naringenin either alone, or as a HPβCD-naringenin complex. Blood samples were collected sequentially at 0, 15, 30, 60, 120, 240, 360, 510, and 600 min, and subsequently analyzed for naringenin content by LC-MS. Complexation with HPβCD enhanced oral bioavilability as measured by $AUC_{0\text{-}10}$ of naringenin from 2.0 ± 0.5 hr*μg/mL to 15.0 ± 4.9 hr*μg/mL representing a 7.4-fold increase in bioavailability (p=0.005, n=3); and maximal concentration, C_{max} increased from 4.3 ± 1.2 μg/mL to 0.3 ± 0.1 μg/mL representing a 14.6-fold increase (p=0.002, n=3). (b) Plasma concentrations were fitted to a two-compartment pharmacokinetic model. Naringenin is transported from the lumen into plasma over 4000-fold the rate than when it is not complexed with cyclodextrin ($k_{1,complexed}$ = 74.6834s-1 vs. $k_{1,uncomplexed}$ = 0.0177 s-1). The k_2 clearance parameter was assumed to be constant, and calculated to equal 0.3138 s-1.

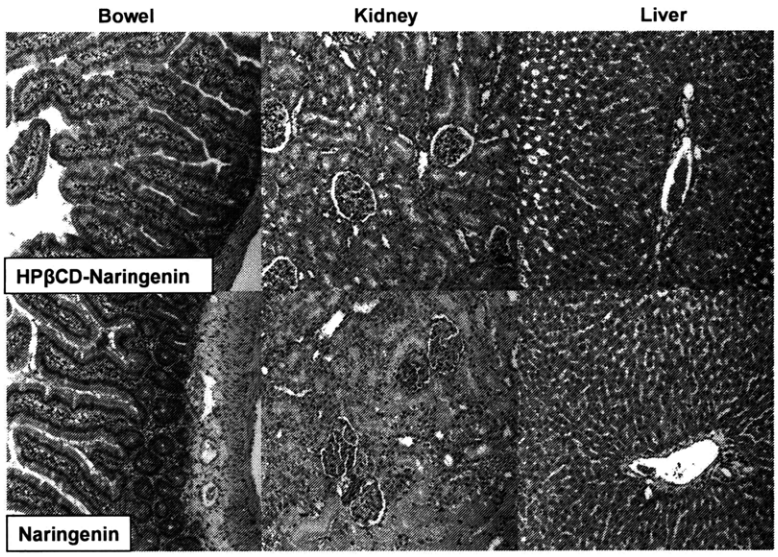

Figure 4 – Rats were fed either naringenin (*bottom*) or naringenin complexed with HPβCD (*top*) in PBS. Blood samples were drawn at various time points, and at t=10hrs animals were sacrificed and tissue specimen from each animal was immediately collected and preserved. Representative images of H&E histological preparations from bowel (*left*), kidney (*center*), and liver (*right*) are presented. The tissues appear normal with no signs of inflammation or necrosis.

		Na+	K+	Cl-	Glu	Ca	Bun	Cre	ALP	ALT	AST	TBil	Alb	TP
NNCD	Avg	139.0	5.9	102.0	168.0	9.3	16.7	0.2	147.3	56.7	307.3	0.3	1.6	5.6
	SD	1.0	0.6	1.0	14.4	0.7	3.1	0.0	84.6	11.1	107.8	0.0	0.2	0.5
NN	Avg	138.0	5.3	102.0	157.0	9.7	19.3	0.3	135.3	61.3	248.3	0.3	1.6	5.6
	SD	1.0	0.3	2.0	6.1	0.2	5.1	0.0	37.5	20.3	45.5	0.1	0.3	0.5
Control	Avg	134.3	4.4	89.7	181.2	10.2	14.0	0.4	311.7	59.8	205.7	0.4	2.1	6.2
	SD	2.5	0.7	3.9	26.5	0.5	3.6	0.1	64.6	30.4	124.0	0.0	0.1	0.3

Table 2- Metabolic blood panel of experimental animals compared with untreated controls. Glu, Glucose; BUN, blood urea nitrogen; Cre, Creatinine; ALP, alkaline phosphatase; ALT, alanine transaminase; AST, aspartate transaminase; TP, total protein. Statistically significant values ($p<0.05$) are noted in italics.

5.3 Discussion

Naringenin has been the focus of multiple studies in recent years, which have began to elucidate its clinical potential with anti-atherogenic, antioxidant, anti-inflammatory, and hypolipidemic effects (12). These properties make it an interesting candidate for clinical application. As with other drugs, however, efficacy would depend on the ability to reproducibly deliver the molecule to patients (7). The ability to breakdown naringin to the absorbable naringenin form varies widely between patients, possibly owing to differences in gut flora (13). Thus, a method of enhancing the bioavailability of naringenin itself is required.

Cyclodextrins, a family of cyclical oligosacchrides composed of varying numbers of glucopyranoside rings that form a three-dimensional toroid structure, are widely used in the food and pharmaceutical industries to solubilize hydrophobic drugs. The potential of β-cyclodextrins to enhance the solubility and gut absorption of flavonoids was demonstrated by the complexatoin of the flavonoid-glycoside, rutin, with HPβCD, and found an >10-fold increase in its solubility in aqueous solution and a 3-fold increase in plasma concetration, as measured by area-under-the-curve (AUC) (14)

We began by examining the ability of several β-cyclodextrins to enhance to solubility of naringenin. Naringenin is generally known to suffer from low solubility in aqueous environments, and is generally dissolved in organic solvents (6). Our observations confirmed a low level of solubility in aqueous buffer, reaching 36μM. The addition of increasing amounts of β-cyclodextrins, however, led to enhanced ability to solubilize the flavonoid. Remarkably, the βCDs increased naringenin's solubility by 2-3 orders of magnitude, up to >500-fold. Of the three βCDs, solubility increased in the order mβCD>HPβCD>βCD. Despite the superior ability of mβCD to solubilize naringenin, we chose to conduct further experiments with HPβCD, which does not or exert a detergent-like effect on biological membranes causing irritation and hemolysis (15). HPβCD is generally regarded as safe by the FDA for use as an excipient (9).

We next examined the ability of HPβCD to enhance the delivery of naringenin across the intestinal mucosa. We used the well-characterized Caco-2 transwell model of the human gut epithelium (9). In this experiment, a monolayer of Caco-2 gut epithelial cells was grown on a

transwell membrane, and the ability of naringenin to cross this barrier was measured over time. When complexed to HPβCD, naringenin reached a concentration 11-fold higher than in the absence of the excipient. The integrity of the monolayer was verified both at the beginning and end of the experiment (by measuring the transport of Lucifer yellow), suggesting that neither HPβCD nor naringenin were damaging to the cells at the concentrations and time-scales examined.

Lastly, we examined the ability of HPβCD to enhance the bioavailability of naringenin in a rat model. Two groups of male Sprague-Dawley rats were fed 20mg/kg body weight naringenin. One group was fed naringenin alone, while the other was fed a HPβCD-naringenin complex. Blood samples at different time points were serially collected and subsequently analyzed by LC-MS, and tissue specimen was collected immediately after animals were sacrificed for histological analysis. Our results indicate a substantial improvement in the delivery of naringenin complexed with HPβCD, with $AUC_{0\text{-}10}$ of naringenin increasing 7.4-fold and maximal concentration, $C_{max,}$ increasing 14.6-fold. This increase in bioavailability represents an increase in the absorption rate from $K_a = 63.7\ hr^{-1}$ to $K_a = 26.9x10^4\ hr^{-1}$, a 4200-fold increase. Several effects could explain this increased rate of transport, including enhancement of dissolution kinetics, increase in solubility, decrease in degradation kinetics in the gut, change in the properties of the intestinal membrane, and shuttling and enhancement of drug concentration at the intestinal wall (16). More study is required to distinguish the dominant mechanisms that lead to enhanced bioavailability in this system. It is unlikely that complexation with HPβCD changes the plasma pharmacokinetics of naringenin, as cyclodextrins are very poorly transported across the intestinal wall (17). The calculated half-life for naringenin in plasma was 2.28 hours, consistent with values previously reported in humans (5) and rats (28).

Previous studies have demonstrated naringenin's low bioavailability, consistent with our results for non-complexed naringenin. Niopas and coworkers orally administered 135mg naringenin to six healthy volunteers. Plasma concentrations peaked after 3.5 hours, and bioavailability was estimated to be 5.8% (11). Erlund and coworkers found similarly low bioavailability when the source of naringenin was grapefruit juice. The researchers also noted the high variability in bioavailability, which was hypothesized to be the result of subject-to-

subject variation in gut microflora (11). The low levels of naringenin plasma concentrations that have been attained in these trials are significantly lower than those required to attain a therapeutic effect as measured both *in vitro* and in animal models. Huff and colleagues have demonstrated that in human hepatoma-based HepG2 cells naringenin's peak modulation of lipid metabolism is attained in the range of 100-200μM (2, 14, 18-20). Our recent results demonstrated that 200μM naringenin blocked the production of HCV in chronically infected Huh7.5.1 cells, concomitantly with a reduction in VLDL secretion (21). Furthermore, animal studies that have demonstrated the beneficial effects of naringenin often employ high doses of the flavonoid (1, 22). Attaining a C_{max} of 200μM in a human would be equivalent to absorbing of 0.25-0.5g of naringenin (neglecting clearance), illustrating the importance of enhancing the bioavailability of the flavonoid.

Our results suggest that complexing naringenin with HPβCD would increase the bioavailability of the naringenin substantially, allowing a smaller dose to be administered, while still achieving the therapeutic plasma concentrations predicted by *in vitro* experiments. More work is required to further elucidate the contribution of several possible mechanisms to the enhanced transport of naringenin across the intestinal wall.

5.4 Materials and Methods

Materials

Naringenin, β-cyclodextrin (βCD), methyl β-cyclodextrin (mβCD), and 2-hydroxypropyl-β-cyclodextrin (HPβCD) were purchased from Sigma-Aldrich Chemicals (St. Louis, MO). Caco-2 cells were purchased from the American Type Culture Collection (Rockville, MD). Unless otherwise noted, all chemicals were purchased from Invitrogen Life Technologies (Carlsbad, CA).

Solubility curves of naringenin complexed with cyclodextrin

Stock solutions of naringenin were prepared in ethanol. A calibration curve was prepared by measuring the UV absorbance of the naringenin stock solutions (0.1 to 0.6 mM) at 290 nm using a ND-1000 spectrophotometer (NanoDrop Technologies, Rockland, DE, USA). Standard deviations between triplicate measurements were less than 5% (**Figure 1A**).

Improvements in naringenin solubility when complexed with cyclodextrin were determined and evaluated as follows. Stock solutions of bCD, mbCD, and HPbCD were prepared in distilled water. None of the cyclodextrins absorbed at 290 nm for concentrations from 0 to 50 mM (data not shown). Next, excess amounts of naringenin powder were added to solutions containing variable amounts of each cyclodextrin, vortexed, and incubated with shaking at 37°C for 3-5 days. Naringenin-cyclodextrin solutions were filtered through a 0.45 μm filter to remove the undissolved naringenin, diluted by 20 or 50-fold, and absorbance was measured at 290 nm. The complex stability constant K was calculated from the linear portion of the solubility diagram assuming a 1:1 complex, that the concentration of free naringenin is equivalent to 36μM (solubility in absence of cyclodextrin), and using the equation:

$$K_{eq} = \frac{[Naringenin \bullet CD]}{[Naringenin][CD]}$$

Caco-2 cell culture

Caco-2 human epithelial colorectal adenocarcinoma cells were cultured in tissue culture flasks (Becton Dickinson and Co., Lincoln Park, NJ). The growth medium was Dulbecco's modified Eagle's medium supplemented with 10% fetal bovine serum, 1% nonessential amino acids, and 4 mM glutamine without antibiotics. The monolayer cultures were grown in a humidified incubator at 37°C and 5% CO_2. The cells were harvested with 0.25% trypsin and 0.2% EDTA (0.5 to 1 min at 37°C), resuspended, and seeded into a new flask. Cells between 30 to 53 passages were used.

Intestinal transport assay

For the transport studies, Caco-2 cells were seeded on Transwell (0.4-µm pore size, 1-cm^2 growth area; Corning Costar Co.) at a cell density of $1x10^5$ cells/filter. Cell growth and maintenance were kept as previously described (23). The cell monolayer was fed fresh growth medium every 2 days and was then used on Day 21 for the transport experiments. To evaluate the integrity of the monolayer, transepithelial HBSS supplement with 20 mM d-glucose and 10 mM HEPES (pH 7.35) was used as the transport medium. To determine the amount of drug crossing the polarized Caco-2 cell monolayer from the donor to the receiver (i.e., apical to basolateral), the Caco-2 cells were rinsed twice with pre-warmed transport medium and were incubated by pre-warmed transport medium 0.2 ml for apical chamber and 0.5 ml for basolateral chamber at 37 °C for 30 min. A 60 mg/ml (1% DMSO in HBSS) stock solution of test compounds, either naringenin or HPβCD-naringenin, was added and samples from both apical and basolateral were taken (30 µl) at different time points: 30, 60, 120, 150 180, 240, and 300 min. The integrity of the culture was confirmed microscopy and by detecting fluorescently labeled cells using 60µM of Lucifer Yellow as a standard. The concentrations of naringenin or HPβCD-naringenin were determined as described and plotted as a concentration on the basolateral side vs. time. Concentrations were corrected by the dilution factor as fresh buffer was added after sampling.

Animal experiments

Adult male Sprague-Dawley rats were purchased from Charles Rivers Laboratories (Wilmington, MA). Upon arrival, each rat was isolated for 5 days towards adaptation to the new

environment. Animals were housed under 12h cycle of day/night with free access to drinking water and fed *ad libitum*. Briefly, rats weighing between 280 and 300 g were anaesthetized using intraperitoneal injections of ketamine and xylazine at 110 and 0.4 mg/kg, respectively. The left carotid artery was cannulated using a 0.76-mm diameter x 60-cm length heparanized catherter. The catheter was tunneled subcutaneously from the opening made in the anterior face of the neck to the dorsal site of the neck and permanently anchored in the skin. The catheter was secured by the use of a rat jacket. Animals were placed in their cages during the term of the study. Animals were orally administered with 20 mg/kg body weight of naringenin in either water or complexed with 320 mg/kg body weight HPbCD using a rat oral gavage (18G x 1 1/2" plastic feeding tube from Instech Laboratories, Inc, PA, USA). Blood samples (0.5 ml) were collected at 0, 15, 30, 60, 120, 240, 360, 510, and 600 min from the carotid artery using the previously placed catheter. In two additional experiments, animals were placed in metabolic cages and urine was collected a pooled for the duration of the experiment. All animals were treated in accordance with National Research Council guidelines and approved by the Subcommittee on Research Animal Care at the Massachusetts General Hospital.

LC-MS detection of naringenin

LC-MS analysis was performed on an Agilent Technologies series 1100 LC-MSD system (Santa Clara, CA), which included an Agilent 1100 quaternary pump, autosampler, column oven, on-line vacuum degassor, and single quadrupole mass spectrometer equipped with electrospray ion source (ESI).

Mass spectrometry conditions: Electrospray ionization (ESI), positive, selected ion monitoring scan (SIM); SIM: naringenin m/z 273.1; IS (hesperetin) m/z 303.1. LC conditions: Eclipse XDB-C18 column (4.6×150mm, 5.0μm). The mobile phase was composed of methanol-water with 0.1% formic acid (65:35,v/v). The isocratic flow rate was set at 0.8 ml/min and injection volume was only 10μl.

To each 100 μl of rat serum sample, 100 μl of 0.1N sodium acetate (pH=5.0) and 100 μl of β-glucuronidase enzyme (5000 units/mL, type HP-2 from Helix Pomatia) were added and vortexed for 5 seconds. This process hydrolyzes the conjugated form of naringenin to determine total

naringenin in plasma. After addition of 20 μl IS buffer solution (5 μg/mL), the sample was then incubated at 37°C water bath for 18h.

The sample was extracted with 0.8mL of ethyl acetate after 18 h incubation, and centrifuged at 13000rpm for 10 min. The supernatant was collected and evaporated to dryness under nitrogen at room temperature. The residue was reconstituted with 100 μl of mobile phase and filtered through a micro nylon n filter (0.45 μm). 10 μl of the filtrate was forwarded to LC-MS analysis. A calibration curve was established and QC samples conducted (data not shown). Data acquisition was performed using ChemStation software (Agilent). Linear regression (weighted by 1/x) between serum concentration and peak area ratio of naringenin to IS was constructed using SPSS11.0 statistical software. The concentrations of naringenin in samples were calculated by interpolation of the linear equation.

Liver Histology

Histological sections of each organ were taken 10 hours after treatment. Formalin-fixed, paraffin-embedded liver, intestine, and kidney samples were sectioned at 4 μm and stained with hematoxylin & eosin (H&E). Histological characterization was performed by a blinded observer using standard assessment of damage.

Modeling naringenin transport in the gut

In this model, the first compartment represents the lumen, and the second compartment represents the circulatory system. These two compartments are governed by the following mathematical equations (16):

$$\frac{dL}{dt} = -k_1[L]$$

$$\frac{dC}{dt} = k_1[L] - k_2[C]$$

Here we assume that the cyclodextrin is absorbed through the lumen [L] at a rate of k_1, and cleared from the circulation [C] at a rate k_2; and that there is no loss of cyclodextrin in feces, and thus all orally administered cyclodextrin will pass through circulation. In order to obtain the values for k_1 and k_2, we fit the response of [C] which is the amount of naringenin in the

circulation, assuming that the initial amount of naringenin in the lumen is assumed to be 5 mg. We further assume that the primary difference between the two cases is captured by k_1 reflective of the increase in transport of naringenin across the lumen due to the formation of a complex with cyclodextrin, whereas k_2 which is reflective of naringenin clearance from circulation is constant.

Modeling was done using MATLAB, and code for curve fitting is given in Appendix I.

Statistics

Data are expressed as the mean ± standard deviation. Statistical significance was determined by a one-tailed Student's t-test. A *P*-value of 0.05 was used for statistical significance.

5.5 Refernces

1. Mulvihill EE, Allister EM, Sutherland BG, Telford DE, Sawyez CG, Edwards JY, Markle JM, et al. Naringenin prevents dyslipidemia, apoB overproduction and hyperinsulinemia in LDL-receptor null mice with diet-induced insulin resistance. Diabetes 2009.

2. Allister, Borradaile, Edwards, Huff. Inhibition of microsomal triglyceride transfer protein expression and apolipoprotein B100 secretion by the citrus flavonoid naringenin and by insulin involves activation of the mitogen-activated protein kinase pathway in hepatocytes. Diabetes 2005;54:1676-1683.

3. Jeon SM, Kim HK, Kim HJ, Do GM, Jeong TS, Park YB, Choi MS. Hypocholesterolemic and antioxidative effects of naringenin and its two metabolites in high-cholesterol fed rats. Transl Res 2007;149:15-21.

4. Rajewski, Stella. Pharmaceutical applications of cyclodextrins. 2. In vivo drug delivery. Journal of pharmaceutical sciences 1996;85:1142-1169.

5. Stella, Rajewski. Cyclodextrins: their future in drug formulation and delivery. Pharm Res 1997;14:556-567.

6. Miyake, Arima, Hirayama, Yamamoto, Horikawa, Sumiyoshi, Noda, et al. Improvement of solubility and oral bioavailability of rutin by complexation with 2-hydroxypropyl-beta-cyclodextrin. Pharmaceutical development and technology 2000;5:399-407.

7. .

8. Tommasini, Raneri, Ficarra, Calabrò, Stancanelli, Ficarra. Improvement in solubility and dissolution rate of flavonoids by complexation with beta-cyclodextrin. Journal of pharmaceutical and biomedical analysis 2004;35:379-387.

9. Stella VJ, He Q. Cyclodextrins. Toxicol Pathol 2008;36:30-42.

10. Notice of a GRAS exemption for beta-cyclodextrin. In: Approval CfFSaANOoP, editor.; 2001.

11. Kanaze, Bounartzi, Georgarakis, Niopas. Pharmacokinetics of the citrus flavanone aglycones hesperetin and naringenin after single oral administration in human subjects. Eur J Clin Nutr 2006:6.

12. Crozier A, Jaganath IB, Clifford MN. Dietary phenolics: chemistry, bioavailability and effects on health. Natural product reports 2009;26:1001-1043.

13. U.S. Food and Drug Administration C. Guidance for Industry: Bioavailability and Bioequivalence Studies for Orally Administered Drug Products--General Considerations. In: Research USFaDACfDEa, editor.: Office of Training and Communications, Division of Communications Management, Drug Information Branch; 2003.

14. Erlund I, Meririnne E, Alfthan G, Aro A. Plasma kinetics and urinary excretion of the flavanones naringenin and hesperetin in humans after ingestion of orange juice and grapefruit juice. J Nutr 2001;131:235-241.

15. Wilcox, Borradaile, Huff. Antiatherogenic Properties of Naringenin, a Citrus Flavonoid. Cardiovascular Drug Reviews 1999.

16. Gao J, Hugger ED, Beck-Westermeyer MS, Borchardt RT: Estimating Intestinal Mucosal Permeation of Compounds Using Caco-2 Cell Monolayers. In: Enna SJ, Williams M, eds. Current Protocols in Pharmacology, 2000.

17. Carrier RL, Miller LA, Ahmed I. The utility of cyclodextrins for enhancing oral bioavailability. J Control Release 2007;123:78-99.

18. Borradaile, Dreu d, Huff. Inhibition of net HepG2 cell apolipoprotein B secretion by the citrus flavonoid naringenin involves activation of phosphatidylinositol 3-kinase, independent of insulin receptor substrate-1 phosphorylation. Diabetes 2003;52:2554-2561.

19. Borradaile, Dreu d, Barrett, Huff. Inhibition of hepatocyte apoB secretion by naringenin: enhanced rapid intracellular degradation independent of reduced microsomal cholesteryl esters. J Lipid Res 2002;43:1544-1554.

20. Wilcox, Borradaile, Dreu d, Huff. Secretion of hepatocyte apoB is inhibited by the flavonoids, naringenin and hesperetin, via reduced activity and expression of ACAT2 and MTP. J Lipid Res 2001;42:725-734.

21. Allister, Mulvihill, Barrett, Edwards, Carter, Huff. Inhibition of apoB secretion from HepG2 cells by insulin is amplified by naringenin, independent of the insulin receptor. J Lipid Res 2008;49:2218-2229.

22. Nahmias, Goldwasser, Casali, Poll v, Wakita, Chung, Yarmush M. Apolipoprotein B-dependent hepatitis C virus secretion is inhibited by the grapefruit flavonoid naringenin. Hepatology 2008;47:1437-1445.

23. Kurowska EM, Borradaile, Spence JD. Hypocholesterolemic effects of dietary citrus juices in rabbits. Nutrition Research 2000.

6 Conclusion

6.1 Summary of results

We began our work by examining the link between VLDL and HCV secretion. We demonstrated that HCV was secreted while physically bound to ApoB and that HCV secretion mirrors that of VLDL. We went on to show that HCV core colocalizes with ApoB in the cell, and that inhibition of ApoB production through RNAi could block viral secretion. Notably, concurrently with our work, several other laboratories were conducting research along similar paths, establishing firmly the dependence of HCV on the secretion of VLDL from hepatocytes (1-3).

The close association of VLDL and ApoB secretion led us to search for an agent that could effectively reduce VLDL secretion. Naringenin, a grapefruit flavonoid, seemed like a promising candidate, as it had been shown earlier to block VLDL secretion in *in vitro* models (4-6), and to lower plasma VLDL levels *in vivo* (7-10). We therefore showed naringenin inhibited ApoB and HCV secretion concomitantly. We went on to investigate how naringenin was interfering with the viral lifecycle and narrowed it to the assembly step – the flavonoid was interfering with a later step than protein production and replication, but earlier than export.

We next hypothesized that naringenin reduced the components needed for the production of VLDL. Indeed, we showed that naringenin inhibited MTP, the rate-limiting enzyme in the production on VLDL. Unlike other MTP inhibitors, we did not see an accumulation of triglycerides in cells treated with naringenin (11). These results, as well as observations of other groups, led us to hypothesize that naringenin was activating the PPARα nuclear receptor (NR). In the liver, PPARα drives β-oxidation, leading to the breakdown of lipids – components required for VLDL production. We showed that naringenin activates PPARα in HCV-infected cells and that a known PPARα agonist,

WY14,643, had similar inhibitory effects on virus production as naringenin. A 7-day experiment confirmed that naringenin's effects were sustainable, but that withdrawal of treatment leads to a quick rebound in virus production, consistent with our proposed mechanism of action.

We next investigated in more depth the effects of naringenin on NRs. We suggested that naringenin could be modulating the activity of two nuclear receptors (NRs): PPARα and LXRα. LXRα is a pro-lipogenic NR that is activated by oxysterols and glucose, and that drives the production of lipids and cholesterol. We showed that naringenin activated PPARα, and the related PPARγ in reporter cell systems. We further showed that naringenin suppressed the activation of LXRα in reporter cells. Interestingly, a biochemical assay indicated that naringenin functioned as a partial agonist of LXRα, leading to a net inhibitory effect in cells. We confirmed the effects of naringenin on PPAR- and LXR-response elements using reporter plasmids transfected in Huh7.5.1 cells. To understand the effects of this activation at the levels of gene activation and metabolic effects, we first showed that naringenin activated PPARα-controlled genes involved in β-oxidation and downregulated LXRα-controlled genes. We then demonstrated that in primary rat hepatocytes, naringenin decreased the secretion of triglycerides and bile acids from cells, and that WY16,463 inhibited ApoB secretion similarly to naringenin.

Lastly, we wished to explore the possible utility of naringenin in a clinical setting. We demonstrated that the flavonoid was non-toxic to primary human hepatocytes in culture and to rats administered high doses intraperitoneally, consistent with the observations of others regarding its low toxicity. We then showed that naringenin's solubility and bioavailability could be dramatically increased by complexation with β-cyclodextrin.

In summary, we have shown naringenin's potential to inhibit HCV production in cells. We have characterized the mechanism of this inhibition, tracing it to interference with VLDL assembly. We then showed that this effect on VLDL could be traced to the

flavonoid's effects on NRs. Finally, we demonstrated a method of increasing any future clinical utility of the molecule by enhancing its bioavailability.

6.2 Impact

We believe this work may have a large impact on the treatment of HCV. Naringenin is a cheap molecule and has a history of safe use as a food supplement. It could be used as a weapon in the arsenal against HCV, most likely in combination with other drugs.

Importantly, our work helps establish ground for further investigation of methods of modulating metabolism to target HCV and possibly other pathogens. It also demonstrates the value of studying naturally derived molecules for beneficial clinical effects.

6.3 Future directions

Our work thus far has focused on the *in vitro* effects of naringenin – we would also like to examine the effects of naringenin in an *in vivo* model. Unfortunately, few options exist for HCV animal models: either chimpanzees or chimeric mouse models. The latter carry grave ethical and cost considerations, while the latter are more feasible, but less complete. Especially in the context of nuclear receptors, it is not clear that the responses observed in these models would be applicable to human patients.

Of course, the ultimate test of our work would be application to patients. We look forward to the possibility of conducting small clinical trial to examine the effects of naringenin in HCV-infected patients. An early target population would consist of patients who do not respond to the standard of care, and would likely be administered in combination with other medications. It will be important to establish whether the expected reduction in HCV production by hepatcytes will lead to improvement in clinical outcomes, and whether the treatment and its outcomes are truly sustainable over months and years.

Our work also sets the stage for examining the effects of other flavonoids and natural products as possible modulators of metabolism, and thus of the HCV viral

lifecycle. Furthermore, evidence that hepatitis B virus proteins modulate LXRα activity (12, 13) suggests that the interaction between hepatitis viruses, lipid metabolism, and nuclear receptors is not unique to HCV, thus expanding the potential of naringenin to treat other infections as well.

6.4 References

1. Huang, Sun, Owen, Li, Chen, Gale, Ye. Hepatitis C virus production by human hepatocytes dependent on assembly and secretion of very low-density lipoproteins. Proc Natl Acad Sci USA 2007;104:5848-5853.
2. Gastaminza, Cheng, Wieland, Zhong, Liao, Chisari. Cellular determinants of hepatitis C virus assembly, maturation, degradation, and secretion. Journal of Virology 2008;82:2120-2129.
3. Gastaminza, Kapadia, Chisari. Differential biophysical properties of infectious intracellular and secreted hepatitis C virus particles. Journal of Virology 2006;80:11074-11081.
4. Wilcox, Borradaile, Dreu d, Huff. Secretion of hepatocyte apoB is inhibited by the flavonoids, naringenin and hesperetin, via reduced activity and expression of ACAT2 and MTP. J Lipid Res 2001;42:725-734.
5. Allister, Borradaile, Edwards, Huff. Inhibition of microsomal triglyceride transfer protein expression and apolipoprotein B100 secretion by the citrus flavonoid naringenin and by insulin involves activation of the mitogen-activated protein kinase pathway in hepatocytes. Diabetes 2005;54:1676-1683.
6. Borradaile, Dreu d, Huff. Inhibition of net HepG2 cell apolipoprotein B secretion by the citrus flavonoid naringenin involves activation of phosphatidylinositol 3-kinase, independent of insulin receptor substrate-1 phosphorylation. Diabetes 2003;52:2554-2561.
7. Mulvihill EE, Allister EM, Sutherland BG, Telford DE, Sawyez CG, Edwards JY, Markle JM, et al. Naringenin prevents dyslipidemia, apoB overproduction and hyperinsulinemia in LDL-receptor null mice with diet-induced insulin resistance. Diabetes 2009.
8. Kurowska EM, Borradaile, Spence JD. Hypocholesterolemic effects of dietary citrus juices in rabbits. Nutrition Research 2000.
9. Lee CH, Jeong TS, Choi YK, Hyun BH, Oh GT, Kim EH, Kim JR, et al. Anti-atherogenic effect of citrus flavonoids, naringin and naringenin, associated with

hepatic ACAT and aortic VCAM-1 and MCP-1 in high cholesterol-fed rabbits. Biochemical and Biophysical Research Communications 2001;284:681-688.

10. Jeon SM, Kim HK, Kim HJ, Do GM, Jeong TS, Park YB, Choi MS. Hypocholesterolemic and antioxidative effects of naringenin and its two metabolites in high-cholesterol fed rats. Transl Res 2007;149:15-21.

11. Chandler CE, Wilder DE, Pettini JL, Savoy YE, Petras SF, Chang G, Vincent J, et al. CP-346086: an MTP inhibitor that lowers plasma cholesterol and triglycerides in experimental animals and in humans. J Lipid Res 2003;44:1887-1901.

12. Na, Shin, Roh, Kang, Hong, Oh, Seong, et al. Liver X receptor mediates hepatitis B virus X protein-induced lipogenesis in hepatitis B virus-associated hepatocellular carcinoma. Hepatology 2008.

13. Kim, Kim, Kim, Cheong. Hepatitis B virus X protein induces lipogenic transcription factor SREBP1 and fatty acid synthase through the activation of nuclear receptor LXRalpha. Biochem J 2008;416:219-230.

Appendix I

MATLAB Code for Modeling

clearance_test.m

```
clear all; close all;
global data;
data = [2988.5  4255.7      5259.0      117.4 55.7  157.4
2502.3    4616.2      1570.4      46.2  55.6  92.2
2182.9    2276.9      435.9 53.8  94.9  301.5
2604.8    2062.0      376.7 101.1 392.8 197.0
1968.8    1177.4      568.2 166.7 325.9 311.9
2370.0    1675.3      1572.6      173.8 307.5 272.9
948.1     1204.3      915.3 172.1 118.1 211.6
434.8     940.3 258.0 164.6 71.8  95.9
];

p = fminsearch(@clearance_fit, [26.7502    0.8100    0.0460]);
```

clearance.m

```
function dx = clearance(t,x)
global c1;
    global c2;
    dx(1) = -1*  c1 * x(1);
    dx(2) = c1 * x(1) - c2 * x(2);
    dx = dx';
```

clearance_fit.m

```
function error = clearance_fit(p)
global c1;
global c2;
global c3;
global data;

c1 = p(1);
c2 = p(2);
c3 = p(3);
tp = [0.25, 0.5, 1, 2, 4, 6, 8.5, 10];
[t,x] = ode23s(@clearance, [0 10], [5000,0]);
flag = false;
xp = interp1(t,x(:,2),[0.25, 0.5, 1, 2, 4, 6, 8.5, 10]);
xp = xp';
ff = mean(data(:,1:3)')';
error = norm(data(:,1) - xp);
%plot(t,x, tp, data(:,1:3));

c1 = p(3);
[t2,x2] = ode23s(@clearance, [0 10], [5000,0]);

x2p = interp1(t2,x2(:,2),[0.25, 0.5, 1, 2, 4, 6, 8.5, 10]);
x2p = x2p';
ffx = mean(data(:,4:6)')';
error = error + norm(ffx - x2p)
plot(tp, data(:,2), t, x(:,2), tp, ffx, t2, x2(:,2));
```